



Faculty of Science and Technology

Bachelor's Thesis

Metabolic Flexibility in Cancer Cells

Study programme / specialization:
Biological Chemistry / Biotechnology

The spring semester, 2022

Author:
Eilin Haave and Camilla Halvorsen

Open / Confidential

Course coordinator:
Cathrine Lilo

Supervisor(s):
Hanne Røland Hagland

Credits (ECTS): 20

Keywords:

colorectal cancer cells, cancer metabolism,
metformin, DCA

Pages: 96

+ appendix: 39

Stavanger, 05/15/2022
date/year

Abstract

Colorectal cancer is the third most occurring cancer type among both men and women in the United States. Even though cancer therapies have been revolutionarily improved over the decades, there is a high demand for more effective treatments, making research within the complex aspect of cancer crucial for the design of highly specific and effective therapies. Manipulation of cancer metabolism has been an interesting topic of research and has shown to be a promising field for future therapeutic methods as a part of cancer therapy.

Metformin (bimethylbiguanide) belongs in a class of drugs named biguanides and is today used as a medication to treat type-II diabetes. Dichloroacetate (DCA) is currently used to treat diabetes mellitus, lipid and lipoprotein disorders, pulmonary arterial hypertension, and acquired and congenital lactic acidosis. Both drugs have shown interesting effects on the metabolism of cancer.

The aim of this study was to examine the effects of metformin and DCA on colorectal cancer cell lines HCT116 and SW948 with the use of alamarBlue- and CCK-8 assays as well as flow cytometry.

The results indicate that metformin has a decreasing effect on the viability in both cell lines, where the most effective treatment was a 6 mM concentration after an exposure period of 48 hours. DCA showed an opposing effect in respect to metformin, where the highest concentration (6 mM) and longest exposure period (48 hours) generated the highest viability. These results indicates that our specific cell lines are more reliant on the mitochondrial metabolism rather than the glycolytic.

The flow cytometry for this study measured the expression of Akt, p-Akt, AMPK, and p-AMPK. Both cell lines showed an increase in the expression of p-Akt and AMPK after the treatment with metformin. SW948 also had a minor shift in the Akt expression. DCA had no impact on neither of the protein expressions.

Table of Contents

Bachelor's Thesis	1
Abstract	2
Abbreviations	6
1 Introduction	8
<i>1.1 General Introduction</i>	8
1.1.1 Cancer.....	8
1.1.2 Cancer Mutations	9
1.1.3 Cancer Survival and Life Expectancy	11
1.1.4 Cancer Therapy	12
1.1.5 Metabolic Pathways and Cancer Metabolism	13
1.1.6 Glycolysis.....	15
1.1.7 The Citric Acid Cycle.....	17
1.1.8 The Electron Transport Chain	19
1.1.9 mTOR pathway	21
1.1.10 Protein kinase B / AKT	22
1.1.11 AMP-activated protein kinase (AMPK).....	24
1.1.12 The Warburg Effect.....	26
<i>1.2 Thesis Introduction</i>	28
1.2.1 Problem Statement	28
1.2.2 Colorectal Cancer Cells.....	29
1.2.3 Metformin and Dichloroacetate.....	30
<i>1.3 Introduction to Instruments and Assays</i>	32
1.3.1 Muse® Cell Analyzer, Count and viability assay	32
1.3.2 Spectrophotometer.....	34
1.3.3 AlamarBlue Assay.....	35
1.3.4 CCK-8 Proliferation Assay	35
1.3.5 Flow Cytometry.....	36
2 Chemicals, Equipment, and Instruments	37
<i>2.1 Chemicals and Reagents</i>	37

2.2	<i>Instruments and Equipment</i>	39
2.3	<i>Experiment Conditions</i>	41
2.3.1	Preparation of Aseptic Working Environment.....	41
2.3.2	Temperature and Humidity Conditions.....	41
3	Procedures	42
3.1	<i>Preparation</i>	42
3.1.1	Cell Growth Medium.....	42
3.1.2	Maintenance of Colorectal Cancer Cells.....	43
3.1.3	Preparation of medication.....	44
3.2	<i>Initial testing</i>	46
3.2.1	Muse Cell Count and Viability Assay.....	46
3.2.2	AlamarBlue Assay.....	47
3.2.3	CCK-8 Proliferation Assay.....	49
3.2.4	Combination treatment.....	50
3.2.5	Flow Cytometry Assay.....	52
4	Results	54
4.1	<i>AlamarBlue</i>	54
4.1.1	AlamarBlue metformin treatment.....	56
4.1.2	HCT116 results.....	56
4.1.3	SW948 results.....	58
4.1.4	AlamarBlue DCA treatment.....	60
4.1.5	HCT116 results.....	60
4.1.6	SW948 results.....	62
4.2	<i>CCK-8</i>	64
4.2.1	CCK-8 metformin treatment.....	65
4.2.2	HCT116 results.....	66
4.2.3	SW948 results.....	68
4.2.4	CCK-8 DCA treatment.....	70
4.2.5	HCT116 results.....	70
4.2.6	SW948 results.....	72

4.3	<i>Combination treatment AlamarBlue</i>	74
4.3.1	HCT116 results.....	75
4.3.2	SW948 results.....	76
4.4	<i>Combination treatment CCK-8</i>	77
4.3.3	HCT116 results.....	78
4.3.4	SW948 results.....	78
4.5	<i>Flow Cytometry</i>	80
4.3.5	HCT116 results.....	81
4.3.6	SW948 results.....	83
5	Discussion	85
5.1	<i>Methodological considerations</i>	85
5.2	<i>Results discussion</i>	87
5.2.1	AlamarBlue and CCK-8	87
5.2.2	Flow Cytometry	89
6	Conclusion	91
7	References	92
8	Appendix	98
5.3	<i>Appendix 1</i>	98
5.4	<i>Appendix 2</i>	104
5.5	<i>Appendix 3</i>	112
5.6	<i>Appendix 4</i>	120
5.7	<i>List of figures</i>	131
5.8	<i>List of tables</i>	132
5.9	<i>List of equations</i>	136

Abbreviations

Abbreviation:	Explanation:
[HIF]-1 α	hypoxia inducible factor
ADB	Antibody Dilution Buffer
ADP	adenosine diphosphate
AMPK	Adenosine 5'-monophosphate-activated protein kinase
ATP	Adenosine triphosphate
BSL-2	Biosafety level 2
CCK-8	Cell Counting Kit-8
CRC	Colorectal cancer
DCA	Dichloroacetate
DHAP	dihydroxyacetone phosphate
ETC	The electron transport chain
F6P	fructose 6-phosphate
FBS	Fetal base serum
G3P	glyceraldehyde 3-phosphate
G6P	glucose-6 phosphate
GLUT	Glucose transporter
HGG	High-Grade Glioma

Met	Metformin
mTOR	Mammalian target of rapamycin
mTORC1	Mammalian target of rapamycin complex 1
NADH	Nicotinamide adenine dinucleotide hydride
PDC	pyruvate dehydrogenase complex
PDH	pyruvate dehydrogenase
PDK	pyruvate dehydrogenase kinases
PEP	phosphoenolpyruvate
PFK-1	phosphofructokinase
PI3K	Phosphoinositide-3-kinase
PIP3	Phosphatidylinositol 3,4,5-trisphosphate
PTEN	Phosphatase and tensin homolog
S.D	Standard deviation
TCA	Tricarboxylic acid
TNM	Tumor, node, and metastasis

1 Introduction

1.1 General Introduction

1.1.1 Cancer

According to the World Health Organization (WHO), cancer caused nearly 10 million deaths in 2020 making it the leading cause of mortality worldwide. (1)

Enormous amounts of research and funding have been put into solving the riddle of cancer. After years of research, there have been made significant progress in fields linked to cancer treatment, prevention, and early detection. Even though the knowledge is rapidly growing, today's scientists and doctors still battle cancer every day and many times the battle is lost. (2)

Cancer is a group of diseases originating from normal tissue. The disease is caused by multiple genetic mutations, and the accumulation of activated oncogenes and loss of tumor suppressors leads to cancer development and progression. Mutations can impact biological pathways and alter the pathways behavior to benefit the cancerous cell.

1.1.2 Cancer Mutations

Cancer driver genes are genes that have been mutated and they create advantages for the cancerous cell. There have been identified 138 such genes. (3) An example of a commonly mutated cancer driver gene is the p53 gene. P53 is a tumor suppressor gene found in ~60% of colorectal cancers. (4) (5) In addition, a greater number of mutations are thought to have a less direct impact on tumor formation, but still facilitates cancerous activity when the cell becomes neoplastic. These mutations can be indels, epigenetic modifications, or a multitude of other changes. Several different mutations can cause the same type of cancer in a variety of people, thus making it difficult to identify and effectively target one specific genetic mutation at a time. (6)

The mutations present in cancer cells lead to the cells stepping away from their normal behaviors and start proliferating beyond control. Normal cells have safeguards to prevent overpopulation and cooperate with surrounding cells. Cancer cells seem to have only one goal; to create as many copies of themselves as possible and thus becoming a form of predatory cell that invade both nearby and distant tissues causing malignant tumors and metastasis. (7)

For a tumor to thrive there are certain biological capabilities needed. These are called the eight hallmarks of cancer and contain:

- sustained proliferation
- evasion of growth suppressors
- death resistance
- replicate immortality
- angiogenesis
- invasion with or without metastability
- reprogrammed energy metabolism
- immune evasion

(3)

One of the benefits in cancer treatment is the fact that all of these hallmarks are supported by one or several of 12 signaling pathways.

Through thoroughly mapping pathways along with the genetic profile of a specific tumor, it might be possible to create a more specific treatment plan by targeting the altered pathways directly instead of targeting each mutation individually.

1.1.3 Cancer Survival and Life Expectancy

A patient's life expectancy and overall survival vary significantly between different cancer types. While some only provide a few months of survival, others can be slow growing and give years to live, and some patients even experience cancer remission. One of the main elements that affect the curability or life expectancy of one's cancer is early detection.

Depending on their development, tumors are categorized into different stages. There are several different staging systems where the Tumor Node Metastases (TNM) system is the most commonly used worldwide. (8) Most staging systems are based on information about the tumor's placement, cell type (such as adenocarcinoma), the size of the tumor, whether the tumor has spread to lymph nodes or not, the presence of distant metastasis, the tumor grade that refers to the degree of abnormality in a cancer cell and how likely it is to spread. (8)

The first-line treatment of choice is surgical resection of the tumor. However, this is only possible if the tumor is detected at an early stage. The longer it goes undetected the further it's likely to have developed, making surgical treatment impossible in many cases, significantly decreasing the life expectancy of the patient. (9)

There are two main tools in early diagnosis: early detection and screening. Early detection is when a patient can discover the symptoms of cancer at an early stage due to increased awareness and knowledge of cancer development and symptoms. Screening on the other hand, are tests such as mammography and pap smears that are performed on people who do not have any clinical symptoms and might be perfectly healthy individuals. (10) The aim is to identify cancers or precancer conditions in people who are asymptomatic.

1.1.4 Cancer Therapy

Cancer therapy has throughout history been challenging due to its varying effectiveness and side effects. Surgery of solid tumors, antitumor drugs and radiation have been the most common approaches for cancer treatment in some cases. In modern times, immunotherapy has become an important and preferable therapeutic alternative for some instances.

Nanotechnology is a fairly new therapeutic approach that uses nanostructures as an alternative for controlled drug delivery, a combination of imaging and treatment, hyperthermia treatment, and targeted therapy. (11)

Cancer tumors possess the ability to become exceedingly heterogeneous during cancer progression. A diverse cell population results in various molecular properties and thus a mixed responsiveness to therapy. Traditional cancer therapy usually treats cancer as a homogeneous disease. Therefore, research within the complex aspect of cancer is crucial for the design of highly specific and effective therapies. (12)

Sidney Farber discovered in 1947 that a drug named aminopterin had the ability to cause remission of acute lymphoblastic leukemia in children. Aminopterin is the precursor of modern drugs that inhibit essential reactions necessary for de novo nucleotide synthesis. This clinical success led to the discovery and development of “antimetabolites”; a class of drugs that interferes with the activity of enzymes involved in nucleotide metabolism. (13)

1.1.5 Metabolic Pathways and Cancer Metabolism

An enormous number of cells working together through signaling pathways creates a network of communication. This is the basis for complex life. These pathways are essentially biochemical reactions that ultimately produce or break down cellular components through several steps of conversion. Every organ in the human body is composed of specialized cells that are structured to perform certain tasks created for the specific cell type.

Cell communication is performed through chemical signaling and signaling pathways that initiate either a stimulatory or inhibitory effect. These pathways are powered essentially by enzymes - flexible catalyst proteins that bind to substrates and/or act as an on/off switch for a specific pathway. (14)

The cells can both receive and send information regarding situations such as injury and stress. Among other tasks, the cells are responsible for creating usable energy in the form of adenosine triphosphate (ATP). (15), (16) Some of the most well-known pathways such as the glycolytic pathway, citric acid cycle, and oxidative phosphorylation are involved in cell metabolism, and are shown in Figure 1.

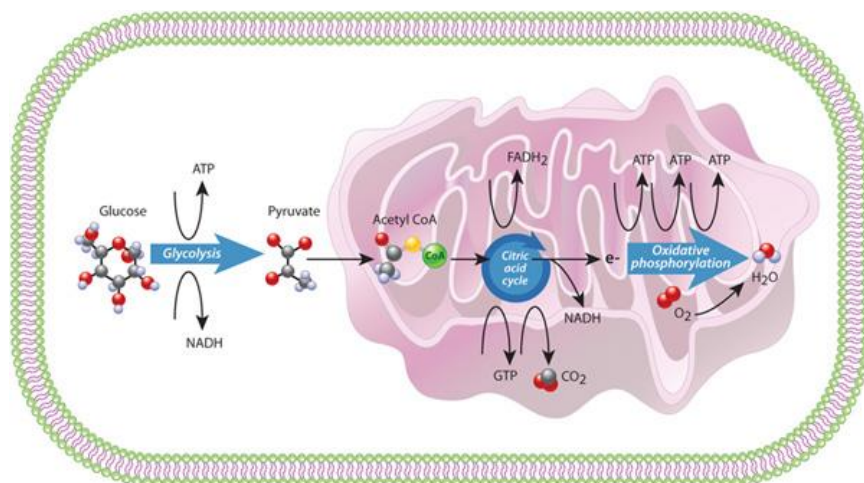


Figure 1: showing a simplified overview showing the cell metabolism. The glycolysis, citric acid cycle and oxidative phosphorylation are depicted. (17)

ATP synthesis takes place in metabolic pathways. Pathways such as the glycolytic pathway, citric acid cycle, and oxidative phosphorylation are multistep processes in the cell that utilize the nutrients we ingest to synthesize ATP and molecules that are needed for cellular

processes. These metabolic pathways might be modified through mutations, and can result in a metabolism that promotes a carcinogenic process. Metabolic targeting of cancer cells is an active research topic for identifying molecules that inhibit key metabolic steps linked to tumorigenesis. (18)

1.1.6 Glycolysis

Glycolysis is a multistep process in the cell's cytosol. During glycolysis, glucose is catabolized into two three-carbon keto-acids (pyruvate) under aerobic conditions, and lactate if the environment is hypoxic. The process generates 4 ATP, 2 NADH molecules, 2 H⁺, and 2 H₂O molecules with a total net gain of 2 ATP per invested glucose molecule. Despite its low ATP output per glucose molecule, the glycolysis can be an effective pathway for ATP synthesis due to its rapid process. The glycolytic pathway is shown in Figure 2, and consists of one investment phase and one pay-off phase. The glycolysis provides the cell with important energy and building blocks required for cell maintenance and proliferation. (19)

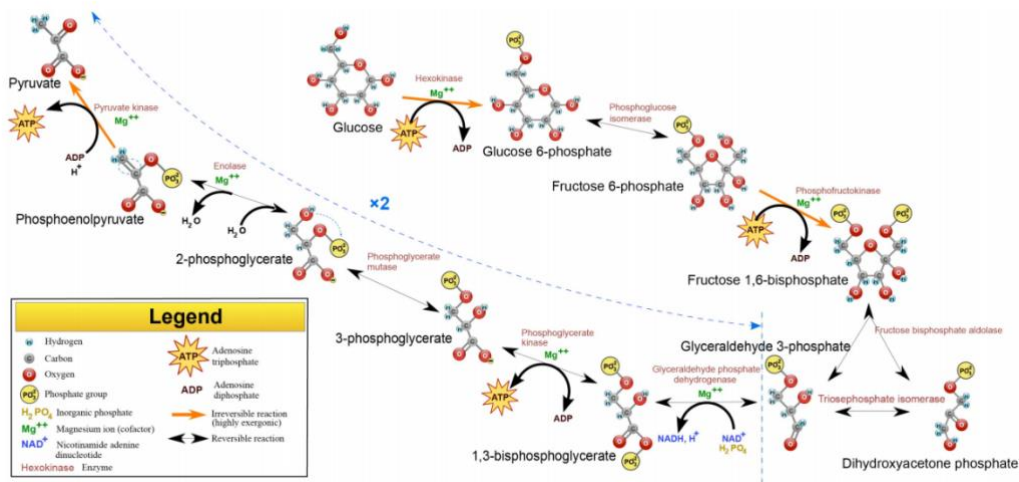


Figure 2: Drawing of the glycolytic pathway, showing the intermediate steps, reactants, and products. (20)

In the investment phase, glucose is imported into the cell by glucose transporters (GLUTs).

The glucose is trapped in the cell as it is phosphorylated by hexokinase and turned into glucose-6 phosphate (G6P), a process that requires the cell to spend ATP. (21)

(21) The next step is the isomerization of G6P into fructose 6-phosphate (F6P) before another phosphate is added by the enzyme phosphofructokinase (PFK-1). The PFK-1 further phosphorylates the F6P into fructose 1,6-bisphosphate, which is then lysed to create two separate molecules that function as substrates as dihydroxyacetone phosphate (DHAP) and glyceraldehyde 3-phosphate (G3P) are created.

During the pay-off phase ATP is produced in two steps, and the cell enters the energetically favorable stage of glycolysis. One part of the ATP production happens through multiple steps, where NAD⁺ are reduced, generating NADH by the help of glyceraldehyde-3-phosphate

dehydrogenase. This process is a part of the metabolization of G3P into 1,3-diphosphoglycerate, which in turn will be dephosphorylated by phosphoglycerate kinase, turning it into 3-phosphoglycerate and along the way ATP is produced. Phosphoglycerate mutase will furthermore convert 3-phosphoglycerate into 2-phosphoglycerate. 2-phosphoglycerate is converted into phosphoenolpyruvate (PEP), and one of the phosphate groups of PEP will be used to phosphorylate adenosine diphosphate (ADP) molecules to create the last 2 ATP molecules of the glycolysis. During this phosphorylation step, PEP is reverted to pyruvate which can continue through the pathways and proceed into oxidative phosphorylation.

Each step in the glycolysis is catalyzed by enzymes, where the main rate-controlling enzyme is phosphofructokinase. (21) The product of glycolysis depends on the environmental conditions in the cell. If the glycolysis occurs under aerobic conditions, the pyruvate created will proceed to the citric acid cycle as shown in Figure 3, and ultimately generate 32 ATP molecules. If the process occurs under anaerobic conditions, lactate will be formed at the expense of pyruvate.

1.1.7 The Citric Acid Cycle

The citric acid cycle, or the tricarboxylic acid (TCA) cycle, is a critical metabolic pathway that drives cellular respiration. The TCA cycle converts the products of glycolysis into NADH, FADH₂ and ATP molecules. The stored energy is then easily harvested either directly as ATP or indirectly through the electron transport chain for NADH and FADH₂.

The cycle is present both in eukaryotes and prokaryotes, with the difference that in the former it takes place in the matrix of the mitochondria, while in the latter it takes place in the cytoplasm. It is catalyzed by oxaloacetate, a four-carbon molecule that is used to initiate the first step of the cycle and is then recreated in the final step. However, a total of eight separate enzymes are used to catalyze the steps of the cycle. (22)

In the first step of the pathway, acetyl CoA reacts with oxaloacetate to produce citrate, a six-carbon molecule. Two of the carbons are then consecutively released in the form of CO₂ with the help of isocitrate dehydrogenase and α -ketoglutarate dehydrogenase, producing a four-carbon molecule of succinyl CoA and two molecules of NADH. Those two enzymes act as key regulators of the process, with their presence accelerating it while their lack of presence decelerating it to adjust to the cell's needs.

The next steps of the cycle replace the CoA of succinyl CoA with a phosphate group, which is then transferred to either ADP or GDP to create the energy carrying ATP or GTP. This process creates succinate, which can then be oxidized in the next step to form fumarate, while simultaneously transferring two hydrogen molecules to a FAD receptor and producing FADH₂. (23)

The fumarate is then hydrated in a process that converts it to malate. The malate is used to complete the cycle by being oxidized back into oxaloacetate, the original catalyst used to start the circle. This process reduces one more NAD⁺ molecule into NADH for a total of three. Those three electron carriers, together with the electron carrier molecule of FADH₂ and the energy yielding molecule of ATP/GTP, are the primary products of the pathway. The electron carriers can then be used by the oxidative phosphorylation pathway to create more ATP

molecules, making the citric acid cycle the primary pathway that drives cellular respiration. (24)

The Warburg effect helps cancer cells bypass this pathway completely and preferentially create lactate instead of pyruvate. However, research has shown that certain cancer cells with special genetic characteristics, primarily those with deregulated oncogene and tumor suppression expression, not only utilize the citric acid cycle pathway but depend upon it both for their energy needs and for their macromolecule synthetic process. This has led to increasing therapeutic research which attempts to apply small molecule inhibitors to re-regulate the cycle and prevent it being used for tumor growth.

An important differentiator between the normal and aberrant utilization of the pathway is that, while several different types of fuels can be catabolized by both normal and cancerous cells, there is significant preferentiality in the fuel used by the two groups. Normal cells thrive mostly on glucose, which is the primary source of pyruvate entering the cycle. Cancer cells, however, because of the Warburg effect, direct glucose towards the anaerobic glycolysis pathway, thus creating a need for increased amounts of glutamine and fatty acids to power the cycle. (24)

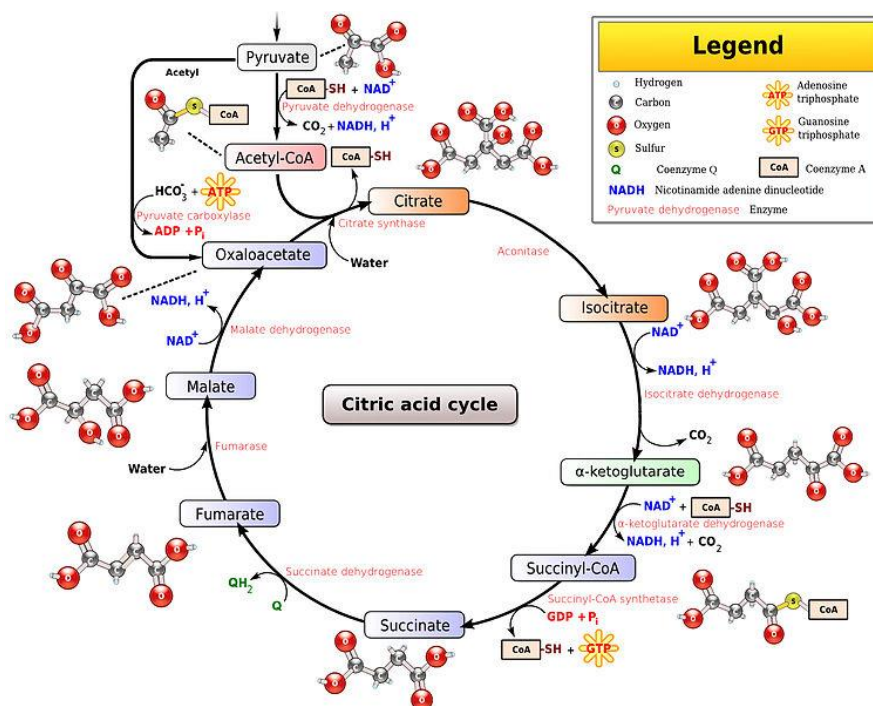


Figure 3: The Citric Acid Cycle (25)

1.1.8 The Electron Transport Chain

The electron transport chain (ETC) is one of the body's main sources of ATP synthesis. Following the glycolysis and the citric acid cycle, the ETC is the last process that is involved in cellular respiration.

Inside the inner membrane of the mitochondria there are five main protein complexes numbered I, II, III, IV and V that all play a part in the ETC along with the electron transporters ubiquinone and cytochrome c. (26)

NADH and FADH₂ are the two common electron carriers which, by being oxidated, give their electrons to complex I and complex II initiating the start of the ETC. Once NADH and FADH₂ have passed off their electrons to each of their respective complexes they are oxidized into NAD⁺ and FAD⁺.

The electrons given up by NADH and FADH₂ are then passed along from complex to complex in a chain of events that create energy. The energy produced from the moving electrons is utilized to drive a hydrogen pump, which in turn moves hydrogen ions into the intermembrane space creating a hydrogen ion gradient between the matrix and the intermembrane space (Figure 4).

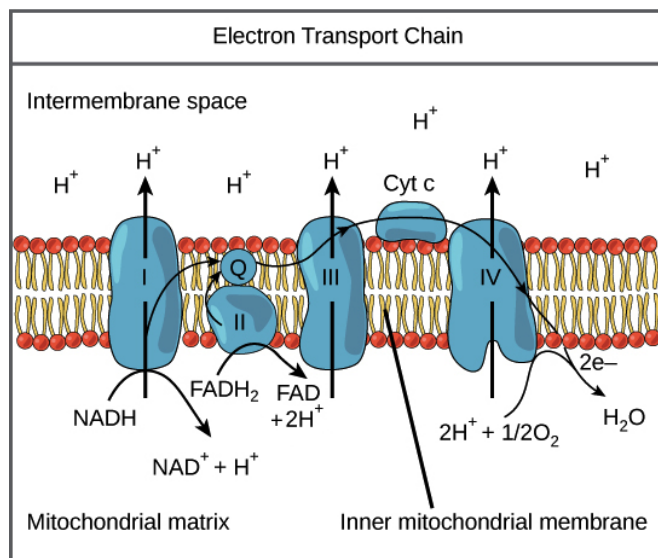


Figure 4: The Electron Transport Chain (27)

The hydrogen ions are capable of moving back into the matrix through complex V (ATP synthase) in a process that creates ATP though combining PO₄³⁻ and adenosine diphosphate

(ADP). The ETC has a negative feedback regulation which ensures that more ADP is utilized by ATP synthase to create ATP when ADP is plentiful, and the process is slowed down if the availability of ADP is scarce. (28)

Due to a lack of efficiency, electron- and proton leaks in the ETC may occur. The O₂ should function as an electron acceptor and through intermediary steps the electrons cause a reduction of O₂ to H₂O, but that is not always the case. In fact, many of the leaking electrons will react with oxygen in different ways, creating reactive oxygen species (ROS). The ROS will get involved with several different pathways, affecting cell death, proliferation, and survival. Normal cells achieve a homeostatic balance regarding the ROS, keeping their population to controlled levels. Cancer cells, however, alter the ETC in ways that create more electron leaks, thus increasing the presence of ROS and upsetting the homeostatic balance. The cancer cells then utilize oncogenic pathways that can take advantage of the increased presence of ROS to create a vicious cycle that allows the cancer cells to proliferate at the expense of normal cells, enhancing tumorigenesis. (29)

1.1.9 mTOR pathway

The mammalian target of rapamycin (mTOR) pathway is involved in multiple signalling pathways. Under normal activation, the mTOR functions as a regulator for cell proliferation, but it also plays a key role in tumor development through tumorigenesis that affects cell's proliferation, metabolic regulation and cell survival.

mTOR contains two complexes: mammalian target of rapamycin complex 1 (mTORC1) and mammalian target of rapamycin complex 2 (mTORC2). While mTORC1 plays a role in promoting both cell proliferation, regulation of metabolism, and catabolic activity if there is energy shortage, mTORC2 also controls proliferation and cell survival. (30)

Among other pathways, the mTOR pathway is involved in both the phosphoinositide-3-kinase (PI3K)/AKT pathway and LKB1/adenosine 5'-monophosphate-activated protein kinase (AMPK) pathway.

The mTOR pathway is linked to conditions like cancer and insulin resistance, and is known to play a significant role in tumorigenesis. Overactivation of the AKT/mTOR pathway is linked to the presence of tumors. Due to the connections found between the mTOR pathway and the development of tumors, inhibition of the mTOR pathway is of large interest when it comes to targeted cancer treatment. (31)

1.1.10 Protein kinase B / Akt

Akt is a gene coding for Akt proteins, and is linked to the development of cancers. The Akt1 protein can be activated by insulin (32) and through phosphorylation by phosphoinositide 3-kinase (PI3K). It can also be deactivated by dephosphorylation by protein phosphatases (33) like the caspase-9. PTEN phosphatase is a main deactivator of Akt making it a tumor suppressor.

The phosphorylated version of Akt is called the p-Akt, and its presence is related to poor prognosis in cancer patients. (34) The Akt1 protein can be phosphorylated at different sites and both threonine residue 308 and serine residue 473 need to be phosphorylated to achieve full activation of the Akt1 protein. (33)

The protein phosphatases mentioned above can dephosphorylate both Akt and phosphatidylinositol 3,4,5-trisphosphate (PIP3). The dephosphorylation of PIP3 will have an inhibitory effect on availability of Akt proteins in the membrane. (33) Phosphorylated Akt1 proteins can inhibit apoptosis, and the PI3K/Akt pathway plays a significant role in tumor progression. Especially in colorectal cancer, changes in the hyperactivation of the PI3K/Akt pathway are often seen in the form of IGF2 overexpression, PIK3CA mutations and PTEN mutations and deletions. (35)

Hyperactivation of Akt/PI3K is a common trait in most tumors and the Akt/PI3K pathway plays a role in multiple pathways, such as the mTOR pathway, where it directly phosphorylates mTOR and causes mTOR activation by inactivating tuberin which is an inhibitor of mTOR. Due to the Akt/PI3K impact seen on cell proliferation, metabolism and cell survival, (36) it can be a target for cancer therapy. The activation of Akt proteins in cells can be measured using specific antibodies such as the Phospho-Akt (Ser473) antibody. This antibody is specific to the phosphorylation that occurs at the Ser473 residue and will only detect Akt1, Akt2 and Akt3 proteins who carry this protein expression. (32) The results of antibody treatment to detect certain protein expressions in cells can be measured by FLOW cytometry.

The activation of Akt can be therapeutically impacted using medication, one of which is metformin. Metformin will inhibit the Akt activation both through phosphorylating IRS-1 at Ser789, which will inhibit Akt activation, (37) and through its effectiveness in insulin reduction making it an interesting topic in cancer prevention and treatment.

DCA has also given indications to be effective in inhibiting Akt activation by upregulating PTEN expression. It has also been shown that under certain conditions, the treatment of colorectal cancer cells with DCA reduced chemoresistance by manipulating the mTOR pathway. (38)

1.1.11 AMP-activated protein kinase (AMPK)

AMPK plays a role in energy homeostasis and through sensing the AMP:ATP ratio. (39) AMPK can both activate catabolic pathways that synthesize ATP, and shut down processes that require ATP consumption, therefore inhibiting proliferation. When the ATP availability is low, AMPK will be activated. The activation of AMPK will stimulate oxidative metabolism. (39) The activation of AMPK shown in Figure 5 can be facilitated by kinase LKB1, increase in intracellular Ca^{2+} , glucose starvation, the AMP:ATP and ADP:ATP ratio and certain DNA damages. (39)

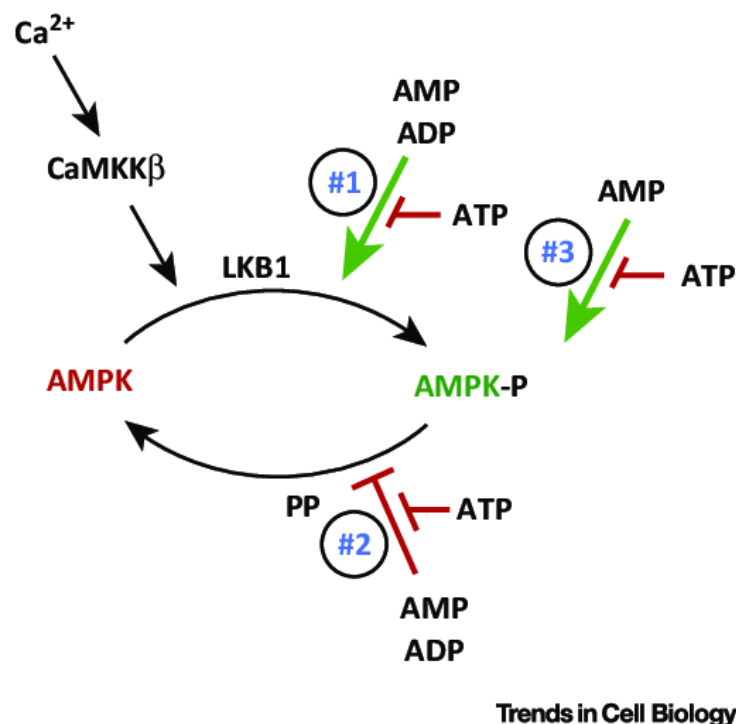


Figure 5: Activation of AMPK (40)

AMPK has a complex role in the development of tumors, and it can function both as a tumor suppressor and as a tumor promotor. It has been hypothesized that the increase in tumorigenesis and viability in cancerous cells caused by AMPK is linked to stress protection for the cancerous cell. (39)

Due to the complex mechanisms of AMPK, both AMPK activators and AMPK inhibitors could prove beneficial to a patient, depending on the specific case and the cancer development. (39), (41)

One medication known to affect the activation of AMPK is the antidiabetic drug metformin. Metformin functions as an AMPK activator and long term use of the drug is linked to less

likelihood of tumor development. (41) Metformin inhibits complex I in the mitochondrial respiratory chain and the mitochondrial ATP synthase leading to an increase in both ADP: ATP and AMP: ATP ratios. (39)

Additionally, DCA has been linked to the reduction of chemoresistance in cancer cells by upregulating the activation of AMPK. (42) The activation of AMPK can be measured using the Phospho-AMPK α (Thr172) Antibody. This antibody will only detect AMPK α when it has been phosphorylated at threonine 172. (43)

1.1.12 The Warburg Effect

Cancer cells tend to carry changes that effect their metabolism. These changes often contribute significantly to the formation and development of tumors. One such effect is the Warburg effect.

Otto Warburg discovered that glucose fermentation occurred through the glycolytic pathway, even when oxygen was available. This process is termed the Warburg effect or aerobic glycolysis. (24)

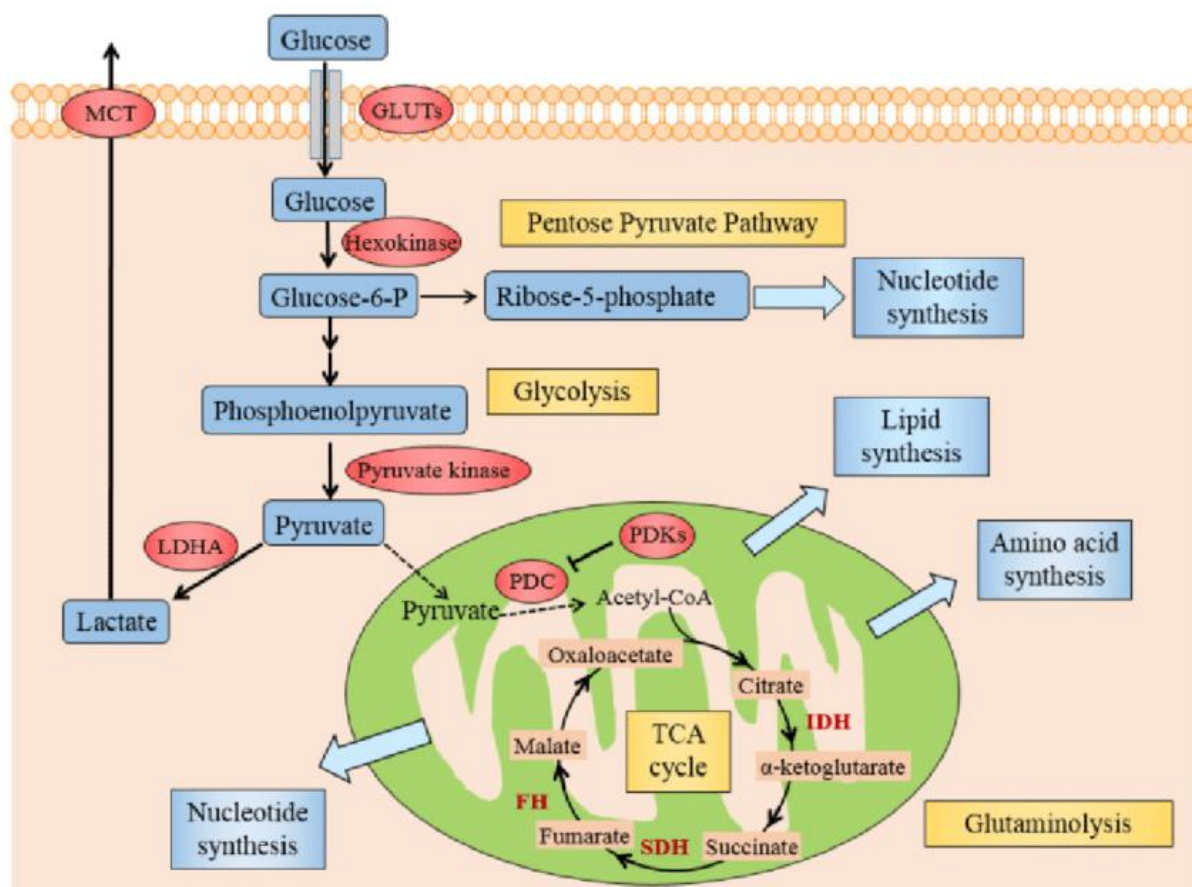


Figure 6: The Warburg Effect in Cancer Cells (44)

The Warburg effect is the ability of cancerous cells to increase the glycolytic flux by reverting to using aerobic glycolysis for its main ATP production rather than using mitochondrial oxidative phosphorylation like a normal cell would in the presence of oxygen. For a normally differentiated cell, glycolysis is an unfavorable and ineffective way to produce energy. Tumor cells however have a deregulated glucose metabolism, meaning they can efficiently create ATP and synthesize cellular ingredients by utilizing glucose-derived carbons which

supports cell proliferation, invasiveness, and creating a higher immunity against radiation therapy. (24)

Many ways have been identified to therapeutically attempt to restore the regulation of the glucose metabolism, using approaches that range from master regulators that control the glucose metabolism such as (hypoxia inducible factor [HIF]-1 α , c-Myc) to using key enzymes to control the rate limiting steps in the glycolytic pathways. (24)

1.2 Thesis Introduction

1.2.1 Problem Statement

One of the challenges in cancer therapy is the metabolic abilities of cancer cells. Two colorectal cell lines will be treated using the two metabolic drugs: metformin and dichloroacetate. These drugs have the opposite effect of each other. Metformin inhibits the electron transport chain, forcing the cells to go back to using glycolysis and therefore limiting the mitochondrial metabolism.

On the other hand, DCA was recently shown to be able to mitigate the Warburg effect in cancer cells by triggering a metabolic switch from glycolysis to oxidative phosphorylation in mitochondria, which was not an effect observed in normal cells. Essentially DCA can increase the amount of pyruvate going into the TCA cycle as opposed to that converted into lactate. (45)

Both drugs will be tested on cell line HCT116 and SW948 to measure their toxicity and the role they play in affecting key signaling pathways. The PI3K-AKT-mTOR pathway will be monitored using flow cytometry and fluorescently labelled antibodies. The project aims to discover and quantify the effects of treatments with metformin and dichloroacetate in different concentrations, combinations, and time frames.

1.2.2 Colorectal Cancer Cells

Colon cancer, or colorectal cancer (CRC), is the third most occurring type of cancer in both men and women in the United States, and around 5% of the average individual has a life-time risk of developing CRC. (46)

CRC most commonly affects older individuals and first establish itself as benign polyps in the interior of the colon through genetic modifications and transformation of normal colonic epithelium (46), (47) Adenomatous polyps generate minor symptoms and thus frequently develop into malignant tumors before being identified. Factors related to age, family history of CRC, and lifestyle increase the risk of developing CRC. Healthy lifestyle changes or certain medication for higher risk patients can reduce the risk of, or prevent, the formation of polyps. (47)

SW948 [SW-948] (ATCC® CCL-237™) is a cell line harvested from colon tissue in an elderly female patient diagnosed with Dukes' type C, grade III colorectal adenocarcinoma. HCT116 (ECACC 91091005) is a cell line isolated from colon tissue in a male patient diagnosed with colonic adenocarcinoma.

The cell lines are intended for research use only, and not therapeutic or diagnostic use for any animal or human. Both cell lines have mutations in the PIK3CA gene. PIK3CA provides instructions for the construction of a subunit in the phosphatidylinositol 3-kinase (PI3K) enzyme. (48)

1.2.3 Metformin and Dichloroacetate

Metformin (bimethylbiguanide) belongs in a class of drugs named biguanides and is today used as a medication to treat type-II diabetes by controlling the amount of glucose in the blood and increasing the body's response to insulin. (49)

It is suggested that metformin reduces tumor growth by two mechanisms; by decreasing the level of circulating insulin, which is a known cancer cell mitogen, and by inhibiting the mitochondrial complex 1. (50)

The group of Xavier Leverve was the first to report the effects of metformin on the mitochondrial metabolism on hepatocytes in rats in the beginning of 2000. They proved that metformin selectively inhibits the mitochondrial respiratory-chain complex 1 in the electron transport chain, and consequently diminish NADH oxidation, decrease the proton gradient across the inner mitochondrial membrane, and reduce the rate of oxygen consumption. (51)

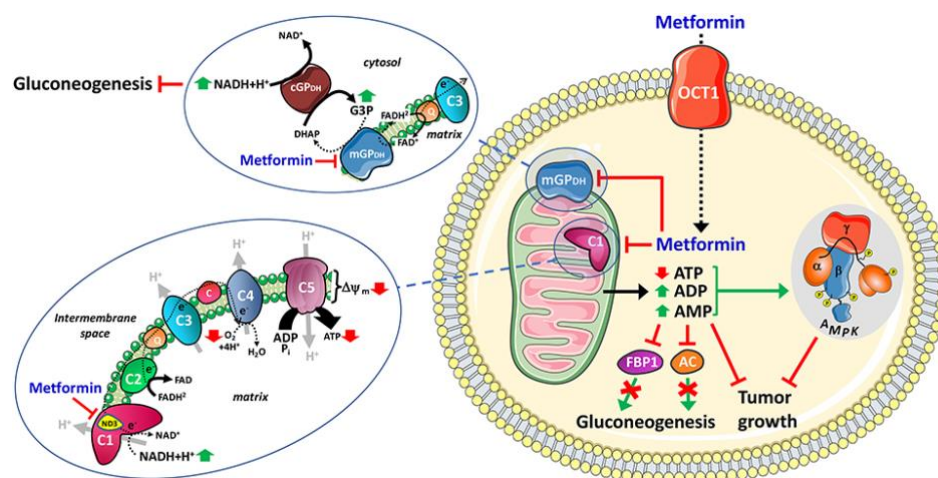


Figure 7: The mechanism of action for Metformin

By the disruption of mitochondrial respiratory-chain complex 1, metformin consequently activates adenosine monophosphate-activated protein kinase (AMPK), an enzyme controlling cell survival, and a mediator of cell activation and metabolism, which leads to an increased AMP:ATP ratio. <https://www.ncbi.nlm.nih.gov/pmc/articles/PMC3224599/>

Dichloroacetate (DCA) is currently used to treat diabetes mellitus, lipid and lipoprotein disorders, pulmonary arterial hypertension, and acquired and congenital lactic acidosis. Recent studies have shown promising effects of DCA, and DCA derivatives, for tumor treatment for its ability to modify carbohydrate metabolism, specifically the mitochondrial pyruvate dehydrogenase complex (PDC). PDC is a multienzyme complex positioned in the mitochondrial matrix linking glycolysis to the tricarboxylic acid (TCA) cycle and oxidative phosphorylation. DCA has an inhibiting effect on pyruvate dehydrogenase kinase (PDK) and as a consequence reactivates PDC and oxidative phosphorylation which leads to a decline in hypoxia-inducible factor 1 alpha (HIF1 α) expression. HIF1 α is a major driver for aerobic glycolysis in cancer cells and a transcriptional activator for glycolytic enzymes and all PDKs.

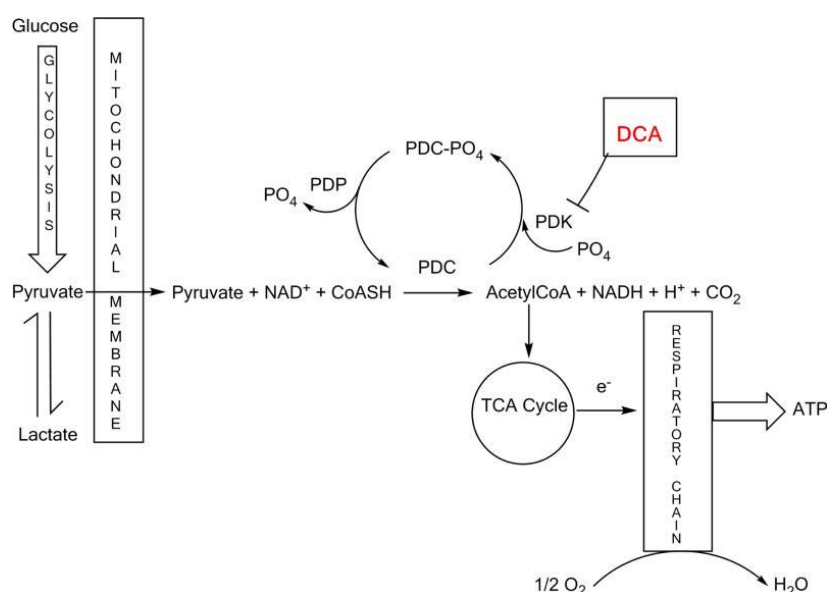


Figure 8: The mechanism of action for Dichloroacetate (DCA) (52)

According to the paper “Targeting Glucose Metabolism of Cancer Cells with Dichloroacetate to Radiosensitizer High-Grade Gliomas” published by Int J Mol Sci, the specialized glucose metabolism can be targeted to increase the radiosensitivity of the High-Grade Glioma (HGG) cells. By treating the HGG cells with DCA, the goal is to activate mitochondrial oxidative phosphorylation by inhibiting pyruvate dehydrogenase kinases (PDK). Inhibiting the PDK will leave the pyruvate dehydrogenase (PDH) unphosphorylated and thus keeping the PDH in its active form. This will block the glycolytic pathway forcing the cell back to utilizing the mitochondrial oxidative phosphorylation as its main metabolic pathway. (24)

1.3 Introduction to Instruments and Assays

1.3.1 Muse® Cell Analyzer, Count and viability assay

The Muse® Cell Analyzer is a fluorescent detecting instrument capable of performing quantitative cellular assays. Among the assays the analyzer can perform are «Muse® Count & Viability Assay» which basically determines both total cell count and separates between viable and dead cells, giving both the percentage and actual numbers. (53)

This assay was used frequently during our project, and it provided information about viability percentage as well as the number of cells/mL. The instrument is capable of quantifying the cells very accurately using fluorescent signals. The machine can distinguish between cell size and will treat small cells/debris as dead cells. This limit can however be manually adjusted by the user by dragging a red line across the screen including or excluding cell colonies. (53)

Figure 9 illustrates an example of a count and viability report using the Muse® Cell Analyzer. One can manually drag the threshold for the debris in both the population- and viability profile before the quantitative results are generated. The results are given in viable cells/mL as well as a viability percentage.

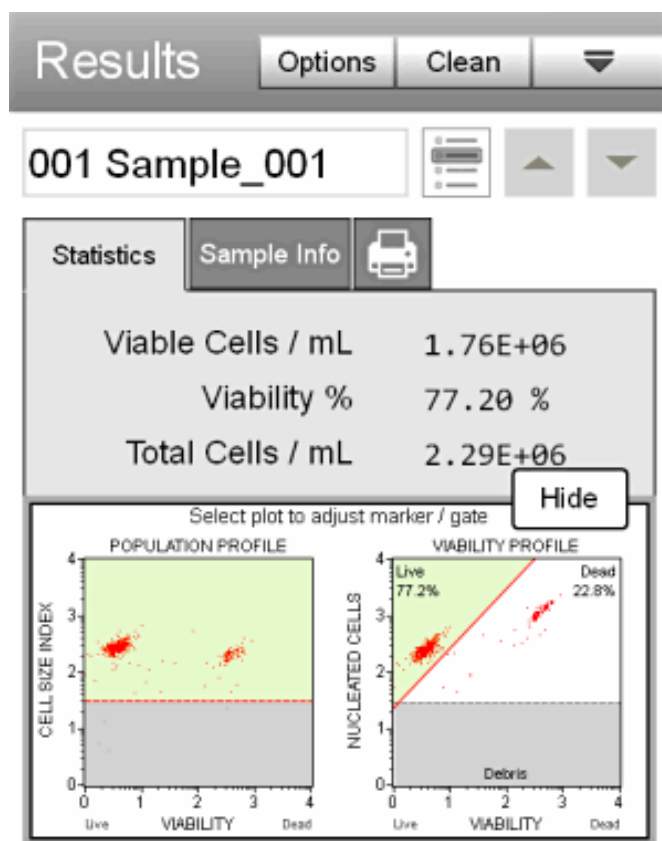


Figure 9: Example of results from Muse® Cell Analyzer count and viability assay. (54)

1.3.2 Spectrophotometer

A spectrophotometer emits laser to quantify the amount of light that is reflected or absorbed by a substance. Each chemical substance has its own reflection or emission wavelength. The spectrophotometer is able to evaluate emission and wavelengths with high precision making it a popular tool for work within fields like clinical diagnostics, biomedical research and to measure how much of a specific substance is present. (55)

The spectrometer and the photometer make up what is called the spectrophotometer. These two components each have their own function and where the spectrometer creates, disperses and measures light. The photometer measures the intensity of this light using a photoelectric detector. A simple drawing of the concept is figured below in Figure 10.

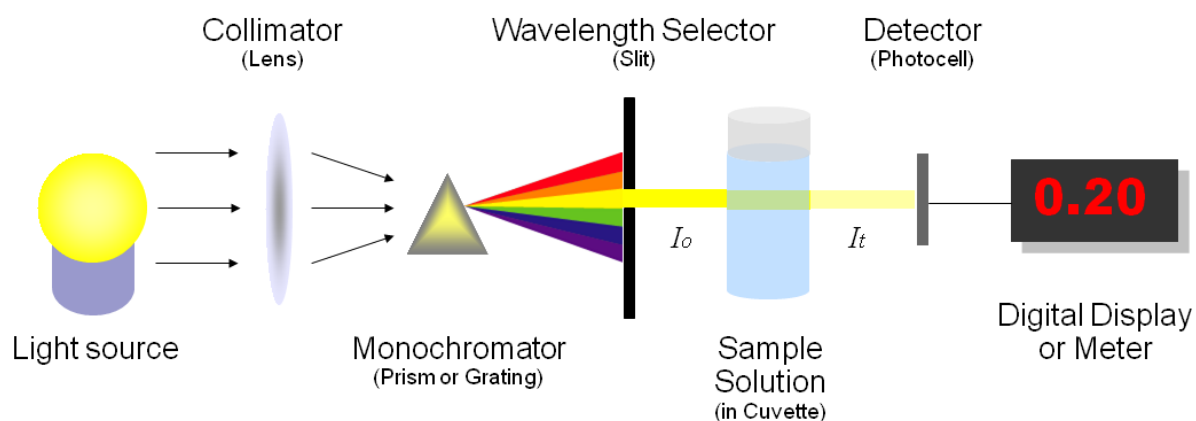


Figure 10: Basic structure of spectrophotometers (55)

During this experiment spectrophotometer has been frequently used for the detection of fluorescence and absorbance to determine the cell viability and activity after medication treatment.

1.3.3 AlamarBlue Assay

AlamarBlue Cell Viability Reagent is a dye used for the quantification of cellular metabolic activity which in turn can determine the concentration of viable cells in a sample. The dye undergoes a redox reaction that changes its color and fluorescent ability after the conversion from oxidized to reduced form. In its oxidized form, the dye projects a blue color and is non-fluorescent. When reduced, due to the viable and actively growing cells, the dye changes to a fluorescent red. This shift can be detected using a fluorescent or absorbance detector.

1.3.4 CCK-8 Proliferation Assay

Cell Counting Kit-8 (CCK-8) uses 2-(2-methoxy-4-nitrophenyl)-3-(4-nitrophenyl)-5-(2,4-disulfophenyl)-2H-tetrazolium (WST-8) and is a convenient quantification method for determining cell viability by utilizing the water-soluble tetrazolium salt which produces an orange formazan dye when reduced in the presence of an electron mediator, 1-Methoxy PMS (1-Methoxy-5-methylphenazinium methyl sulfate). CCK-8 / WST-8 is reduced by cell dehydrogenases to give the orange formazan product which is soluble in the tissue cell medium. The amount the formazan dye produced is proportional to the number of viable cells, and the absorbance can be measured using a microplate reader. The detection sensitivity is higher than any other tetrazolium salts. (56)

1.3.5 Flow Cytometry

Flow cytometry is used for the analysis of physical and chemical characteristic of a single cell suspension injected into a flow cytometer instrument. The technique is used to quickly quantify characteristics of cells and particles. It can process great amounts of cells in a matter of seconds, some can analyze as many as 32 parameters at 200,000 events/s, 100,000 cells/s can be arranged in a 6-way sorting. Flow can also be used to separate sub populations. (57)

By injecting a heterogenous population of cells the flow cytometer will create a flow of cells on a one-by-one basis passing single cells through a laser beam. The cell will make the light scatter, the scattered pattern can reveal characteristics of the cell such as its components and size. Flow cytometry have a wide range usage and are utilized for cell counting, cell sorting, microorganism detecting, fluorescent protein detection and so on. (57)

During our project, we will measure the protein expression of four different proteins: protein kinase B, also known as Akt, plus its phosphorylated hence active form p-Akt, and adenosine monophosphate-activated protein kinase (AMPK), plus its phosphorylated active form p-AMPK. Both proteins are essential for glucose homeostasis.

2 Chemicals, Equipment, and Instruments

2.1 Chemicals and Reagents

Table 1: List of hazardous chemicals related to our project and their hazard/precaution classifications.

Chemical:	Caution: *
HyClone™ Penicillin-Streptomycin Solution Cytiva Norway	<u>Hazard:</u> H315, H317, H319, H334, H335. <u>Precaution:</u>
ICF Instrument Cleaning Fluid Luminex Corporation	<u>Hazard:</u> H319, H315. <u>Precaution:</u> P280, P264, P305+P351+P338
Methanol Merck Life Science AS/Sigma Aldrich Norway AS	<u>Hazard:</u> H225, H301+H311+H331, H370. <u>Precaution:</u> P210, P260, P280, P301+P310, P311.
Paraformaldehyde Merck Life Science AS/Sigma Aldrich Norway AS	<u>Hazard:</u> H301+H332, H315, H317, H318, H335, H341, H350 <u>Precaution:</u> P201, P280, P301+P312+P330, P304+P340+P312, P305+P351+P338+P310, P308+P313
Sodium dichloroacetate Merck Life Science AS/Sigma Aldrich Norway AS	<u>Hazard:</u> H315, H319, H335, H351 <u>Precaution:</u> P302+P352, P305+P351+P338, P308+P313
Trypan Blue 0.4% in aqueous solution Cell Culture Reagent VWR International AS, part of Avantor	<u>Hazard:</u> H350. <u>Precaution:</u> P201, P280, P308+P313.
Metformin	*Information not available
Dichloroacetate	*Information not available
Antibody Dilution Buffer	*Information not available

Table 2: List of non-hazardous chemicals related to our project.

Chemical:
D-(+)-Glucose , Merck Life Science AS/Sigma Aldrich Norway AS
Fetal Bovine Serum, Biowest SAS
L-Glutamine, 200 mM solution, Corning
Muse® Count & Viability Kit, Merck KGaA
Phosphate Buffered Saline (PBS) Tablets, Life Technologies Europe BV
Trypsin-EDTA solution , Merck Life Science AS/Sigma Aldrich Norway AS
CCK-8 , *Information not available

2.2 Instruments and Equipment

Table 3: Listing of every instrument used in our project and their description.

Instrument:	Description:
Muse® Cell Analyzer	Instrument for miniaturized fluorescence detection and microcapillary cytometry in single cell analysis.
SpectraMax Paradigm Multi-Mode Microplate Reader	Microplate Reader for detecting absorbance, fluorescence, luminescence, FP, TRF, FRET, western blot, and cell imaging.
SoftMax Pro Software	Software that provides advanced data analysis.
Cytoflex B3 R1 V0	Instrument from Beckman Coulter created for flow cytometry
Kubota2800	Centrifuge

Table 4: Listing of equipment used in our project and their description.

Equipment:	Description:
T75 Tissue Culture Flask	Specialized flasks for cell cultivation
T150 Tissue Culture Flask	Specialized flasks for cell cultivation
96-well plate	Well plates used during cultivation and treatment

2.3 Experiment Conditions

Viable colorectal cancer cells were handled in a biosafety level 2 (BSL-2) cell lab. The cells were only handled inside a ventilated biosafety cabinet with an integrated UV-function and/or incubated in a MCIO-18AIC CO₂ incubator. The cells have also been relocated to other sites within the building for cell counting by Muse® Cell Analyzer and analysis by SprectraMax Paradigm.

2.3.1 Preparation of Aseptic Working Environment

To enter the biosafety level-2 (BSL-2) cell lab protective shoe covers and coats has been worn at all times. Both shoe covers and coats were kept in a negative air pressure pre-room. There are two doors entering this room, and only one door could be open at any given time. In this room there is a clearly marked line on the floor, this line may only be crossed wearing protective shoe covers. Once in the lab gloves and facial masks have been worn, the gloves have been disinfected using 70% ethanol before touching a new item.

Biosafety cabinets have been cleaned using 70% ethanol before and after use, and every item brought into the cabinet has been thoroughly sprayed down before it's taken into the cabinet. The cabinet has been left for 30 minutes with UV light after use. Sterile equipment such as pipette tips, bottles, and containers have been autoclaved, and only opened inside the biosafety cabinet to avoid contamination.

2.3.2 Temperature and Humidity Conditions

The colorectal cancer cells have been stored in tissue culture flasks, both 75- and 150 cm², depending on the requirement and necessity for the passage, inside an incubator set to 37°C and 5% CO₂ which simulates the physiological conditions *in vivo*. The tissue culture flasks have been removed from the incubator to the microscope or the biosafety cabinet for the splitting procedure or medium renewal. The appropriate medium and the components needed for subculturing were prewarmed to 37 °C in a water bath.

3 Procedures

3.1 Preparation

3.1.1 Cell Growth Medium

The growth medium used in our project aimed to achieve a similar environment as the one found *in vivo*, and the final glucose concentration created was 5 mM.

The cell growth medium consisted of the following components:

- 500 mL Dulbecco's modification of eagle's medium.
- 5 mL glutamine 200 mM
- 50 mL Fetal base serum (FBS)
- 5 mL pen-strep 1 M, (mixture of penicillin G and streptomycin)
- 2.5 mL 1 M glucose

The medium has been stored in the fridge in the original 500 mL bottle from the Dulbecco's medium. From this container the medium that was needed has been aliquoted into 50 mL tubes. To mimic the natural *in vivo* environment, these tubes have been placed in a water bath until they reached the temperature of 37°C before the medium has been in contact with the cells. To keep the medium as sterile as possible, all aliquotation and handling happened solely in the biosafety cabinets. Separate tubes were made for each cell line. The tubes were not reused, instead new tubes were made once the previous ones were emptied. The penicillin added had the purpose of keeping bacterial growth at a minimum as to not contaminate the medium and thus affecting the colorectal cancer cells.

3.1.2 Maintenance of Colorectal Cancer Cells

The colorectal cancer cells have been stored in a cryotube, with appropriate cell culture medium, inside a tank containing liquid nitrogen.

Cell growth medium have been replaced every 2-3 days to maintain and promote growth to the colorectal cancer cells. Old medium was removed and replaced with an equivalent amount of prewarmed (37°C) cell growth medium to the cell tissue flask.

The colorectal cancer cells have been subcultivated based on the individual cell line's confluency rate, although roughly every 2-3 days. All the necessary reagents for the splitting procedure, e.g., cell growth medium, PBS, and trypsin, were prewarmed in a water bath to a temperature of 37°C before the outside of the containers were sterilized with 70% ethanol and inserted into the biosafety cabinet. The cell growth medium in the tissue culture flask was removed and the adherent cells were rinsed with either 5.0- or 10.0 mL PBS for 75- or 150 cm² tissue cell flasks, respectively. 2- or 4 mL trypsin was then added, and the cells were incubated until they lost its adherence. The effect of trypsin was neutralized by an appropriate volume of complete cell growth medium, either 3- or 6 mL, depending on the size of the tissue cell flask. A varying amount of cell suspension was added to a new tissue cell flask, depending on the necessary subcultivation ratio, and cell growth medium was added to a total volume of either 10- or 20 mL.

SW948 had a tendency to form clusters after reaching a higher percentage of confluency. Because of this trait, it was essential to both homogenize by a pipette, and strain the cell suspension through a 100 nm pore strainer before measuring the cell concentration by Muse® Cell Analyzer for a more accurate result.

3.1.3 Preparation of medication

Dichloroacetate (DCA) and metformin were the two medications used to treat the colorectal cancer cells during this experiment. Both medications were used in concentrations of 0.25-, 0.5-, 1-, 3-, and 6 mM. The cells were treated for periods of 24- and 48 hours, both with each medication separately as well as with medication combinations.

In addition to treating the cells with metformin and DCA, there were a set of control cells where only medium was added and on some experiments a control group was also made by adding water instead of medication to rule out any effect the dilution of the medium might have created.

The concentrations needed to create 100 mM stock solutions were calculated using the following equation:

Equation 1

$$X = C_{stock} * V_{target} * Mw_{med}$$

The molecular weights on DCA and metformin are 150,92g/mol and 165,62g/mol respectively. While the goal was to create 10 mL of 100 mM solution, the ultimate mass of each medication was calculated as follows:

$$X_{DCA} = 0.1M * 10mL * 150,92 \frac{g}{mol} = 150,92mg$$

$$X_{met} = 0.1M * 10mL * 165,62 \frac{g}{mol} = 165,62mg$$

A standard stock solution of 100mM DCA was made by mixing 150,92 mg DCA with 10 mL autoclaved water. DCA was weighed on an analytical scale inside a biosafety cabinet, mixed with the water and properly covered before it was taken out of the biosafety cabinet. The solution was then filtered through a syringe filter with a pore size of 0.2 nm before it was ready for use.

Following the same process as described above, a 100 mM metformin stock solution was created by adding 165,62 mg metformin in powder form to 10 mL of autoclaved water.

Both medications were used in concentrations of 0.25-, 0.5-, 1.0-, 3.0-, and 6 mM. The medications were also used in combination with each other as depicted in Table .

Each of these concentrations was created by diluting the standard medicine solutions with complete cell medium to create a total of 2 mL for the desired concentration. The biosafety cabinet and sterile techniques were used during this procedure, and the calculated amount of cell growth medium was aliquoted before the medications were added and the mixture was vortexed.

To calculate the amounts of medium and medications needed for each solution, the following formulas were used.

Equation 2

$$V_{target} = V_{met} + V_{DCA} + V_{medium} = 2ml$$

$$V_{met} = \frac{C_{t_{met}} * V_{target}}{C_{met}}$$

$$V_{DCA} = \frac{C_{t_{DCA}} * V_{target}}{C_{DCA}}$$

Equation 3

$$C_{met} = C_{DCA} = 0,1M \text{ (concentration of the stock solution)}$$

The solution for the control group treated with water was calculated based on the highest combination treatment; thus, using the volumes from 6 mM metformin and 6 mM DCA in the form of water. Therefore, a total of 480 μ L water were added to 1520 μ L medium.

3.2 Initial testing

3.2.1 Muse Cell Count and Viability Assay

To perform the count and viability assay, 250 μL Muse™ Count & Viability Reagent were preheated to room temperature. 50 μL of testing compound was added to the reagent, vortexed and left to incubate for five minutes in room temperature. The Muse™ Count & Viability Reagent is a light sensitive compound and were therefore kept under dark conditions as far as possible to avoid contamination of the results. Once the incubation was complete, the assay was run on the Muse® Cell Analyzer, using Muse® Count & Viability Assay. The results were noted, interpreted, and used for further analysis on the cells.

3.2.2 AlamarBlue Assay

The viable cell count per mL was firstly determined by Muse® Cell Analyzer and testing compound was prepared based on 1) alamarBlue assay and 2) alamarBlue treatment assay. The standard alamarBlue assay with untreated colorectal cancer cells was performed for the purpose of finding the most suitable cell density for the alamarBlue and CCK-8 treatment assays.

1) The volume of cell suspension and cell growth medium for each individual well was calculated based on the following equations:

Equation 4

$$\text{cell suspension (mL)} = \frac{\text{viable cells per well}}{\text{viable cells/mL}}$$

Equation 5

$$\text{cell growth medium} = 200 \mu\text{L} - \text{cell suspension}$$

A 96-well plate was prepared by seeding four parallels of 200 μL /well of ~ 5000 - 30000 viable cells with an interval of 5000. 200 μL /well blank control containing only cell growth medium and 200 μL /well of PBS was also added for the remaining wells as displayed in Table .

The 96-well plate containing testing compound and controls were incubated for 24 hours followed by a renewal of 100 μL cell growth medium and then incubated for another 24 hours.

20 μL of resazurin, making up 10% (v/v) of the total volume, was added to each well containing testing compound and controls, carefully shaken for a homogenous solution, and incubated for 4 hours. Fluorescence was measured by SpectraMax Paradigm at 540 nm excitation wavelength and 590 nm emission wavelength and analyzed using SoftMax Pro 6 Software.

2) The volume of cell suspension and cell growth medium was determined based on Equation 4 and Equation 5 as described in 1). A 96-well plate was prepared by seeding 11*4 parallels, four parallels of each concentration of metformin and DCA and four parallels of untreated colorectal cancer cells, with a volume of 200 μL /well of ~ 10000 - and ~ 15000 viable cells for

HCT116 and SW948, respectively. 4 parallels of 200 μL /well blank control containing only cell growth medium and 200 μL /well of PBS for the remaining wells was also added as displayed in Table .

After incubating the 96-well plate for 24 hours, 100 μL of medium was removed from each individual well excluding the blank controls and PBS, and 100 μL of 0.25-, 0.5-, 1.0-, 3.0-, and 6 mM metformin and DCA were added according to the setup in

Table . In the 0 mM wells, 100 μ L of cell growth medium was added. The 96-well plate, now containing treated colorectal cancer cells, was further incubated for either 24- or 48 hours.

20 μ L of resazurin, making up 10% (v/v) of the total volume, was added to each well containing testing compound and controls, carefully shaken for a homologous solution, and incubated for 4 hours. Fluorescence was measured by SpectraMax Paradigm at 540 nm excitation wavelength and 590 nm emission wavelength and analyzed using SoftMax Pro 6 Software.

3.2.3 CCK-8 Proliferation Assay

The viable cell count per mL was firstly determined by Muse® Cell Analyzer, and the volume of cell suspension and cell growth medium, for either ~10000- or ~15000 viable cells for HCT116 and SW948 respectively, was calculated based on Equation 4 and Equation 5.

The same protocol as the 2) alamarBlue treatment assay as described in 3.2.1 were executed for the CCK-8 proliferation assay, including the setup for the 96-well plate as depicted in

Table

After the 96-well plate containing the treated cells were done incubating for 20- or 44 hours, 100 μ L of medium was removed from all wells except those containing PBS, 10 μ L of CCK-8 was added to each well, making up 10% (v/v) of the total volume. The plate was carefully shaken to create a homologous solution, and further incubated for an additional 4 hours. Absorbance was measured by SpectraMax Paradigm at 450 nm wavelength and analyzed using SoftMax Pro 6 Software.

3.2.4 Combination treatment

Cancer is an extraordinarily complex disease and multiple medications are often used to treat the same patient to target different structures within the tumor cells in question. Combination treatment combining metformin and DCA to treat both cell lines was performed during this experiment to see if and how they impacted the cells and if the combination has an effect on the effectiveness of the medications themselves. However, both medications are metabolic drugs purposed for other medical conditions and neither of the two are approved cancer treatments and are not expected to kill or show excessive impact on the cells.

Before the combination treatment was performed, each drug had been tested individually in various concentrations.

Using the Muse® Cell Analyzer the cell count was determined before the following steps were taken:

- 1) For both cell lines Equation 6 was used to perform calculations on the cell suspension volume needed. The target for the HCT116 cell line was 10000 cells pr well and for the SW948 cell line the target amount was 15000 cells in each well. The total volume in each well with cell suspension and medium combined were 200 μL , the volume medium needed was calculated using Equation 7

Equation 6

$$\text{cell suspension (mL)} = \frac{\text{viable cells per well}}{\text{viable cells/mL}}$$

Equation 7

$$\text{cell growth medium} = 200 \mu\text{L} - \text{cell suspension}$$

- 2) In a 96-well plate the plates outer wells were filled with 200 μL PBS for isolation purposes. The remaining wells were filled with 200 μL cell suspension/medium as calculated in Equation 6 and Equation 7 The only exception being 3-4 blank parallels only containing 200 μL medium the setup is displayed in Table

- 3) The 96-well plate was incubated at 37 °C for 24 hours, after the initial 24-hour incubation period 100 µL of the cell growth medium was removed and 100 µL of medication was added to all wells except the three wells containing the blank. Concentrations of 1 mM, 3 mM, and 6 mM metformin were combined with 1 mM, 3mM, and 6 mM DCA so that all combinations were accounted for. Also, 4 parallels were not treated with medication but received fresh medium. During the experiment, there were used two different setups for the combination treatment. One setup as shown in Table , where there were parallels made as a control group treated with water instead of medication, and one setup where this was not the case, seen in Table 5.
- 4) After the new volume with or without medication was added to the wells, the plate was further incubated. The experiment was performed on incubation periods of 24 and 48 hours. After for 20 – 44 hours incubation the plates were taken out and CCK-8 cell counting kit or alamarBlue reagent were added to the wells in a concentration making up 10% (v/v) of the total volume. The plates were shaken for a homologous solution and further incubated at 37°C for 4 hours. ‘
- 5) Using SpectraMax Paradigm at 540 nm excitation wavelength and 590 nm emission wavelength and analyzed using SoftMax Pro 6 Software the fluorescence was measured.

3.2.5 Flow Cytometry Assay

Viable cell count per mL was firstly determined by Muse® Cell Analyzer, and the volume of cell suspension and cell growth medium, for ~2 000 000 viable cells was calculated using equation 6 and 7. The cells were, preparatory to the flow cytometry protocol, treated with 6 mM of either metformin or DCA for 48 hours in individual T75 cell flasks, plus a flask containing untreated cells as a control, containing ~2 000 000 viable cells per flask. The flow cytometry assay protocol was divided into three distinct steps: Fixation, permeabilization and immunostaining, and was performed in the following fashion:

Fixation:

Cell suspension was centrifuged for a period of 5 minutes at 1000 rpm, and the supernatant was carefully removed. The cells were resuspended in 200 μ L 4% formaldehyde and furthermore vortexed for the purpose of dissolving the pellet to a homogenized solution. Lastly, the cells were fixed at room temperature (20-25 $^{\circ}$ C).

Permeabilization:

The cells were permeabilized by the addition of ice-cold 100% methanol, whilst being vortexed, to a final concentration of 90% methanol, and stored overnight at -20 $^{\circ}$ C.

Immunostaining:

The cells were firstly aliquoted into tubes containing 0,5 mL cell suspension which equaled to 500 000 cells/tube; two parallels for each of the treatments and four controls, where two were marked with secondary antibodies. To remove the methanol, the cells were washed in 1X PBS and supernatant was removed in appropriate waste container. Furthermore, the cells were resuspended in 100 μ L diluted primary antibody, prepared in Antibody Dilution Buffer (ADB) at recommended dilution. The following antibodies were added in individual tubes, one for each treatment:

- a) AKT (pan) (11E7) Rabbit mAb #4685 Ref. number: 10/2017, Lot 6, dilution ratio 1:100
- b) Phospho-Akt (Ser473) Antibody #927 Ref. Number: 03/2017, Lot 14, dilution ratio 1:400
- c) AMPK α (D5A2) Rabbit mAb #5831 Ref. number: 07/2017, Lot 4, dilution ratio 1:100
- d) Phospho-AMPK α (Thr172) (40H9) Rabbit mAb #2535 Ref. number 07/2017, Lot 4, dilution ratio 1:400

The cells were incubated at room temperature for one hour and washed by centrifugation, firstly in 500 μ L ADB and once more with 500 μ L 1X PBS. Supernatant was discarded after each wash. The cells were resuspended in 100 μ L of fluorochrome-conjugated secondary antibody diluted in ADB to a 1:200 ratio, and further incubated for 1 hour at room temperature. The cells were washed in 1X PBS and supernatant was discarded. Lastly, the cells were resuspended in 250 μ L of 1x PBS and analyzed on a flow cytometer.

4 Results

4.1 AlamarBlue

The colorectal cancer cell density for cell lines HCT116 and SW948 have been quantified using Muse® Cell Analyzer to a concentration of ~10000- or ~15000 viable cells/well, respectively. The seeded cells in the 96-well plate have been treated with metformin in various concentrations and incubated for either 20- or 44 hours before resazurin, in a final concentration of 10% per well, was added and incubated for an additional 4 hours. The fluorescence of resazurin was measured by SpectraMax Paradigm at 540 nm excitation wavelength and 590 nm emission wavelength and analyzed using SoftMax Pro 6 Software.

Outlying parallels have firstly been discarded with the use of Dixon's Q-test for the identification of outlying parallels:

$$Q_n = \frac{(x_a - x_b)}{R}$$

Where:

R: the range of all data points

x_a: the suspected outlier

x_b: the data point closest to x_a

We used the Q-test decision level at 90% confidence interval:

Table 5: Threshold values for Dixon's Q-test with a 90% confidence interval. N = number of replicates and Q = the threshold value.

N	3	4	5	6	7	8	9	10
Q	0.94	0.76	0.64	0.56	0.51	0.47	0.44	0.41

The quantitative raw data from the analysis of resazurin of every parallel have firstly been normalized to the blank control by subtraction. The arithmetic means from each passage for both 24- and 48 hours are calculated along with the total arithmetic mean and its S.D. and are represented in appendix 2, Table 6 - Table 13

The data is further normalized to the untreated control using Equation 8, and the results are represented in appendix 2,

Table 14 - Table 21 coupled with the total arithmetic mean and the S.D.

Equation 8

$$\textit{normalization} = \left(\frac{\textit{replicate value}}{\textit{control}} \right) * 100\%$$

4.1.1 AlamarBlue metformin treatment

The following results exhibit the fluorescence value of resazurin from colorectal cancer cells treated with various concentrations of metformin for a period of either 24- or 48 hours. The fluorescence value of the dye is proportional to the viability of the cells.

4.1.2 HCT116 results

Figure 11 (Appendix 2, table 11-12) depicts the fluorescence value of resazurin for the HCT116 cell line after 24 and 48 hours of exposure to metformin. The trend show that the fluorescence decreases with increasing metformin concentrations as well as with longer exposure time.

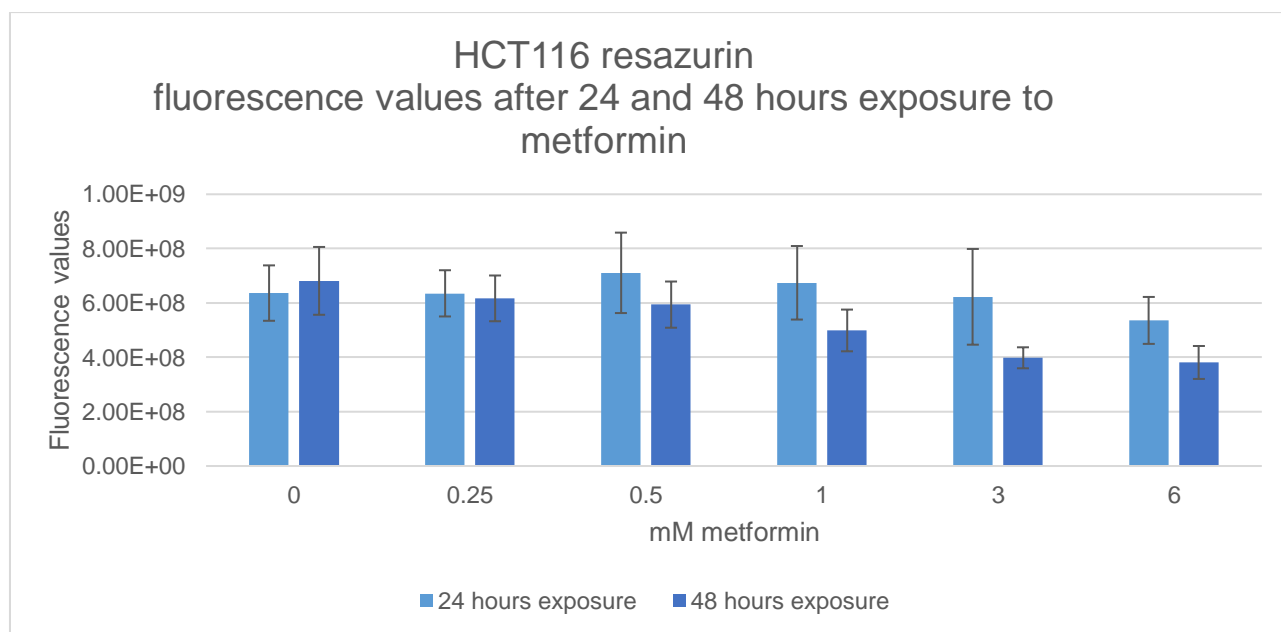


Figure 11: Total arithmetic mean (N=3) and S.D. of resazurin fluorescence values for HCT116 colorectal cancer cells with 24- and 48-hours exposure to different concentrations of metformin.

The results for the normalized values for the HCT116 cell line that have been exposed to resazurin and treated with metformin for 24 and 48 hours are shown in Figure 12 (Appendix 2, table 19-20) the results show a decrease in percentage fluorescence as the concentrations of metformin increase as well as a drop in fluorescence from 24 to 48 hours.

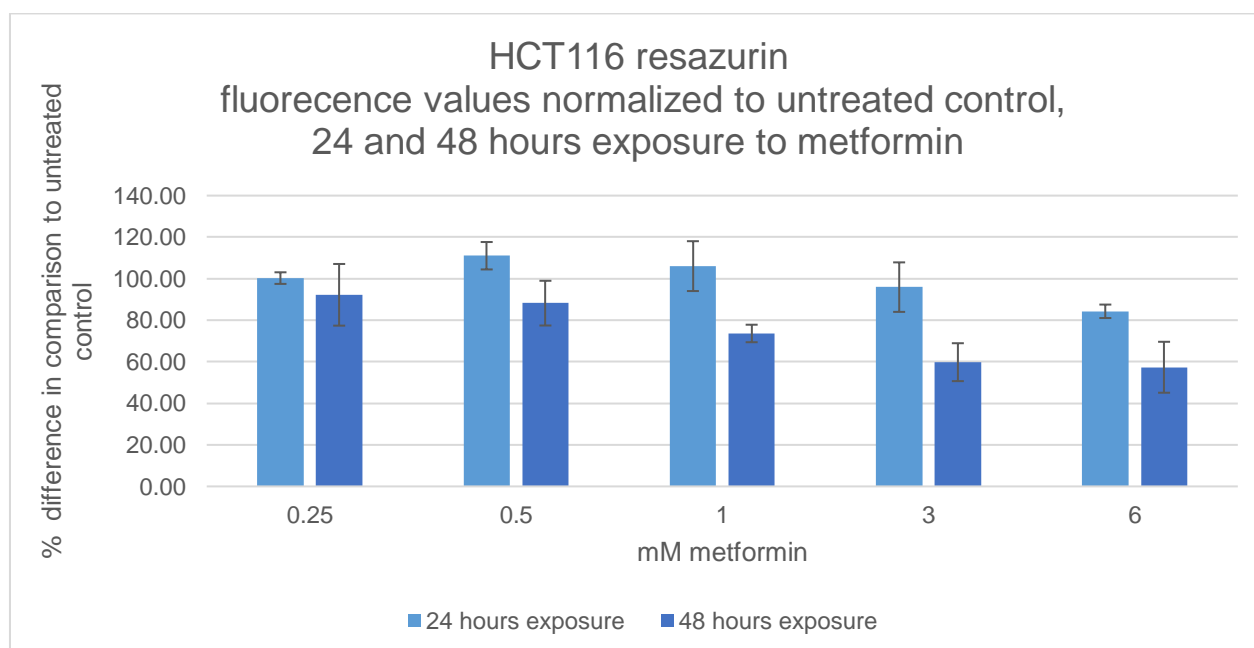


Figure 12: Total arithmetic mean (N=3) and S.D for resazurin fluorescence values normalized to the untreated control of HCT116 cell line with 24- and 48-hours exposure to various metformin concentrations.

4.1.3 SW948 results

The results of 24 hours exposure to metformin using resazurin are seen in Figure 13 (Appendix 2, table 13-14) and have little to no decrease of viability relative to the untreated control (0 mM) for 0.25-, 0.5-, and 1.0 mM. Furthermore, the viability shows a significant decrease for both 3-, and 6 mM metformin. The results of 48 hours exposure to metformin reveal a more obvious decrease correlated to heightened concentration, where 6 mM clearly displays the lowest fluorescence value, and thus the most effective treatment in all.

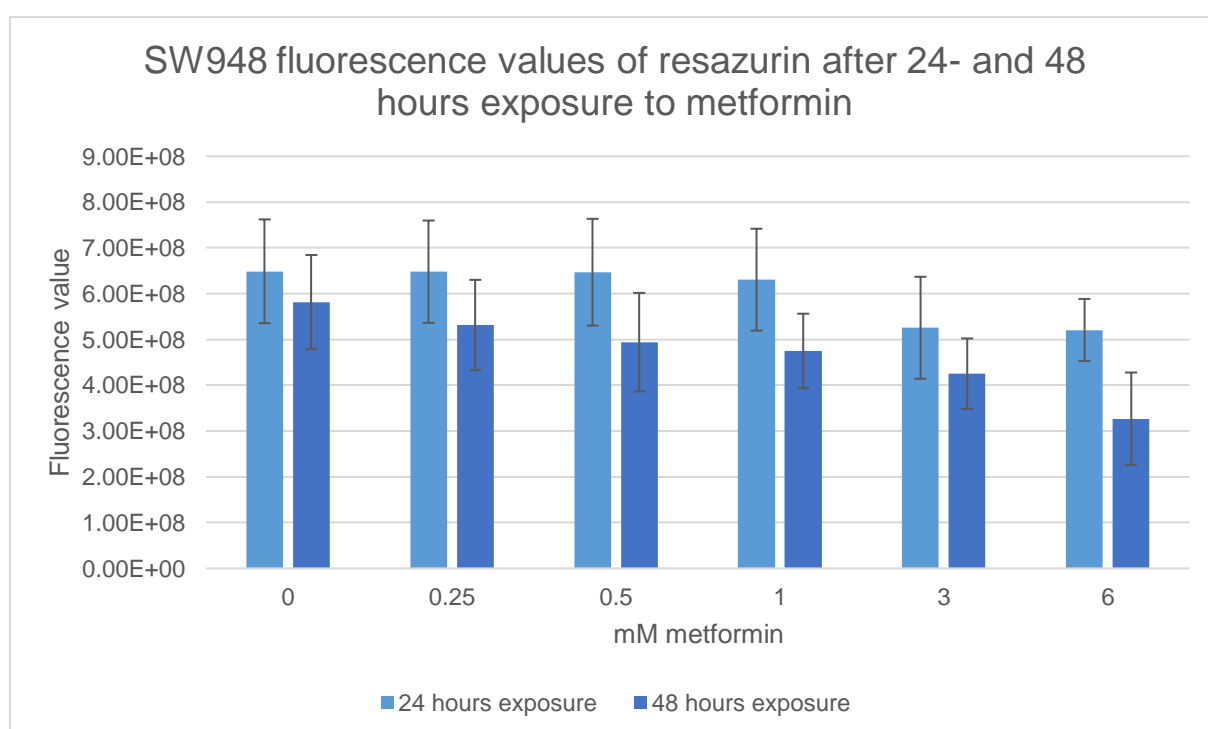


Figure 13: Total arithmetic mean ($N=4$) and S.D. of resazurin fluorescence value from SW948 colorectal cancer cells with 24- and 48 hours treatment with various concentrations of metformin.

Figure 14 (Appendix 2, table 21-22) depicts the normalized total arithmetic mean of all replicates in percentage for both 24- and 48 hours exposure to metformin. The viability only shows a significant decrease for 3- and 6 mM of metformin for the 24-hour exposure, but the S.D. values for these two concentrations have a higher margin in comparison to the three lowest concentrations. For the 48-hour treatment, the values have a higher decrease relative to

the 24 hours treatment for all concentrations. 6 mM metformin after 48 hours has the lowest viability, but the highest S.D.

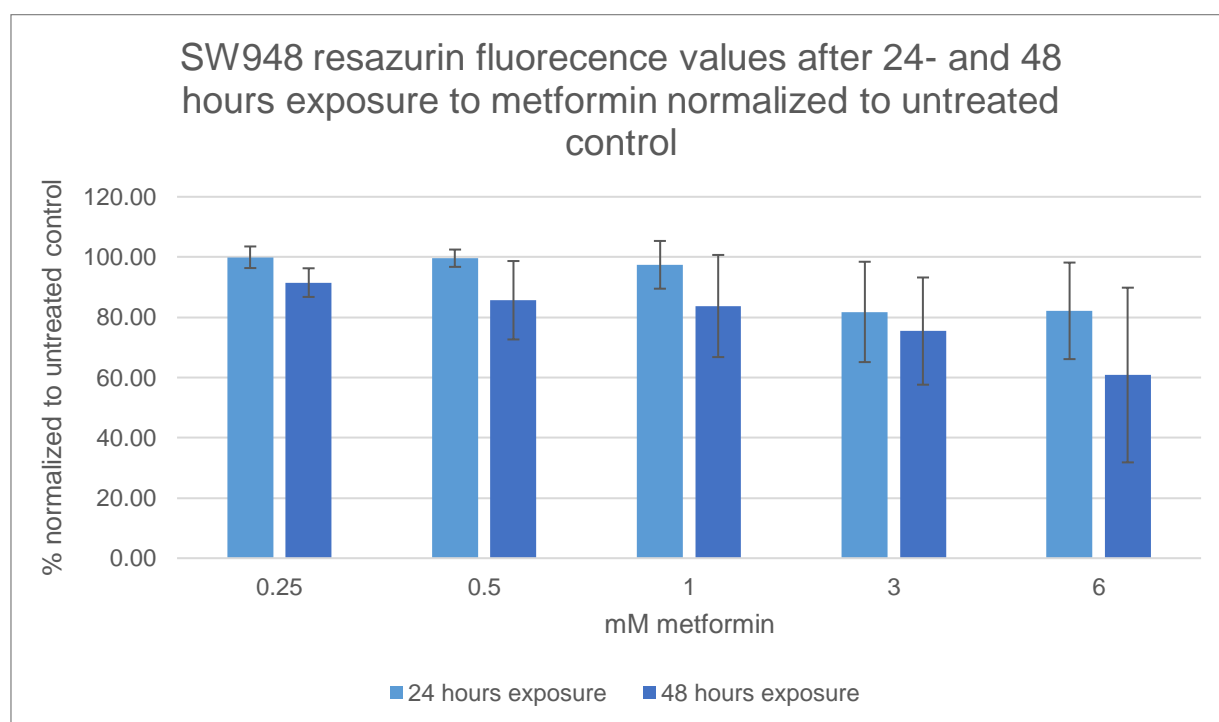


Figure 14: Total arithmetic mean ($N=4$) and S.D. of resazurin fluorescence values normalized to the untreated control of SW948 with 24- and 48 hours treatment with metformin.

4.1.4 AlamarBlue DCA treatment

The following results exhibit the fluorescence value of resazurin from colorectal cancer cells treated with various concentrations of DCA for a period of either 24- or 48 hours. The fluorescence value of the dye is proportional to the viability of the cells.

4.1.5 HCT116 results

The resazurin results for the DCA treatment after both 24 and 48 hours for the HCT116 cells are shown in Figure 15 (Appendix 2, table 15-16). The result indicates that DCA treatment does not provide any inhibitory effects and the fluorescent increased both during longer exposure and to higher concentrations. It is also shown that the S.D is at its largest for the 24-hour treatment with 6 mM DCA.

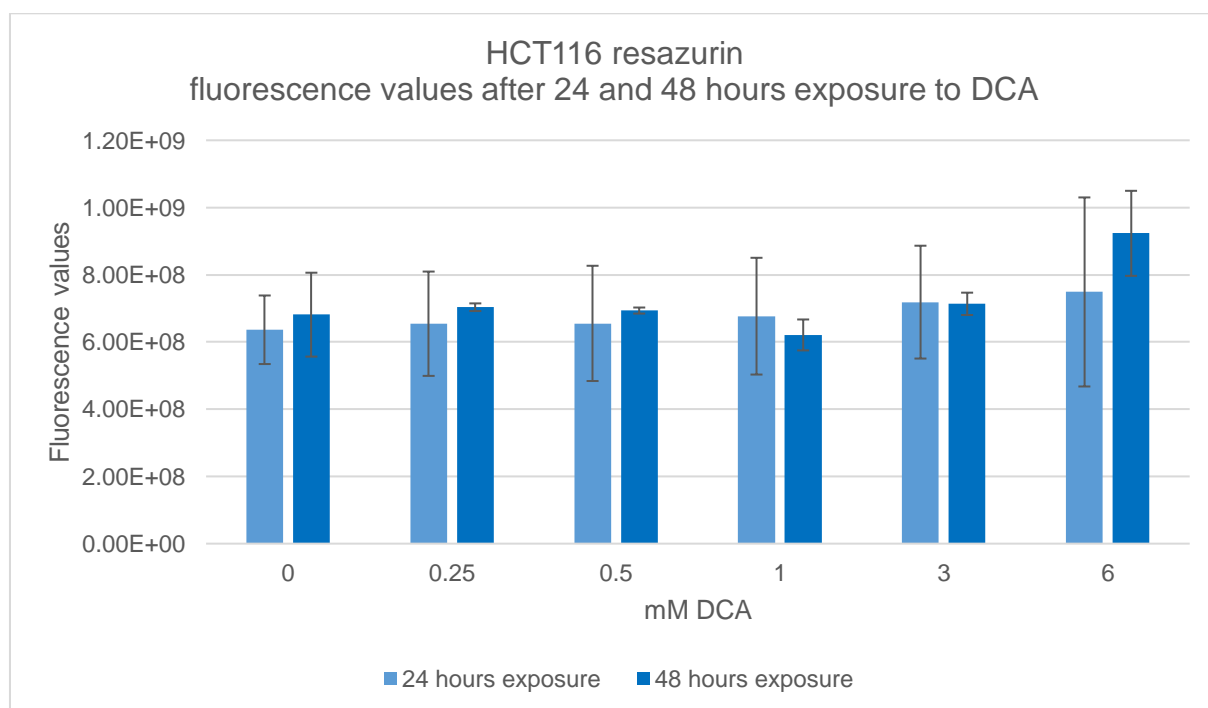


Figure 15: Total arithmetic mean ($N=3$) and S.D. of resazurin fluorescence values for HCT116 colorectal cancer cells with 24 and 48 hours of exposure to different concentrations of DCA.

Figure 16 (Appendix 2, table 23-24) exhibits the HCT116 cell lines normalized values for resazurin fluorescence for cells treated with various concentrations of DCA for 24 and 48 hours. Total arithmetic means and S.D. are shown, and the figure depicts the percentage change in absorbance between untreated control and the different concentrations. The diagram is slightly uneven and goes down for 1 mM DCA before it has a sharp increase in viability at 6 mM DCA.

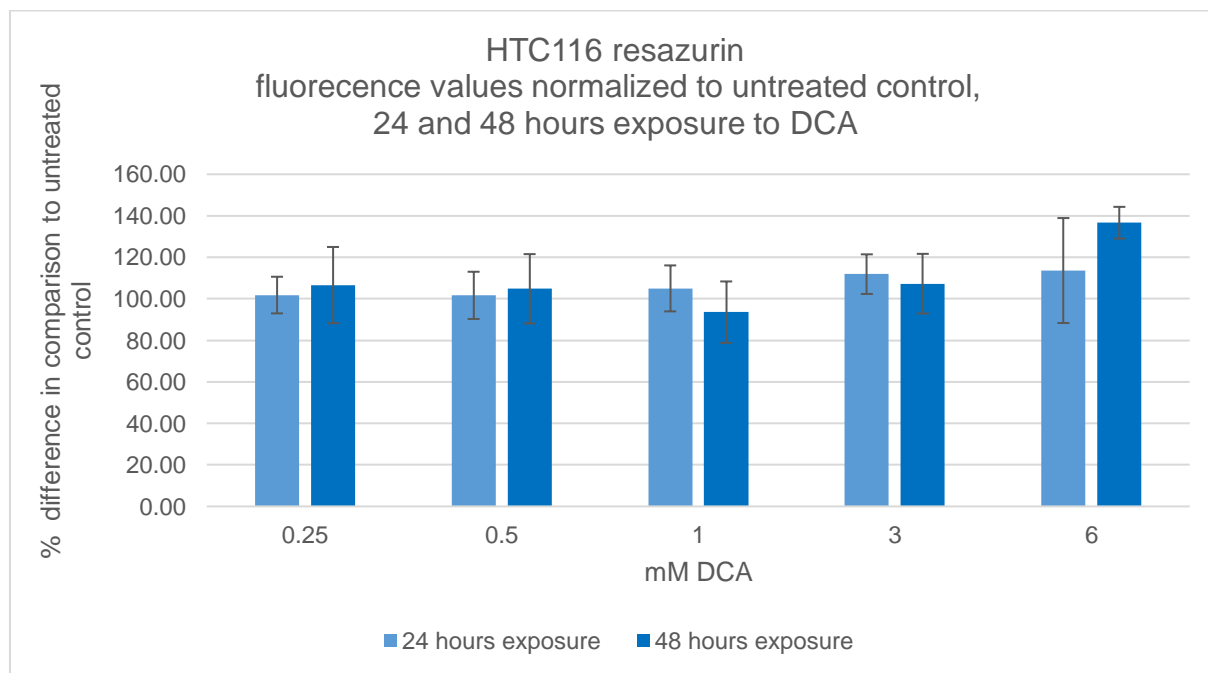


Figure 16: Total arithmetic mean (N=3) and S.D for resazurin fluorescence values normalized to the untreated control of HCT116 cell line with 24- and 48-hours exposure to various DCA concentrations.

4.1.6 SW948 results

Figure 17 (Appendix 2, table 17-18) shows the arithmetic mean of the fluorescence values from all the replicates from SW948 treated with DCA for both 24- and 48 hours. For the 24 hours exposure, the graph illustrates a decrease correlated to higher concentrations of DCA. For the 48 hours exposure, the viability increases along with the concentration value.

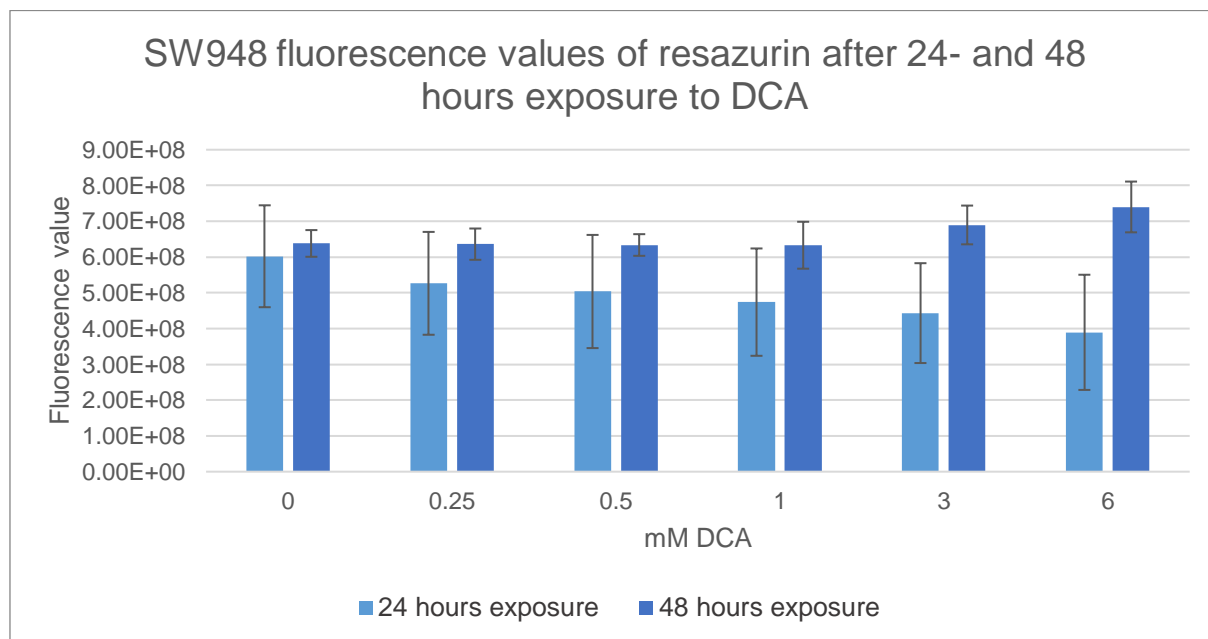


Figure 17: Total arithmetic mean (N=4) and S.D. of resazurin fluorescence value from SW948 colorectal cancer cells with 24- and 48 hours treatment with various concentrations of DCA.

The values are furthermore normalized to their internal untreated control, and the results are illustrated in Figure 18 (Appendix 2, table 25-26). The 48 hours exposure has a persistent higher percentage than the 24 hours exposure for all concentrations of DCA, as well as an increase of viability.

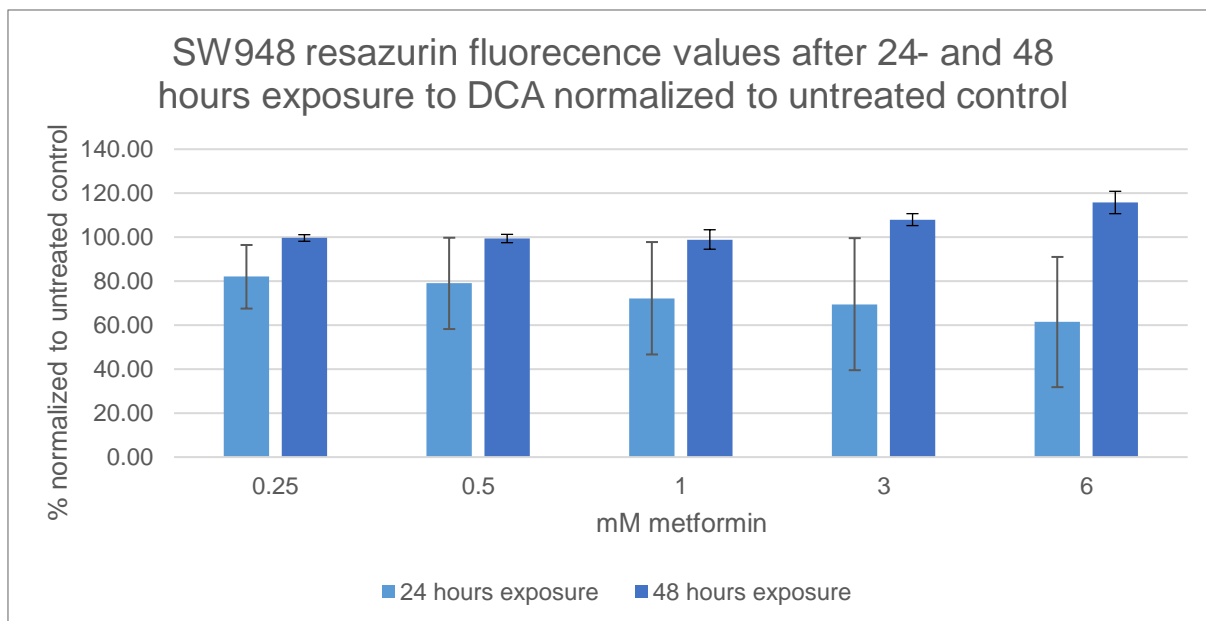


Figure 18: Total arithmetic mean (N=4) and S.D. of resazurin fluorescence values normalized to the untreated control of SW948 with 24- and 48 hours treatment with DCA.

4.2 CCK-8

The colorectal cancer cell density for cell lines HCT116 and SW948 have been quantified using Muse® Cell Analyzer to a concentration of ~10000- or ~15000 viable cells/well, respectively. The seeded cells in the 96-well plate have been treated with metformin in various concentrations and incubated for either 20- or 44 hours before CCK-8, in a final concentration of 10% per well, was added and incubated for an additional 4 hours. The absorbance of CCK-8 was measured by SpectraMax Paradigm at 450 nm wavelength and analyzed using SoftMax Pro 6 Software.

Outlying parallels have firstly been discarded with the use of Dixon's Q-test for the identification of outlying parallels:

$$Q_n = \frac{(x_a - x_b)}{R}$$

Where:

R: the range of all data points

x_a: the suspected outlier

x_b: the data point closest to x_a

Q-test were used to evaluate a decision level at 90% confidence interval:

Table 5: Threshold values for Dixon's Q-test with a 90% confidence interval. N = number of replicates and Q = the threshold value.

N	3	4	5	6	7	8	9	10
Q	0.94	0.76	0.64	0.56	0.51	0.47	0.44	0.41

The quantitative raw data from the analysis of CCK-8 of every parallel have then been normalized to the blank control by subtraction. The arithmetic means from each passage for both 24- and 48 hours are calculated along with the total arithmetic mean and its S.D. These values are represented in appendix 3, Table 22 - Table 29.

The data is further normalized to the untreated control using Equation 8, and the results are represented in appendix 3, Table 30 - Table 37 coupled with the total arithmetic mean and the S.D.

4.2.1 CCK-8 metformin treatment

The following results exhibit the absorbance value of CCK-8 from colorectal cancer cells treated with various concentrations of metformin for a period of either 24- or 48 hours. The absorbance value of CCK-8 is proportional to the viability of the cells.

4.2.2 HCT116 results

Illustrated in Figure 19 (Appendix 3, table 27-28) are the CCK-8 absorbance values for the HCT116 cell line after exposure to metformin in 24 and 48 hours. Total arithmetic means and S.D are expressed.

A slight decrease is seen after 24 hours, but the alteration is significant after 48 hours and the higher the concentration the more effective treatment.

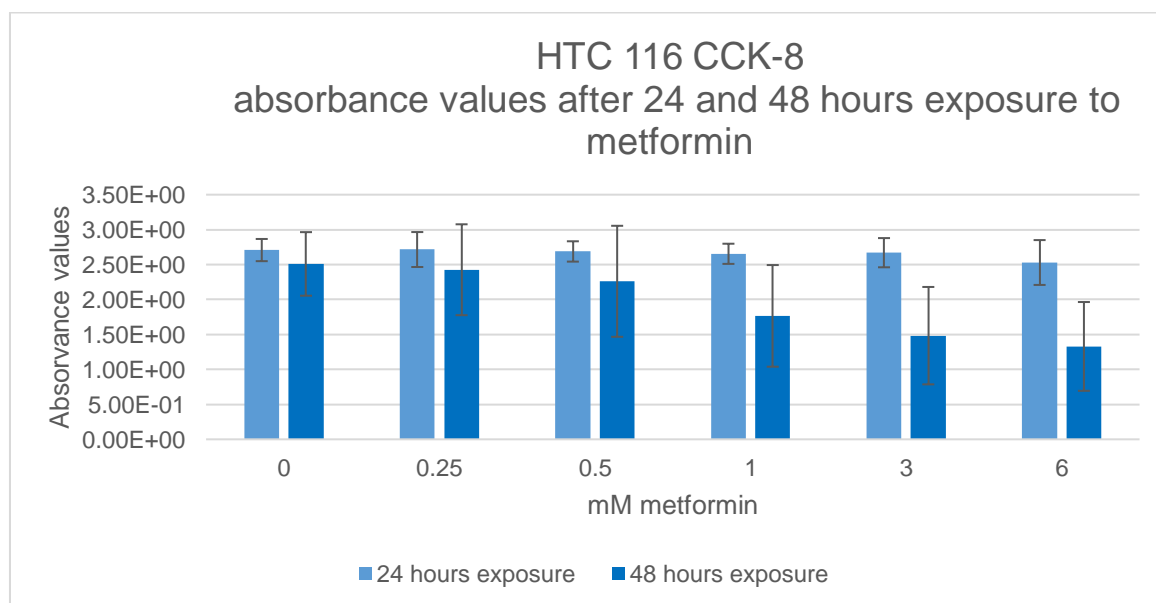


Figure 19: Total arithmetic mean ($N=3$) and S.D. of CCK-8 absorbance values for HCT116 colorectal cancer cells with 24- and 48-hours exposure to different concentrations of metformin.

Figure 20 (Appendix 3, table 35-36) depicts the normalized CCK-8 absorbance values for HCT116 cell line after 24 and 48 hours of metformin treatment. The figure shows the change in percentage between untreated control and cells exposed to metformin in various concentrations. This figure shows a clear indication on inhibitory effect of metformin on the viability of the cells, the higher metformin concentration and/or longer exposure time causes a significant decrease in cell viability.

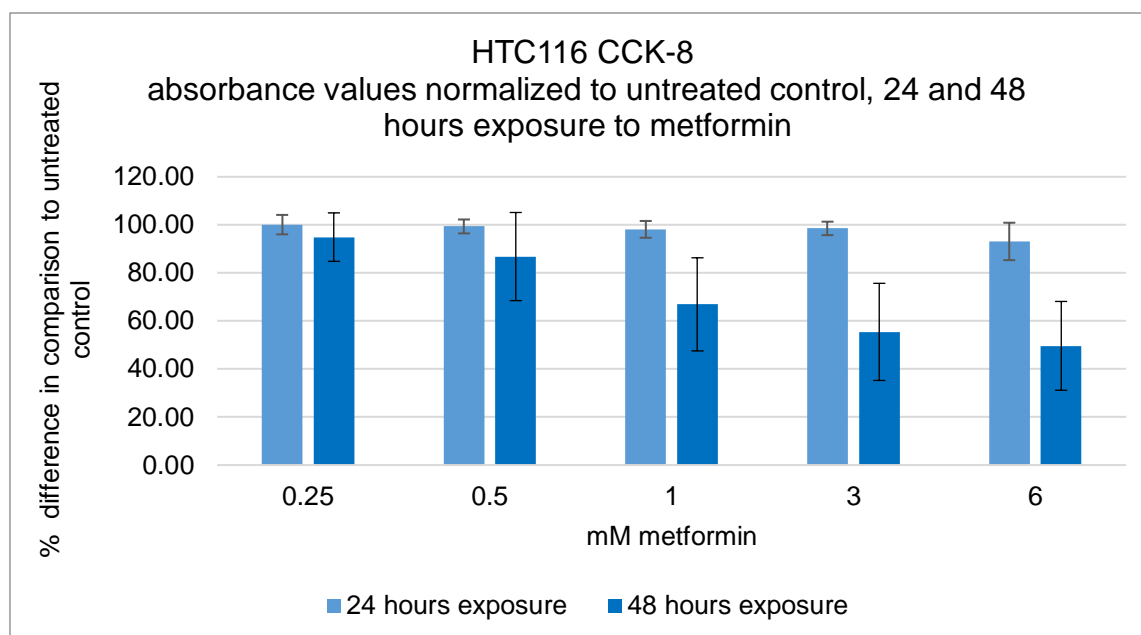


Figure 20: Total arithmetic mean (N=3) and S.D. for CCK-8 absorbance values normalized to the untreated control of HCT116 cell line with 24- and 48-hours exposure to various metformin concentrations.

4.2.3 SW948 results

The results from the analysis of the CCK-8 absorbance values generated from SW948 exposed to 24- and 48 hours with metformin is represented in Figure 21 (Appendix 3, table 29-30). For both the 24- and 48 hours treatments, the viability has a continuous decrease proportional to the increasing concentration of metformin, except the 24 hours treatment with 6 mM. All the values for the 48 hours treatment are persistently lower than the 24 hours treatment within the same concentration. Hence, the effectiveness of the treatment supposedly increases with a longer exposure to this specific medication.

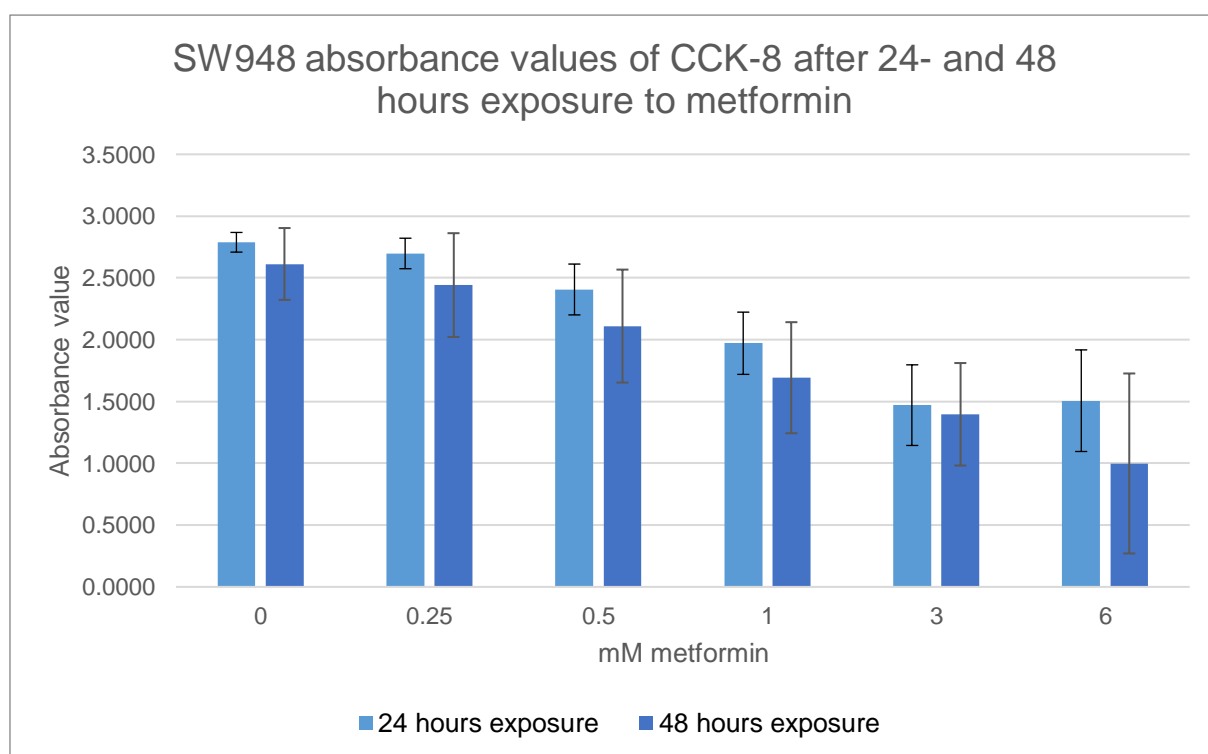


Figure 21: Total arithmetic mean ($N=4$) and S.D. of CCK-8 absorbance value from SW948 colorectal cancer cells with 24- and 48 hours treatment with various concentrations of metformin.

The normalized data more accurately describe the changes in viability since each replicate is normalized to its internal control. Figure 22 (Appendix 3, table 37-38) depicts both the 24- and 48 hours exposure of DCA to SW948 colorectal cancer cells. There is a clear indication of difference between the length of exposure, where 48 hours is persistently more effective in

relation to the viability of the cells after the treatment. For the 6 mM concentration, the 48 hours exposure has the lowest value in all.

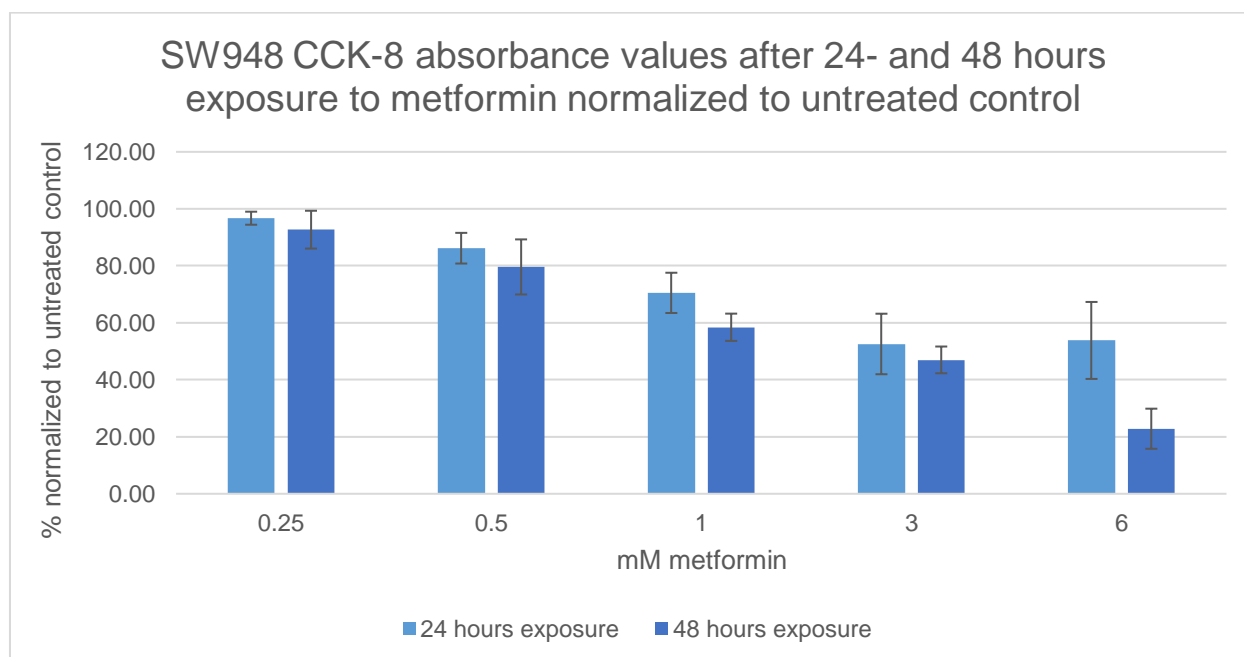


Figure 22: Total arithmetic mean ($N=4$) and S.D. of CCK-8 absorbance values normalized to the untreated control of SW948 with 24- and 48 hours treatment with metformin.

4.2.4 CCK-8 DCA treatment

The following results exhibit the absorbance value of CCK-8 from colorectal cancer cells treated with various concentrations of DCA for a period of either 24- or 48 hours. The absorbance value of CCK-8 is proportional to the viability of the cells.

4.2.5 HCT116 results

The results in Figure 23 (Appendix 3, table 30-31) show the total arithmetic mean and S.D of the CCK-8 absorbance values for HCT116 cell line after 24- and 48-hours exposure to DCA in concentrations ranging from 0-6 mM. the highest viability is seen after 24 hours exposure to 6 mM DCA. The viability seems to increase along with increase in medication.

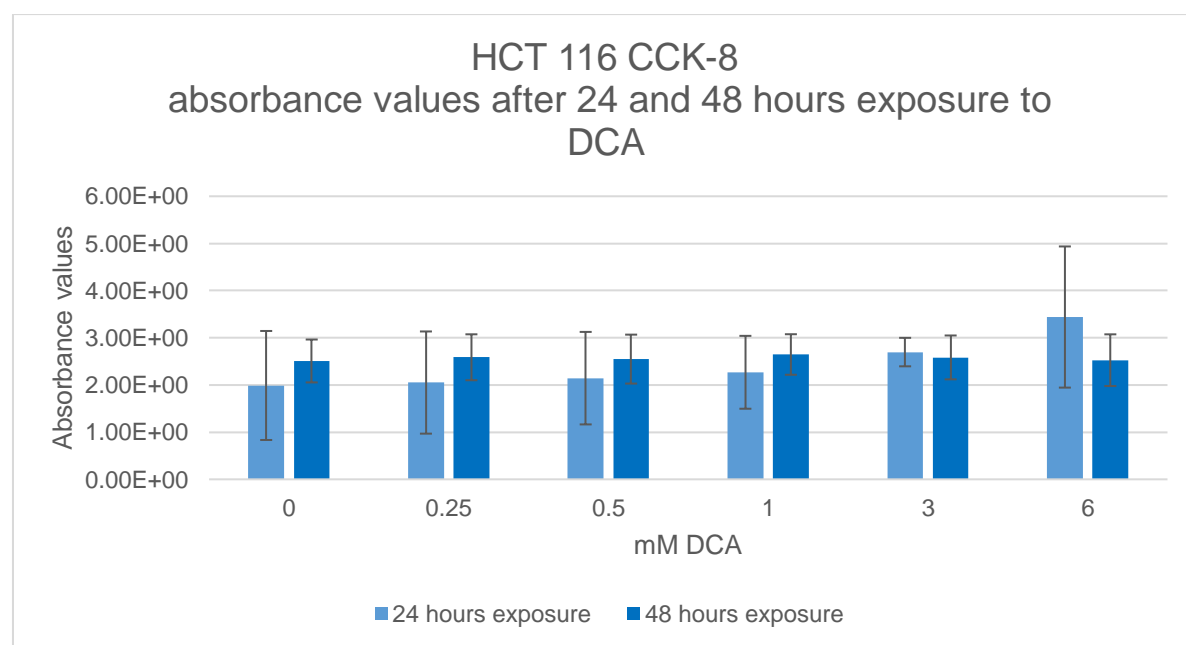


Figure 23: Total arithmetic mean (N=3) and S.D. of CCK-8 absorbance values for HCT116 colorectal cancer cells with 24- and 48 hours exposure to different concentrations of DCA.

Figure 24 (Appendix 3, table 39-40) shows the percentage deviation between the CCK-8 absorbance levels for the untreated control and cells exposed to DCA in concentrations ranging from 0-6 mM for 24 and 48 hours. Total arithmetic means and S.D are depicted. The figure shows an increase in cell viability after 48 hours of treatment compared to 24 hours. The highest viability is seen after 48 hours exposure to 1 mM DCA.

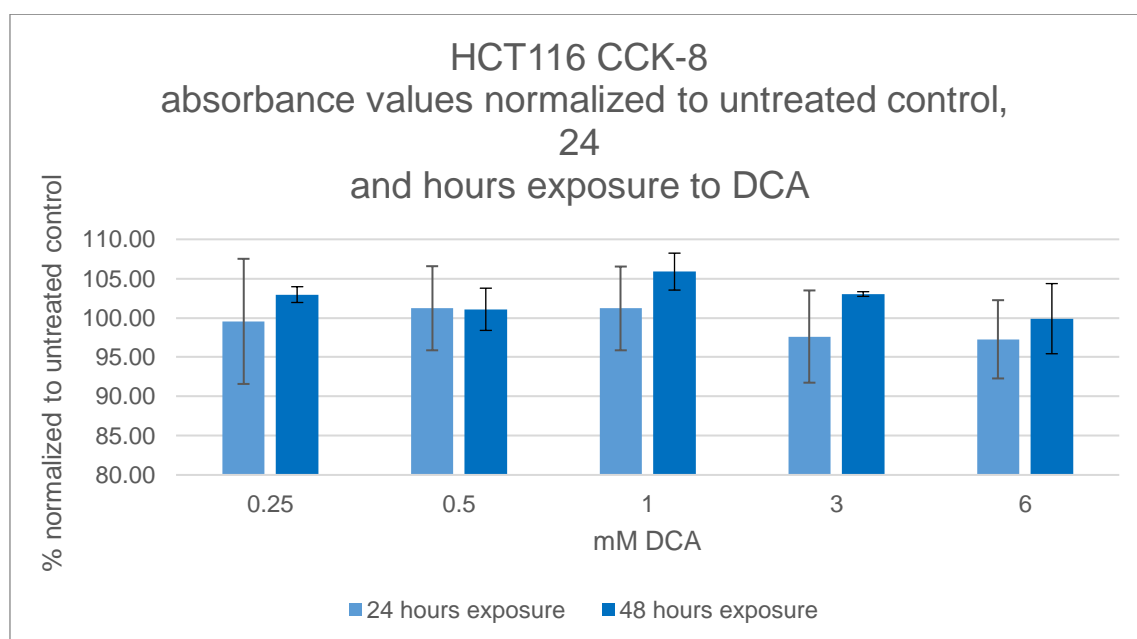


Figure 24: Total arithmetic mean (N=3) and S.D for CCK-8 absorbance values normalized to the untreated control of HCT116 cell line with 24- and 48 hours exposure to various DCA concentrations.

4.2.6 SW948 results

The results from the absorbance values of CCK-8 from SW948 treated with DCA exhibit variable results with increasing concentration of DCA for both the 24- and 48 hours treatments shown in Figure 25 (Appendix 3, table 33-34).

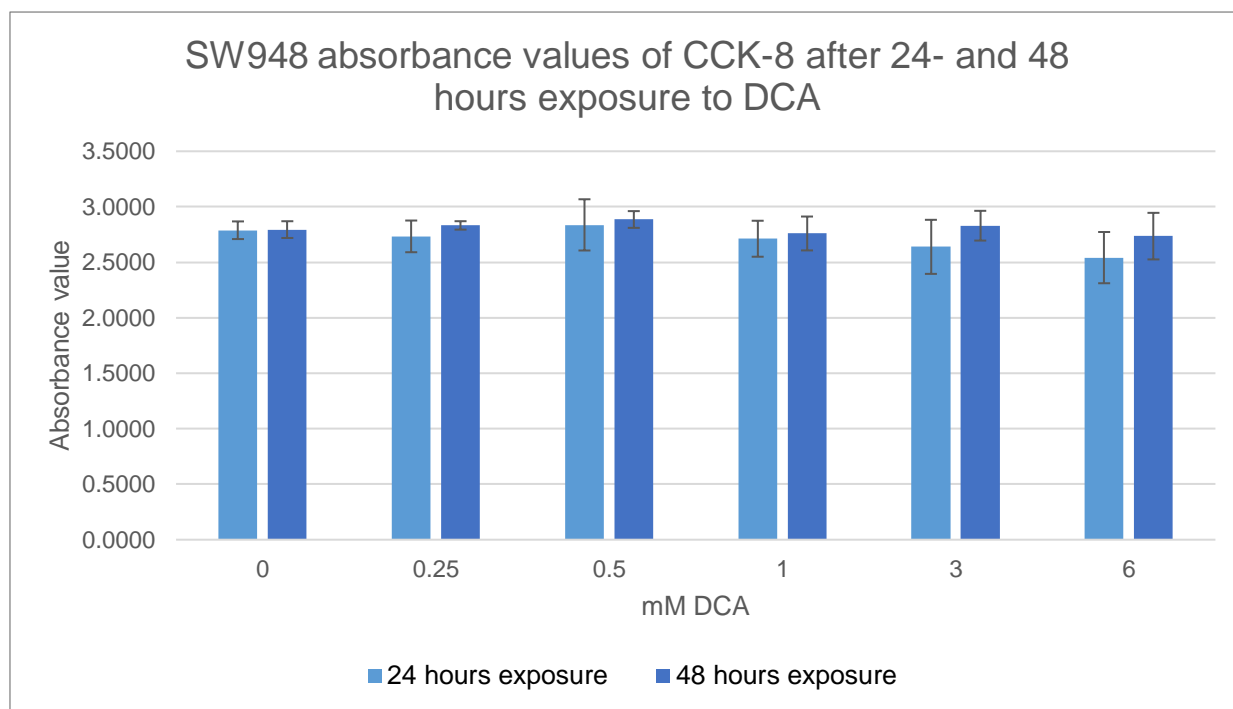


Figure 25: Total arithmetic mean ($N=4$) and S.D. of CCK-8 absorbance value from SW948 colorectal cancer cells with 24- and 48 hours treatment with various concentrations of DCA.

The normalized data in Figure 26 (Appendix 3, table 41-42) shows no significant change in viability for any concentration used to treat the colorectal cancer cells in relation to the untreated control. The viability for the 48 hours treatments has a consistently higher value than the 24 hours exposure to DCA.

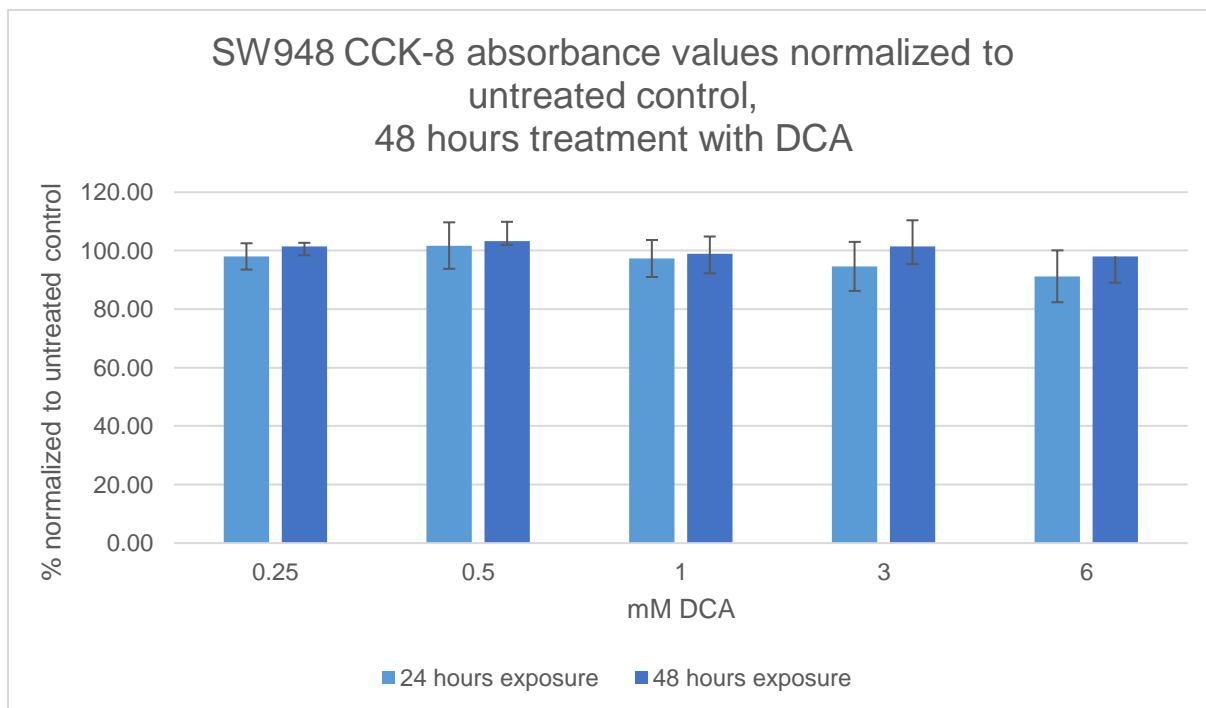


Figure 26: Total arithmetic mean ($N=4$) and S.D. of CCK-8 absorbance values normalized to the untreated control of SW948 with 24- and 48 hours treatment with DCA.

4.3 Combination treatment AlamarBlue

The colorectal cancer cells in the 96-well plate were treated with various combinatorial concentrations ranging from 1- to 6 mM of both metformin and DCA and incubated for either 20- or 44 hours before resazurin was added to a final concentration of 10% (v/v).

Fluorescence was measured using SpectraMax Paradigm at 540 nm excitation wavelength and 590 nm emission wavelength and analyzed using SoftMax Pro 6 Software.

The arithmetic means of each individual replicate, the total arithmetic mean, and the S.D. for the individual cell lines are calculated. Furthermore, the results have been normalized to the corresponding singular metformin treatment using Equation 8 and the results are represented in **Error! Reference source not found.** The purpose for the normalization is to observe the difference of the effects between a singular treatment and a combinatory treatment.

4.3.1 HCT116 results

Illustrated in Figure 27 (Appendix 4, table 43-44) are the percentage differences in resazurin fluorescence values for the HCT116 cell line between the equivalent singular metformin treatment and cells exposed to 24- and 48-hours treatment with various combined concentrations using DCA and metformin. Higher concentrations of DCA (6 mM) increases the viability of the cells for both exposure periods, whereas lower concentrations decrease the viability.

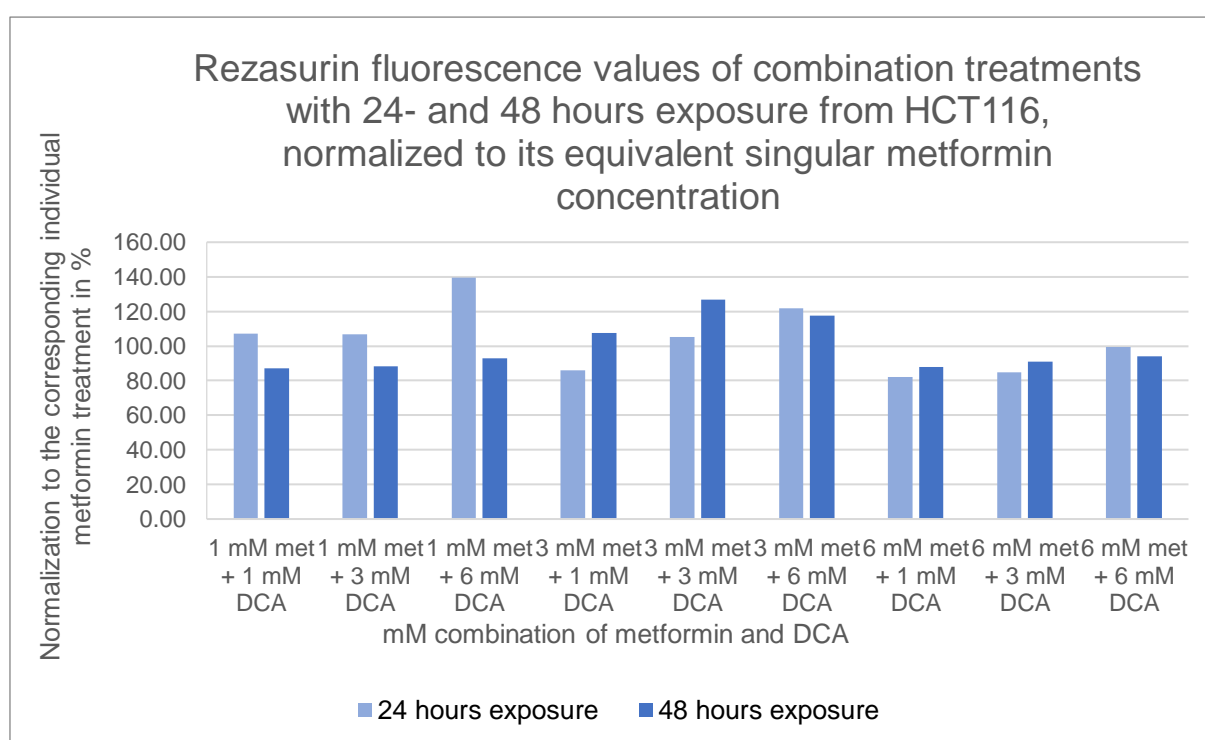


Figure 27: Resazurin fluorescence values in percent normalized to its internal corresponding singular metformin treatment of HCT116 cell line with 24- and 48 hours exposure to various combinations of metformin and DCA.

4.3.2 SW948 results

When we normalize the data to the singular treatment with metformin, as seen in Figure 28 (Appendix 4, table 45-46), we see the effects of the combinatory treatments. 24 hours exposure generally lowers the viability of the cells, in contrast to the 48 hours treatment, where the viability seems to increase with higher concentrations of DCA as previously observed in the singular treatments of DCA.

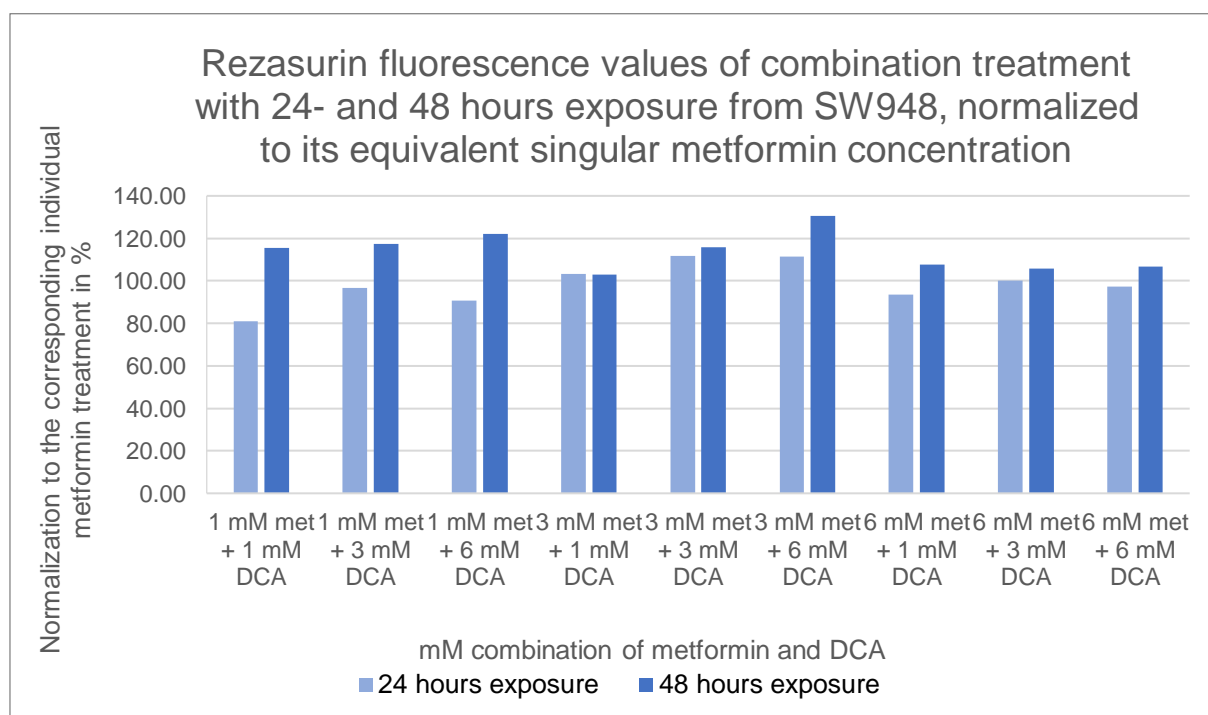


Figure 28: Resazurin fluorescence values in percent normalized to its internal corresponding singular metformin treatment of SW948 cell line with 24- and 48 hours exposure to various combinations of metformin and DCA.

4.4 Combination treatment CCK-8

The colorectal cancer cells in the 96-well plate were treated with various combinatorial concentrations ranging from 1- to 6 mM of both metformin and DCA and incubated for either 20- or 44 hours before CCK-8 to a final concentration of 10% (v/v) was added and further incubated for four hours. Absorbance was measured using SpectraMax Paradigm at 450 nm wavelength and analyzed using SoftMax Pro 6 Software.

The arithmetic means of each individual replicate, the total arithmetic mean, and the S.D. for the individual cell lines are calculated. Furthermore, the results have been normalized to the corresponding singular metformin treatment using Equation 8 and the results are represented in Table 50. The purpose for the normalization is to observe the difference of the effects between a singular treatment and a combinatory treatment.

4.4.1 HCT116 results

Illustrated in Figure 29 (Appendix 4, table 47-48) are the percentage differences in CCK-8 absorbance values for the HCT116 cell line between the equivalent concentration of metformin and cells exposed to 24 and 48 hours of treatment with various combined concentrations using DCA and metformin. The lowest concentrations of metformin in the combination treatment (1 mM) lowers the viability slightly, whereas the 3 mM metformin and 3- and 6 mM DCA combination has a stronger effect than any other combination.

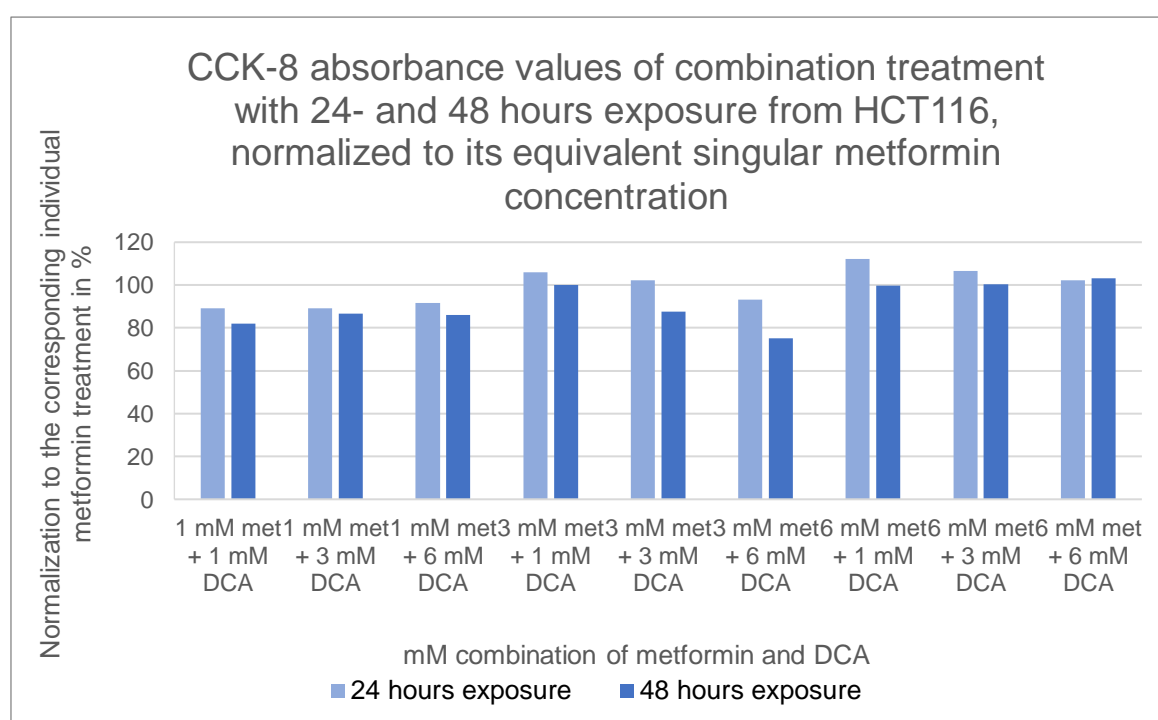


Figure 29: CCK-8 absorbance values in percent normalized to its internal corresponding singular metformin treatment of HCT116 cell line with 24- and 48 hours exposure to various combinations of metformin and DCA.

4.4.2 SW948 results

Figure 30 (Appendix 4, table 49-50) illustrates the normalized values of the combination treatments to the singular equivalent metformin concentration. All of the combinatorial concentrations have an increasing effect, especially the 48 hours exposure, on SW948 in

comparison to the singular treatments. This observation correlates to the singular DCA results.

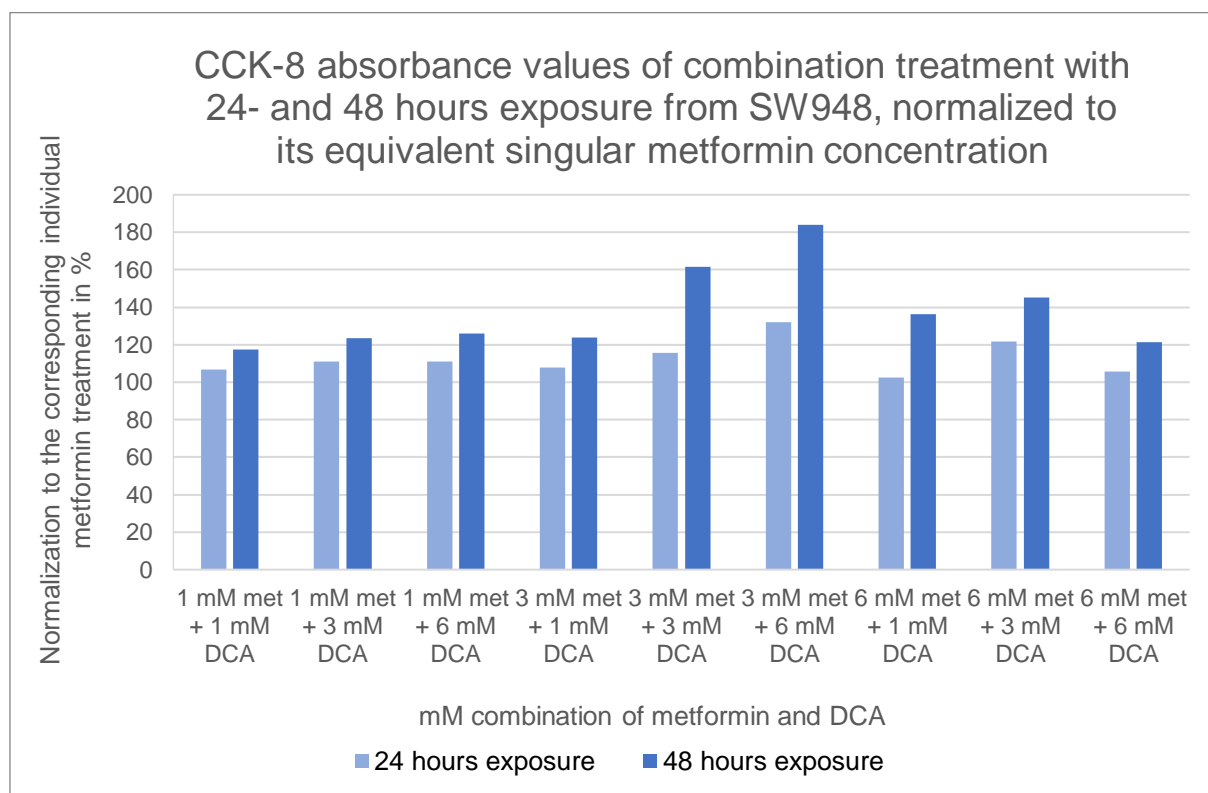


Figure 30: CCK-8 absorbance values in percent normalized to its internal corresponding singular metformin treatment of SW948 cell line with 24- and 48 hours exposure to various combinations of metformin and DCA.

4.5 Flow Cytometry

Flow cytometry is used for the analysis of physical and chemical characteristic of a single cell suspension injected into a flow cytometer instrument. Flow cytometry has a wide range of applications, including fluorescent protein detection, this was the application used during this project. We measured the effect of metformin and DCA on cell lines HCT116 and SW948 on the protein expression of Akt, p-Akt, AMPK, and p-AMPK. These proteins play a significant role in cellular energy homeostasis, specifically glucose metabolism. By measuring the protein expression on the colorectal cancer cells before and after treatment, we can better understand their effects on the metabolism of these cancer cells.

The following data are measured by a fluorescein isothiocyanate (FITC)-A x-axis, where increasing value indicates higher protein expression.

The first figure (Figure 31) illustrates the cell characteristics of the cells from the negative control testing compound for HCT116 and SW948. The FSC-A axis increases proportional to the diameter of the cell due to the light diffraction around the cell. Essentially it measures and differentiates the cells by size. The SSC-A axis measures light refracted or reflected between the flow cytometry laser and the cells intracellular structures, which can give information about the cell's internal complexity. (58)

The P1 areas are the gated boundaries in the cell population of the testing compound, which were manually marked and used for further analysis of protein expression.

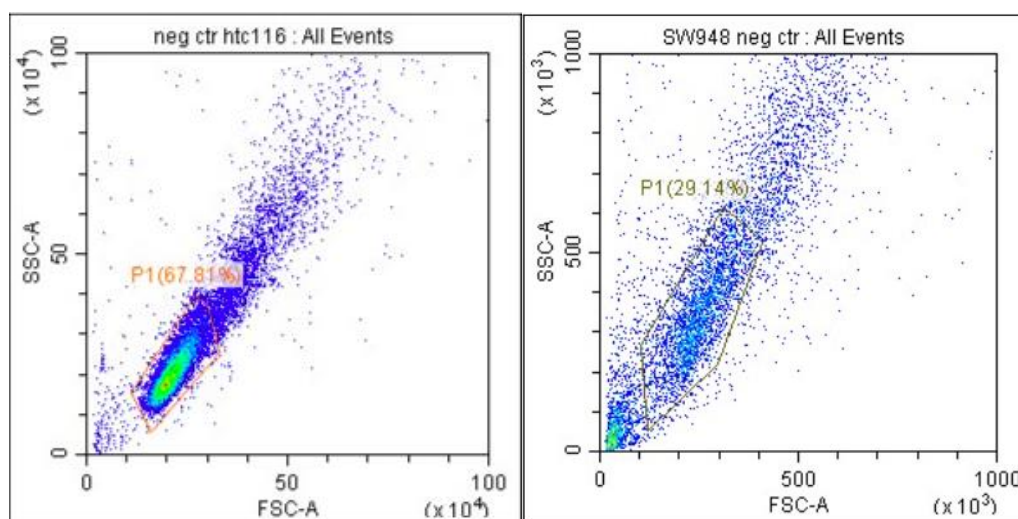


Figure 31: Cell characteristics and gated areas of negative control for HCT116 (left) and SW948 (right) measured by a flow cytometry.

4.5.1 HCT116 results

Figure 32 shows a histogram of the expression of both the Akt- and p-Akt protein on HCT116 after treatment with either metformin or DCA. The red curve is the control of untreated cells for Akt, and the green curve is the control for p-Akt. We can see a shift in the expression of p-Akt treated with metformin in comparison to the control. There is no significant shift on FITC-A for the expression of Akt on neither of the treatments.

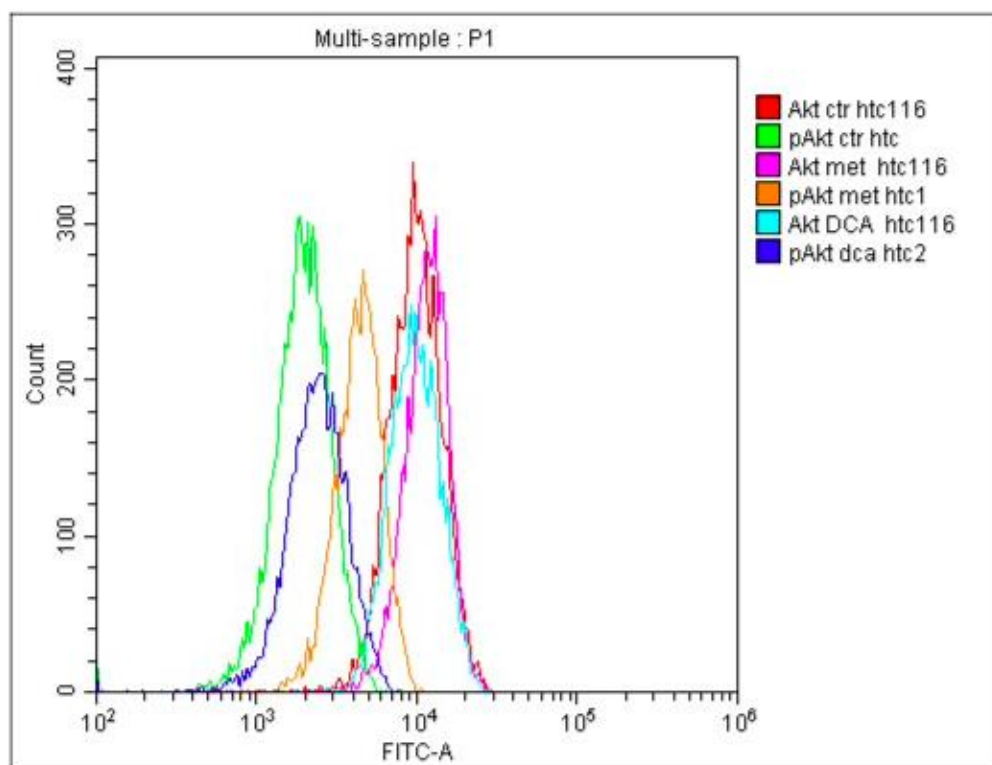


Figure 32: Flow cytometry results of HCT116, treated with 48 hours exposure to metformin and DCA, on the expression of Akt and p-Akt.

In Figure 33 AMPK, and its phosphorylated form p-AMPK are measured after treatment with either metformin or DCA. The red curve is the untreated control of AMPK, and the green curve is the control for p-AMPK. For the AMPK, DCA does not have an effect on the expression of the protein, but metformin gives the expression a significant shift. Furthermore, there is no indication of a shift on neither of the treatments for the p-AMPK expression.

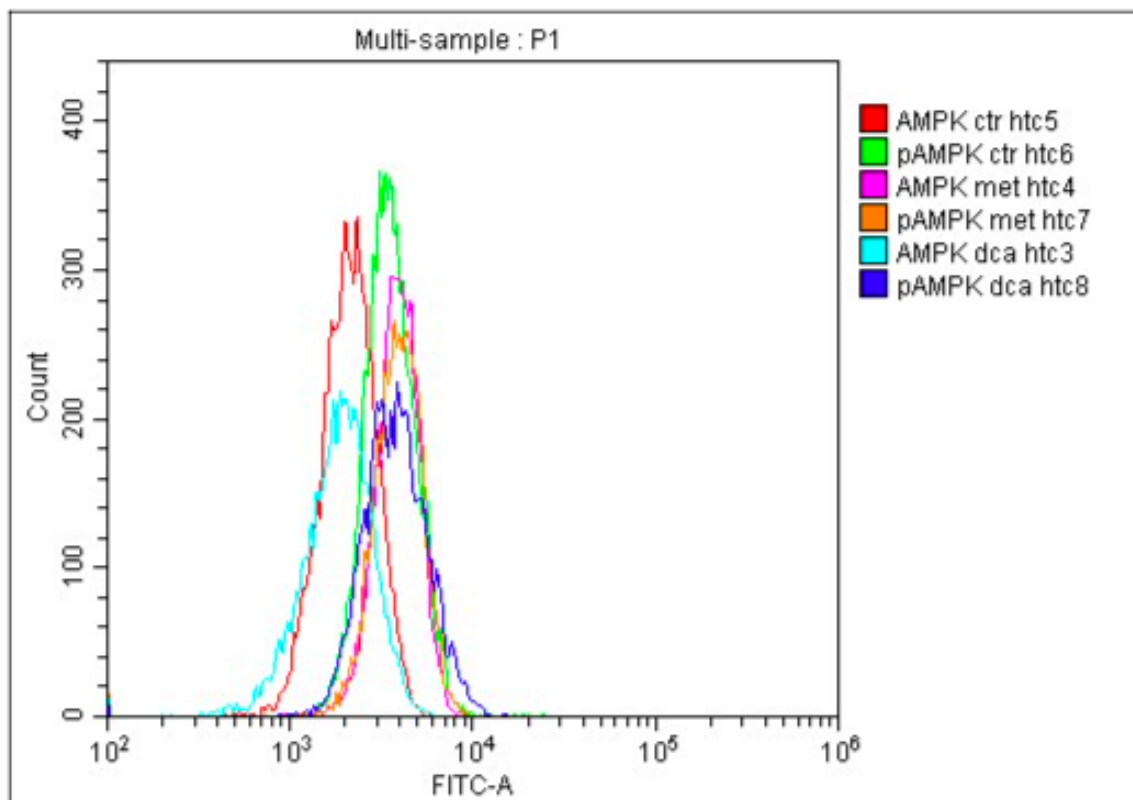


Figure 33: Flow cytometry results of HCT116, treated with 48 hours exposure to metformin and DCA, on the expression of AMPK and p-AMPK.

4.5.2 SW948 results

Figure 34 shows a histogram of the expression of both the Akt- and p-Akt protein on SW948 after treatment with either metformin or DCA. Where the red curve is the control for the Akt protein, the pink curve, which is the metformin treated Akt expression, shows a minor shift on FITC-A. DCA has no significant shift for the Akt. The green curve is the control for the p-Akt protein. DCA, the blue curve, has a slight shift, whereas metformin, the orange curve has a larger shift and thus a higher expression of p-Akt.

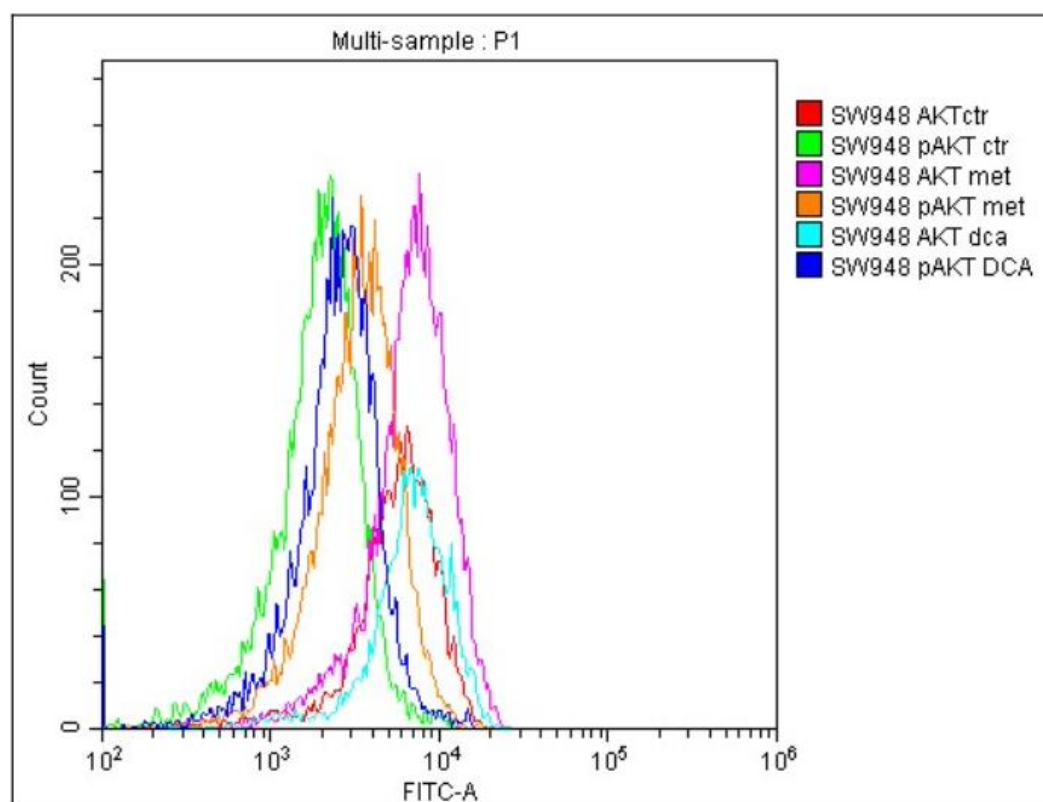


Figure 34: Flow cytometry results of SW948, treated with 48 hours exposure to metformin and DCA, on the expression of Akt and p-Akt.

Figure 35 illustrated the results of measured AMPK and p-AMPK expression of untreated and treated cells of SW948. For the AMPK, the cells treated with metformin (pink) has a shift in FITC-A compared to the untreated control (red). DCA has no significant effect on the expression of AMPK. Metformin also has a major effect on the expression of p-AMPK (orange) for SW948 compared to the green control curve.

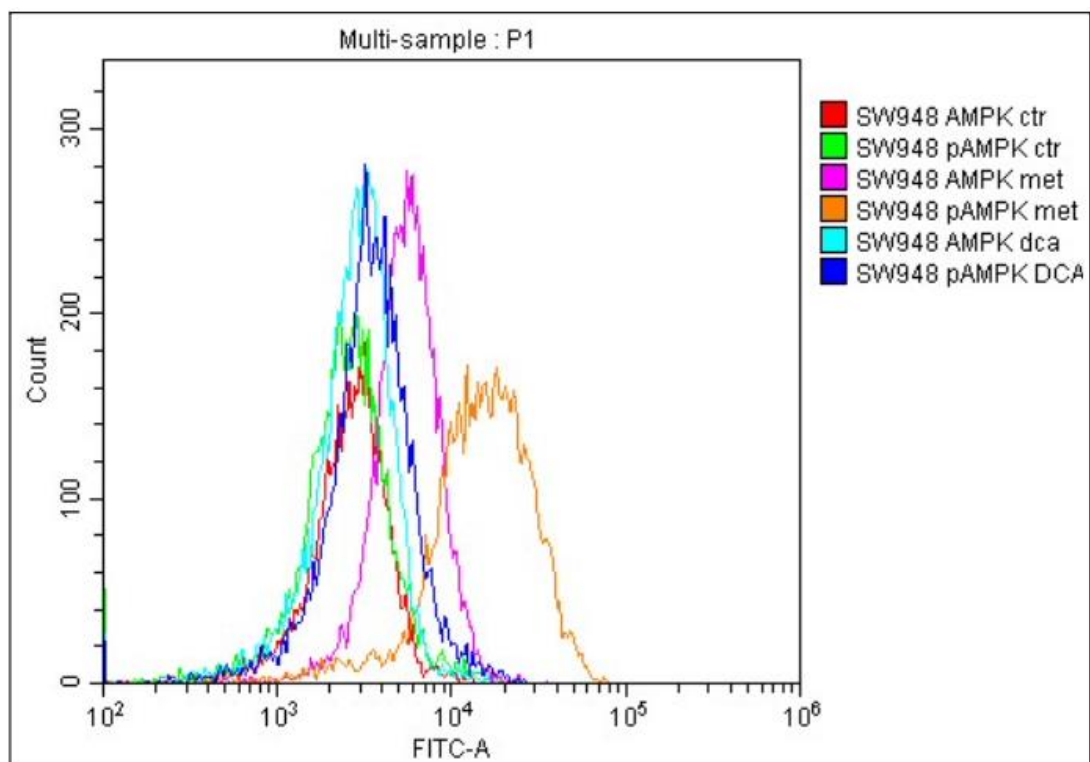


Figure 35: Flow cytometry results of SW948, treated with 48 hours exposure to metformin and DCA, on the expression of AMPK and p-AMPK.

5 Discussion

5.1 Methodological considerations

The splitting of SW948 from one passage to another often resulted in an inadequate amount of cell suspension for the AlamarBlue- and CCK-8 assays, despite having two cell flasks. Because of this, some of the concentrations only had three parallels and one of the 96-well plates had to be excluded (resazurin 48 h). This might have affected the results generated in contrast to the actuality of the results due to fewer replicates and parallels and thus less accurate arithmetic means and consequently higher S.D. values.

Certain individual parallels on CCK-8 (48 h) with 1-, 3-, and 6 mM of DCA for SW948 appeared considerably darker than expected after the incubation of CCK-8, and the result values reflected this difference. After observing the parallels under the microscope there was a substantial difference in cell density. A possible cause for this variability might have been a lack of homogenizing the cell suspension preparatory to the addition to the wells. Considering that the CCK-8 DCA (48 h) well was the last to be prepared, this speculation is very likely. Therefore, it was more accurate to discount the applicable parallels.

During the addition of CCK-8 to one of the plates of HCT16 cell line the pipette malfunctioned. The mistake was attempted corrected by changing pipettes and re-adding CCK-8 to the wells it concerned, but due to both change in pipettes and a uncertainty regarding the question if any reagent had reached the well the first time, this mistake may very well have impacted the results significantly. This plate was removed and does not appear in the final results.

The formation of baubles in the wells created an ongoing topic of discussion, and even though the problem decreased throughout the experiment as practice was gained, the issue was never fully resolved. It was attempted to pop the bubbles using methanol air. The blowing of methanol air against the bubbles gave various results were some popped, and some proved to resistant to be eradicated. It's also unclear whether this process had any impact on the cells or further analysis and may be a source of error in the final results.

During the experiment an incident occurred where some of the treated 96-well plates belonging to the HCR116 cell line were dropped on the floor. These plates could no longer be used and was discarded. The failed experiment was replicated a couple weeks later to get the adequate number of readings and parallels, but it gave rise to the necessity of moving planned runs around and multiple runs had to be done on the same passage, meaning that there are multiple runs being run under identical conditions using the same P. This is not ideal and create a less reliable result and should be taken into consideration.

Flow Cytometry was performed twice during the experiment. The first attempt was problematic for the HCT116 cell line. During the preparation of the suspension, the supernatant had been poured out after centrifugation, the pouring, despite care being taken, led to a loss of cells along with the supernatant, leading to a cell shortage once all steps were completed. The flow cytometry was still performed but the instrument struggled with the low cell concentration. For the second attempt the error was corrected, and a pipetting technique was used to remove the supernatant after each centrifugation, providing a more correct cell concentration.

For the SW948 cell line the second flow cytometry run proved to be the most problematic as the cells showed a strong tendency to clump together making the reading difficult for the instrument. The flow cytometer consequently did not count the actual number of cells, and this might have generated inaccurate results.

Overall, the experiment had several areas of improvement under methodological considerations. Ideally, every assay should have had more replicates for more accurate results. It would also be of interest to measure the effect of even higher concentration values to study the trend of the treatments in a higher margin.

5.2 Results discussion

5.2.1 AlamarBlue and CCK-8

The results from the viability assays for both HCT116 and SW948 show an indication that both prolonged exposure to metformin and increasing metformin concentration decrease the measured values and hence the viability of the treated cells. The most effective treatment for all the replicates for both cell lines is the 48 hours exposure to 6 mM metformin. Metformin has, without a doubt, a strong effect on the viability of the cells in higher concentrations. In contrast, DCA generated variable results on the viability with higher concentrations after the 24 hours exposure period, but a clear increase of viability for the 48 hours exposure for both cell lines.

In Figure 36 the highest and lowest generated normalized values for metformin and DCA with an exposure period of 48 hours for both HCT116 and SW948 are illustrated. Where 100% is the threshold for the untreated control, metformin has a ~40% decrease for both cell lines with resazurin. For the CCK-8, SW948 has a greater response to metformin than HCT116. On the other hand, HCT116 is observed to be more resistant to the DCA treatment with a higher increase in viability.

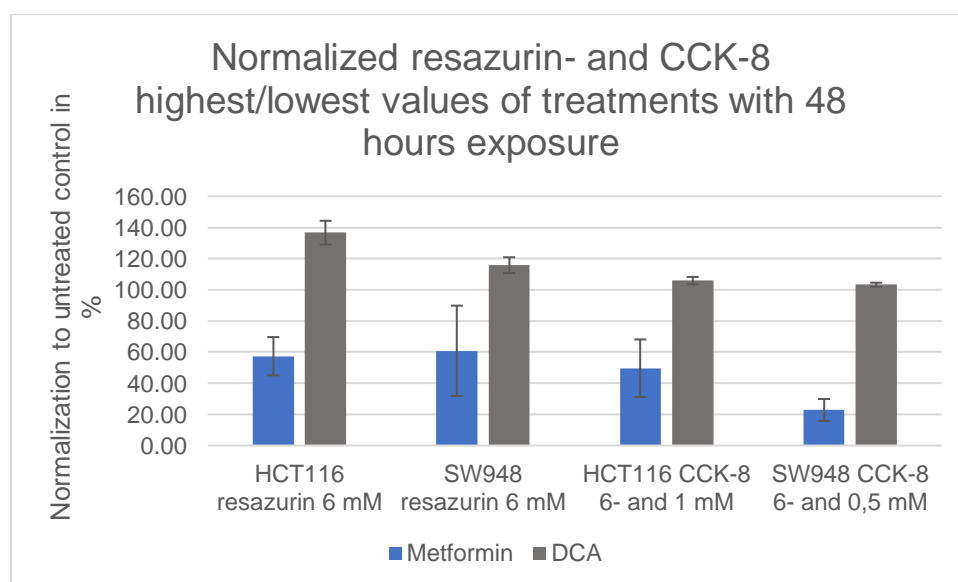


Figure 36: Most and least effective treatments using resazurin and CCK-8, normalized to untreated control for both HCT116 and SW948.

The combination treatments showed a minor increase of viability with increasing DCA concentration in contrast to the singular equivalent metformin treatment for both cell lines.

The results had variable values for both cell lines and protocols, and there was no combination that proved to be the most effective in all.

As previously mentioned, metformin and DCA have an opposing effect in respect of each other. Where metformin inhibits the electron transport chain and consequently forces the cell to retreat to utilizing glycolysis and thus limiting the mitochondrial metabolism, DCA is able to mitigate the Warburg effect in cancer cells by triggering a metabolic switch from glycolysis to oxidative phosphorylation in mitochondria, which was not an effect observed in normal cells. Essentially DCA can increase the amount of pyruvate going into the TCA as opposed to that converted into lactate.

We can interpret the results in this experiment based off the effect metformin and DCA has on the metabolism of cancer cells. A reasonable hypothesis, solely based on our results, is that our specific cell lines are more reliable on the mitochondrial metabolism rather than the glycolysis. This leads to lower viability when treated with metformin, and a higher viability when treated with DCA. The effect of these compounds naturally increases with higher concentration and exposure period as proven in the generated data.

Even though our findings seem convincing as is, many existing papers have covered the characteristics of cell line SW948 and its metabolic phenotypes. Tia R. Tidwell, Ph.D. found SW948 to be highly glycolytic in terms of metabolism. (59) Metformin showed inhibitory growth, but not in the presence of high glucose conditions. The metabolic effect of metformin is therefore strongly based on the abundance of glucose.

5.2.2 Flow Cytometry

During the flow cytometry, the cells were exposed to four different antibodies correlating to four different protein expressions. The expressions that were evaluated were the expression of Akt, in both the phosphorylated form p-Akt and its unphosphorylated form Akt, where p-Akt represents an increase in activation and is known as a cancer promotor. The other set of protein expression measured was the phosphorylated p-AMPK and its unphosphorylated counterpart AMPK.

For the HCT116 cell line, the flow cytometry showed a significant shift in the expression of both AMPK and p-Akt. SW948 did also generate a shift in AMP and p-Akt, but also on the expression of Akt.

Based on the literature and the knowledge about metformin's ability to inhibit activation of AKT, through both phosphorylating IRS-1 at Ser789 and its effect on insulin, the hypothesis for the results was a possible but uncertain increase in Akt and a decrease in p-Akt after metformin treatment.

During DCA treatment similar result as with metformin, due to the effect of DCA on the PTEN, were expected meaning a decrease in p-Akt and a possible but uncertain increase in AKT were hypothesized.

Metformin is known as an AMPK activator. We would therefore expect an increase in the phosphorylated AMPK expression, but none of the cell lines had any increase of p-AMPK. DCA has been proved to have an inhibiting effect on the phosphorylation/activation of Akt, whilst having an activating effect on AMPK. Neither of the cell lines reacted accordingly to this fact.

Overall, the flow cytometry did not provide the results expected. An attempt has been made to find sources to back up the findings in this experiment, but unfortunately that proved very difficult and all the sources that has been utilized clearly state that the expected effects of metformin and DCA should be an inactivation of the p-Akt to Akt as well as an activation of the AMPK to p-AMPK.

As well as the literature indicating a different result, the results from both alamarBlue and CCK-8 lead to the belief that an inhibition of the tumor promoters would be seen after metformin treatment. The metformin proved effective on both cell lines during the other assays. It is possible that its impact on the cells simply were other alterations than the two proteins followed during the flow cytometry. When it comes to DCA the former results from both alamarBlue and CCK-8 gave an indication of possible increase in tumor promoters, meaning an increase in p-Akt and AMPK should have been seen.

Why the flow experiment provided the results that it did is to this date unclear. It might be due to low concentrations in the medications, mistakes made during the experiment preparation, mutations in the cell or multiple other factors not taken into consideration.

6 Conclusion

The results from the experiments of this thesis found that HCT116 and SW948 responds greatly, in terms of decreasing viability, by the exposure of metformin, where 6 mM incubated for 48 hours generated the lowest values for both cell lines. DCA has an opposite effect, and the viability increased proportional to the concentration, where 6 mM incubated for 48 hours generated the highest values. This leads to the conclusion that both HCT116 and SW948 are more reliable on the mitochondrial metabolism rather than the glycolysis, but further testing is required.

The cell lines expressed different results for the proteins tested, but metformin was the only compound that generated significant shifts in the flow cytometry. The results did not resemble the expected protein expressions based on the suggested effects of both metformin and DCA on the specific proteins and their corresponding phosphorylated/activated forms.

7 References

1. World Health Organization. Cancer. 2022 February 3.
2. American Cancer Society. cancer.org. [Online]. [cited 2022 4 19. Available from: <https://www.cancer.org/treatment/understanding-your-diagnosis/history-of-cancer.html>.
3. Mary Crowley Cancer Research. marycrowley.org. [Online]. [cited 2022 04 20. Available from: <https://www.marycrowley.org/groundbreaking-research/cancer-pathways/>.
4. Boris Klimovich SMJS+SEMKANMMOTTS. Loss of p53 function at late stages of tumorigenesis confers ARF-dependent vulnerability to p53 reactivation therapy. PROCEEDINGS OF THE NATIONAL ACADEMY OF SCIENCES. 2019 Oct.
5. Mizuho Nakayama MO. Mutant p53 in colon cancer. Journal of Molecular Cell Biology. 2019 Apr: p. 267–276.
6. National Human Genome Research Institute. genome.gov. [Online].; 2015 [cited 2022 04 20. Available from: <https://www.genome.gov/about-genomics/fact-sheets/Biological-Pathways-Fact-Sheet>.
7. Bert Vogelstein KWK. The multistep nature of cancer. Trends in Genetics. 1993: p. 138-141.
8. National cancer institute. Cancer staging. [Online].; 2015 [cited 2022 04 19. Available from: <https://www.cancer.gov/about-cancer/diagnosis-staging/staging>.
9. Bethune R SMBCAT. What happens when we do not operate? Survival following conservative bowel cancer management. Ann R Coll Surg Engl. 2016 Jul: p. 409-412.
10. World Health Organization. GUIDE TO CANCER EARLY DIAGNOSIS geneva: WHO Document Production Services; 2018.
11. Arruebo M VNSGBea. Assessment of the evolution of cancer treatment therapies. Cancers (Basel). 2011 Aug: p. 3279-3330.
12. Pucci C MCCG. Innovative approaches for cancer treatment: current perspectives and new challenges. Ecancermedicalsecience. 2019 Sep.
13. Luengo A GDVHM. Targeting Metabolism for Cancer Therapy. Cell Chem Biol. 2017 Sep: p. 1161-1180.

14. O'Connor CM&AJU. Essentials of Cell Biology Cambridge, MA: NPG Education; 2010.
15. National Library of Medicine. [Online].; 2021 [cited 2022 05 12. Available from: <https://medlineplus.gov/genetics/understanding/basics/cell/>.
16. National Human Genome Research Institute. Biological Pathways Fact Sheet. [Online].; 2020 [cited 2022 05 12. Available from: <https://www.genome.gov/about-genomics/fact-sheets/Biological-Pathways-Fact-Sheet>.
17. Cell Energy and Cell Functions. [Online]. [cited 2022 05 13. Available from: <https://www.nature.com/scitable/topicpage/cell-energy-and-cell-functions-14024533/>.
18. Jang M,KS&LJ. Cancer cell metabolism: implications for therapeutic targets. Exp Mol Med. 2013 Jan.
19. Kumari A. Chapter 1 - Glycolysis. In Kumari A, editor. Sweet Biochemistry.: Academic Press; 2018. p. 1-5.
20. Rajagopal KA&I. libretexts. [Online].; 2021 [cited 2022 05 13. Available from: [https://bio.libretexts.org/Bookshelves/Biochemistry/Book%3A_Biochemistry_Free_and_Easy_\(Ahern_and_Rajagopal\)/06%3A_Metabolism_I_-_Oxidative_Reductive_Processes/6.03%3A_Glycolysis](https://bio.libretexts.org/Bookshelves/Biochemistry/Book%3A_Biochemistry_Free_and_Easy_(Ahern_and_Rajagopal)/06%3A_Metabolism_I_-_Oxidative_Reductive_Processes/6.03%3A_Glycolysis).
21. Chaudhry R VM. Biochemistry, Glycolysis. [Online].; 2021 [cited 2022 05 13. Available from: <https://www.ncbi.nlm.nih.gov/books/NBK482303/>.
22. Khan Academy. Khan Academy: The Citric Acid Cycle. [Online]. [cited 2022 05 15. Available from: <https://www.khanacademy.org/science/biology/cellular-respiration-and-fermentation/pyruvate-oxidation-and-the-citric-acid-cycle/a/the-citric-acid-cycle>.
23. Veech RL. Tricarboxylic Acid Cycle. In William J. Lennarz MDL, editor. Encyclopedia of Biological Chemistry.: Academic Press; 2013. p. 436-440.
24. Cook KM SHMKGHHE. Targeting Glucose Metabolism of Cancer Cells with Dichloroacetate to Radiosensitize High-Grade Gliomas. International Journal of Molecular Sciences. 2021.
25. Khanna A. Teachme Physiology. [Online].; 2021 [cited 2022 05 13. Available from: <https://teachmephysiology.com/biochemistry/atp-production/tca-cycle-2/>.
26. Zhao RZ JSZLYZ. Mitochondrial electron transport chain, ROS generation and uncoupling. Int J Mol Med. 2019 Jul: p. 3-15.

27. Khan Academy. Khan Academy. [Online]. [cited 2022 05 13. Available from: <https://www.khanacademy.org/science/ap-biology/cellular-energetics/cellular-respiration-ap/a/oxidative-phosphorylation-etc>.
28. Raimondi V,CF&CV. Oncogenic pathways and the electron transport chain: a dangeROS liaison. *British Journal of Cancer*. 2020: p. 168–181.
29. Raimondi V,CF&CV. Oncogenic pathways and the electron transport chain: a dangeROS liaison. *Br J Cancer*. 2020 Jan 21: p. 168-181.
30. Zou Z TTLHZX. mTOR signaling pathway and mTOR inhibitors in cancer: progress and challenges. *Cell & Bioscience*. 2020 Mar 10.
31. S.H A. Targeting mTOR pathway: A new concept in cancer therapy. *Indian J Med Paediatr oncol*. 2020: p. 132-136.
32. Cell Signaling Technology. Phospho-Akt (Ser473) Antibody #9271. [Online]. [cited 2022 05 14. Available from: <https://www.cellsignal.com/products/primary-antibodies/phospho-akt-ser473-antibody/9271>.
33. national library of medicine. national library of medicine. [Online].; 2022 [cited 2022 05 14. Available from: <https://www.ncbi.nlm.nih.gov/gene/207>.
34. Vasou O,SL,AM,PA,PE,&PE. Detection of pAkt protein in imprint cytology of invasive breast cancer: Correlation with HER2/neu, hormone receptors, and other clinicopathological variables. *CytoJournal*. 2015 Mar 25.
35. A.Lothe SADPWEANTGELRAL. Portrait of the PI3K/AKT pathway in colorectal cancer. *Biochimica et Biophysica Acta (BBA) - Reviews on Cancer*. 2015 Jan: p. 104-121.
36. Zou Z,TT,LHea. mTOR signaling pathway and mTOR inhibitors in cancer: progress and challenges.. *Cell Biosci*. 2020 Mar 10.
37. Zakikhani M,BM,PEea. Metformin and rapamycin have distinct effects on the AKT pathway and proliferation in breast cancer cells. *Breast Cancer Res Trea*. 2010 Feb: p. 271–279.
38. Liang Y,ZD,ZL,HY,HL,HX,LL,WY,LL,ZH,WT,YM,WJ,&MX. Dichloroacetate Overcomes Oxaliplatin Chemoresistance in Colorectal Cancer through the miR-543/PTEN/Akt/mTOR Pathway. Liang, Y., Zhu, D., Zhu, L., Hou, Y., Hou, L., Huang, X., Li, L., Wang, Y., Li, L., Zou, H., Wu, T., Yao, M., Wang, J., & Meng, X. (2019).

- Dichloroacetate Overcomes Oxaliplatin Chemoresistance in Colorectal Cancer through the miR-543/PTEN/Akt/mTOR Pathway. 2019: p. 6037-6047.
39. Diana Vara-Ciruelos FMRaDGH. The strange case of AMPK and cancer: Dr Jekyll or Mr Hyde?†. *open biology*. 2019 Jul 10.
40. David G Hardie BESAB. AMPK: An Energy-Sensing Pathway with Multiple Inputs and Outputs. *Trends in Cell Biology*. 2015 Nov.
41. Hardie DG. Molecular Pathways: Is AMPK a Friend or a Foe in Cancer? *Clinical cancer research : an official journal of the American Association for Cancer Research*. 2015 Jul: p. 07.
42. Liang Y,ZD,HLea. MiR-107 confers chemoresistance to colorectal cancer by targeting calcium-binding protein 39. *Br J Cancer*. 2020 Mar: p. 705–714.
43. Phospho-AMPK α (Thr172) Antibody #2531. [Online]. [cited 2022 05 14. Available from: [https://www.cellsignal.com/products/primary-antibodies/phospho-ampka-thr172-antibody/2531#:~:text=Phospho%2DAMPKalpha%20\(Thr172\)%20Antibody,regulatory%20beta%20or%20gamma%20subunits.](https://www.cellsignal.com/products/primary-antibodies/phospho-ampka-thr172-antibody/2531#:~:text=Phospho%2DAMPKalpha%20(Thr172)%20Antibody,regulatory%20beta%20or%20gamma%20subunits.)
44. Wen Zhang SLZXH&KT. Targeting Tumor Metabolism for Cancer Treatment: Is Pyruvate Dehydrogenase Kinases (PDKs) a Viable Anticancer Target? *International Journal of Biological Sciences*. 2015 Nov: p. 1390-1400.
45. Zhou L LLCWZTJXGXHLYC. Dichloroacetic acid upregulates apoptosis of ovarian cancer cells by regulating mitochondrial function. *Onco Targets Ther*. 2019 Feb: p. 1729-1739.
46. Sei-Jung Lee CCY. Colorectal cancer cells – proliferation, survival and invasion by lysophosphatidic acid. *Int J Biochem Cell Biol*. 2010 Dec: p. 1907-1910.
47. Mayo Clinic. *mayoclinic.org*. [Online].; 2021 [cited 2022 04 20. Available from: <https://www.mayoclinic.org/diseases-conditions/colon-cancer/symptoms-causes/syc-20353669>.
48. Medlineplus. PIK3CA gene. [Online].; 2021 [cited 2022 05 14. Available from: <https://medlineplus.gov/genetics/gene/pik3ca/>.
49. Medicine NLo. *medlineplus.gov/*. [Online].; 2020 [cited 2022 04 21. Available from: <https://medlineplus.gov/druginfo/meds/a696005.html>.

50. Wheaton WW WSHRea. Metformin inhibits mitochondrial complex I of cancer cells to reduce tumorigenesis. 2014 May 10.
51. Mohamad-Yehia El-Mir VNEFNAMRXL. Dimethylbiguanide Inhibits Cell Respiration via an Indirect Effect Targeted on the Respiratory Chain Complex I*. Journal of Biological Vhemistry. 2000 Jan: p. 223-228.
52. James MO JSZGSMHZSP. Therapeutic applications of dichloroacetate and the role of glutathione transferase zeta-1. Pharmacol Ther. 2017: p. 166-180.
53. Millipore Corporation. millipore.com. [Online].; 2012 [cited 2022 04 21. Available from:
<http://www.icms.qmul.ac.uk/flowcytometry/instruments/muse/Muse%20Cell%20Analyzer%20-%200500-3115.pdf>.
54. Merck. How Muse Cell Analyzer Works. [Online]. [cited 2022 05 15. Available from:
https://www.merckmillipore.com/NO/en/20130820_202736.
55. LibreTexts. chem.libretexts.org. [Online].; 2022 [cited 2022 04 22. Available from:
[https://chem.libretexts.org/Bookshelves/Physical_and_Theoretical_Chemistry_Textbook_Maps/Supplemental_Modules_\(Physical_and_Theoretical_Chemistry\)/Kinetics/02%3A_Reaction_Rates/2.01%3A_Experimental_Determination_of_Kinetics/2.1.05%3A_Spectrophotometry](https://chem.libretexts.org/Bookshelves/Physical_and_Theoretical_Chemistry_Textbook_Maps/Supplemental_Modules_(Physical_and_Theoretical_Chemistry)/Kinetics/02%3A_Reaction_Rates/2.01%3A_Experimental_Determination_of_Kinetics/2.1.05%3A_Spectrophotometry).
56. Merck. Cell Counting Kit - 8. [Online]. [cited 2022 05 15. Available from:
<https://www.sigmaaldrich.com/NO/en/product/sigma/96992>.
57. Picot J GCLVKCBC. Flow cytometry: retrospective, fundamentals and recent instrumentation. Cytotechnology. 2012 Jan 21: p. 109-130.
58. AAT Bioquest. AAT Bioquest. [Online].; 2020 [cited 2022 05 14. Available from:
<https://www.aatbio.com/resources/faq-frequently-asked-questions/What-is-FSC-and-SSC-in-flow-cytometry>.
59. Tidwell TR. UIS.brage. [Online].; 2021 [cited 2022 05 14. Available from:
https://uis.brage.unit.no/uis-xmlui/bitstream/handle/11250/2985155/PhD_TR_Tidwell_open.pdf?sequence=3.
60. National Human Genome Research Institute. genome.gov. [Online].; 2020 [cited 2022 04 20. Available from: <https://www.genome.gov/about-genomics/fact-sheets/Biological-Pathways-Fact-Sheet>.

61. Diana Vara-Ciruelos FMRaDGH. The strange case of AMPK and cancer: Dr Jekyll or Mr Hyde?†. 2019 Jul 10.

8 Appendix

Appendix 1

Table 6: Final medication concentrations used in our project for metformin and DCA, both separate and combined.

1 mM met
3 mM met
6 mM met
1 mM DCA
3 mM DCA
6 mM DCA
1 mM met + 1 mM DCA
1 mM met + 3 mM DCA
1 mM met + 6 mM DCA
3 mM met + 1 mM DCA
3 mM met + 3 mM DCA
3 mM met + 6 mM DCA
6 mM met + 1 mM DCA
6 mM met + 3 mM DCA
6 mM met + 6 mM DCA

Table 7: Calculations of the amounts of medium and medications needed for each combination solution

Concentration in Well	Target concentration met ($C_{t_{met}}$ mM)	Target concentration DCA ($C_{t_{DCA}}$ mM)	Target Volume Total (V_{target} ml)	Volume stock met (V_{met} μ l)	Volume stock DCA (V_{DCA} μ l)	Medium ($V_{t_{medium}}$ μ l)
1 mM met	2	0	2	40	0	1960
3 mM met	6	0	2	120	0	1880
6 mM met	12	0	2	240	0	1760
1 mM DCA	0	2	2	0	40	1960
3 mM DCA	0	6	2	0	120	1880
6 mM DCA	0	12	2	0	240	1760
1 mM met + 1 mM DCA	2	2	2	40	40	1920
1 mM met + 3 mM DCA	2	6	2	40	120	1840
1 mM met + 6 mM DCA	2	12	2	40	240	1720
3 mM met + 1 mM DCA	6	2	2	120	40	1840
3 mM met + 3 mM DCA	6	6	2	120	120	1760
3 mM met + 6 mM DCA	6	12	2	120	240	1640
6 mM met + 1 mM DCA	12	2	2	240	40	1720
6 mM met + 3 mM DCA	12	6	2	240	120	1640
6 mM met + 6 mM DCA	12	12	2	240	240	1520

Table 8: 96-well plate setup for alamarBlue assay on cell line HCT116 and SW948 containing viable cells ranging from 5000-30000, blank controls, and PBS.

	1	2	3	4	5	6	7	8	9	10	11	12
A	PB S	PBS	PBS	PBS	PBS	PBS	PBS	PBS	PBS	PB S	PB S	PB S
B	PB S	Blan k	Blan k	Blan k	Blan k	3000 0	3000 0	3000 0	3000 0	PB S	PB S	PB S
C	PB S	5000 0	5000 0	5000 0	5000 0	PBS	PBS	PBS	PBS	PB S	PB S	PB S
D	PB S	1000 0	1000 0	1000 0	1000 0	PBS	PBS	PBS	PBS	PB S	PB S	PB S
E	PB S	1500 0	1500 0	1500 0	1500 0	PBS	PBS	PBS	PBS	PB S	PB S	PB S
F	PB S	2000 0	2000 0	2000 0	2000 0	PBS	PBS	PBS	PBS	PB S	PB S	PB S
G	PB S	2500 0	2500 0	2500 0	2500 0	PBS	PBS	PBS	PBS	PB S	PB S	PB S
H	PB S	PBS	PBS	PBS	PBS	PBS	PBS	PBS	PBS	PB S	PB S	PB S

Table 9: 96-well plate setup for alamarBlue treatment assay on cell line HCT116 and SW948 containing 10000- and 15000 viable cells, respectively, with different concentrations of metformin of DCA (mM), blank controls, and PBS.

	1	2	3	4	5	6	7	8	9	10	11	12
A	PBS	PBS	PBS	PBS	PBS	PBS	PBS	PBS	PBS	PBS	PBS	PBS
B	PBS	Blank	Blank	Blank	Blank	6.0	6.0	6.0	6.0	PBS	PBS	PBS
C	PBS	0.0	0.0	0.0	0.0	0.25	0.25	0.25	0.25	PBS	PBS	PBS
D	PBS	0.25	0.25	0.25	0.25	0.5	0.5	0.5	0.5	PBS	PBS	PBS
E	PBS	0.5	0.5	0.5	0.5	1.0	1.0	1.0	1.0	PBS	PBS	PBS
F	PBS	1.0	1.0	1.0	1.0	3.0	3.0	3.0	3.0	PBS	PBS	PBS
G	PBS	3.0	3.0	3.0	3.0	6.0	6.0	6.0	6.0	PBS	PBS	PBS
H	PBS	PBS	PBS	PBS	PBS	PBS	PBS	PBS	PBS	PBS	PBS	PBS

Metformin
DCA

Table 10: 96-well plate setup showing the placement of different medication combinations including wells treated with water rather than medication.

1	2	3	4	5	6	7	8	9	10	11	12	
P B S	PBS	PBS	PBS	PBS	PBS	PBS	PBS	PBS	PBS	PBS	PBS	P B S
P B S	0 mM	0 mM	0 mM	0 mM	3 mM met + 6 mM DCA	3 mM met + 6 mM DCA	3 mM met + 6 mM DCA	3 mM met + 6 mM DCA	1 mM DCA	3 mM DCA	P B S	
P B S	1 mM met + 1 mM DCA	1 mM met + 1 mM DCA	1 mM met + 1 mM DCA	Water	6 mM met + 1 mM DCA	6 mM met + 1 mM DCA	6 mM met + 1 mM DCA	6 mM met + 1 mM DCA	1 mM DCA	3 mM DCA	P B S	
P B S	1 mM met + 3 mM DCA	1 mM met + 3 mM DCA	1 mM met + 3 mM DCA	Water	6 mM met + 3 mM DCA	6 mM met + 3 mM DCA	6 mM met + 3 mM DCA	6 mM met + 3 mM DCA	1 mM DCA	3 mM DCA	P B S	
P B S	1 mM met + 6 mM DCA	1 mM met + 6 mM DCA	1 mM met + 6 mM DCA	Water	6 mM met + 6 mM DCA	6 mM met + 6 mM DCA	6 mM met + 6 mM DCA	6 mM met + 6 mM DCA	6 mM DCA	6 mM DCA	P B S	
P B S	3 mM met + 1 mM DCA	3 mM met + 1 mM DCA	3 mM met + 1 mM DCA	Water	1 mM metfor min	1 mM metform in	1 mM metform in	6 mM metform in	6 mM metfor min	6 mM metfor min	P B S	
P B S	3 mM met + 3 mM DCA	3 mM met + 3 mM DCA	3 mM met + 3 mM DCA	3 mM met + 3 mM DCA	3 mM metfor min	3 mM metform in	3 mM metform in	Blank	Blank	Blank	P B S	

P											P
B											B
S	PBS	PBS	PBS	PBS	PBS	PBS	PBS	PBS	PBS	PBS	S

Table 5: 96-well plate setup showing the placement of different medication combinations in this setup no wells contain added water.

Appendix 2

Table 6: Arithmetic mean and S.D. of every resazurin fluorescence value of each parallel from HCT116 colorectal cancer cells with 24 hours treatment with different concentrations of metformin. Pn displays the passage number for the replicate.

Metformin (mM):	P25:	P27:	P28:	Arithmetic mean:	Standard deviation:
0	6,28E+08	5,16E+08	7,65E+08	6,36E+08	1,02E+08
0,25	6,26E+08	5,36E+08	7,44E+08	6,35E+08	8,51E+07
0,5	6,50E+08	5,68E+08	9,15E+08	7,11E+08	1,48E+08
1	5,60E+08	5,98E+08	8,64E+08	6,74E+08	1,35E+08
3	5,88E+08	4,26E+08	8,53E+08	6,23E+08	1,76E+08
6	5,02E+08	4,51E+08	6,54E+08	5,36E+08	8,64E+07

Table 7: Arithmetic mean and S.D. of every resazurin fluorescence value of each parallel from HCT116 colorectal cancer cells with 48 hours treatment with different concentrations of metformin. Pn displays the passage number for the replicate.

Metformin (mM):	P27:	P28:	P30:	Arithmetic mean:	Standard deviation:
0	6,18E+08	5,70E+08	8,56E+08	6,81E+08	1,25E+08
0,25	6,94E+08	5,00E+08	6,57E+08	6,17E+08	8,42E+07
0,5	6,38E+08	4,75E+08	6,69E+08	5,94E+08	8,50E+07
1	4,91E+08	4,09E+08	5,96E+08	4,99E+08	7,67E+07
3	4,36E+08	3,45E+08	4,13E+08	3,98E+08	3,86E+07

Table 8: Arithmetic mean and S.D. of every resazurin fluorescence value of each parallel from SW948 colorectal cancer cells with 24 hours treatment with different concentrations of metformin. Pn displays the passage number for the replicate.

Metformin (mM):	P12:	P13:	P13:	P17:	Arithmetic mean:	Standard deviation:
0	5,99E+08	8,44E+08	5,61E+08	5,92E+08	6,49E+08	1,13E+08
0.25	6,14E+08	8,32E+08	5,31E+08	6,15E+08	6,48E+08	1,12E+08
0.5	6,22E+08	8,42E+08	5,37E+08	5,86E+08	6,47E+08	1,17E+08
1.0	6,20E+08	8,09E+08	5,90E+08	5,04E+08	6,31E+08	1,11E+08
3.0	5,65E+08	6,38E+08	5,59E+08	3,40E+08	5,26E+08	1,11E+08
6.0	5,35E+08	5,51E+08	5,89E+08	4,08E+08	5,21E+08	6,79E+07

Table 9: Arithmetic mean and S.D. of every resazurin fluorescence value of each parallel from SW948 colorectal cancer cells with 48 hours treatment with different concentrations of metformin. Pn displays the passage number for the replicate.

Metformin (mM):	P12:	P13:	P13:	P17:	Arithmetic mean:	Standard deviation:
0	6,86E+08	5,95E+08	4,12E+08	6,33E+08	5,82E+08	1,03E+08
0.25	6,68E+08	5,27E+08	3,90E+08	5,41E+08	5,32E+08	9,87E+07
0.5	6,63E+08	5,12E+08	3,94E+08	4,07E+08	4,94E+08	1,08E+08
1.0	5,80E+08	5,20E+08	4,34E+08	3,66E+08	4,75E+08	8,14E+07
3.0	5,27E+08	4,50E+08	4,11E+08	3,13E+08	4,25E+08	7,69E+07

6.0	3,18E+08	3,89E+08	4,33E+08	1,67E+08	3,27E+08	1,01E+08
-----	----------	----------	----------	----------	----------	----------

Table 10: Arithmetic mean and S.D. of every resazurin fluorescence value of each parallel from HCT116 colorectal cancer cells with 24 hours treatment with different concentrations of DCA. Pn displays the passage number for the replicate.

DCA (mM):	P25:	P27:	P28:	Arithmetic mean:	Standard deviation:
0	6,28E+08	5,16E+08	7,65E+08	6,36E+08	1,02E+08
0,25	5,81E+08	5,11E+08	8,70E+08	6,54E+08	1,55E+08
0,5	5,64E+08	5,06E+08	8,95E+08	6,55E+08	1,71E+08
1	5,90E+08	5,21E+08	9,19E+08	6,77E+08	1,74E+08
3	6,37E+08	5,66E+08	9,52E+08	7,18E+08	1,68E+08
6	6,95E+08	4,35E+08	1,12E+09	7,49E+08	2,81E+08

Table 11: Arithmetic mean and S.D. of every resazurin fluorescence value of each parallel from HCT116 colorectal cancer cells with 48 hours treatment with different concentrations of DCA. Pn displays the passage number for the replicate.

DCA (mM):	P25:	P27:	P28:	Arithmetic mean:	Standard deviation:
0	6,18E+08	5,70E+08	8,56E+08	6,81E+08	1,25E+08
0,25	7,19E+08	6,99E+08	6,92E+08	7,03E+08	1,14E+07
0,5	7,02E+08	6,81E+08	6,97E+08	6,93E+08	8,99E+06
1	6,73E+08	5,61E+08	6,29E+08	6,21E+08	4,60E+07
3	7,29E+08	6,67E+08	7,44E+08	7,13E+08	3,33E+07
6	8,29E+08	8,38E+08	1,10E+09	9,23E+08	1,27E+08

Table 12: Arithmetic mean and S.D. of every resazurin fluorescence value of each parallel from SW948 colorectal cancer cells with 24 hours treatment with different concentrations of DCA. Pn displays the passage number for the replicate.

DCA (mM):	P12:	P13:	P13:	P17:	Arithmetic mean:	Standard deviation:
0	5,61E+08	8,44E+08	5,22E+08	4,82E+08	6,02E+08	1,42E+08
0.25	5,19E+08	7,57E+08	4,63E+08	3,67E+08	5,26E+08	1,44E+08
0.5	5,09E+08	7,27E+08	4,99E+08	2,80E+08	5,04E+08	1,58E+08
1.0	4,66E+08	6,73E+08	5,05E+08	2,52E+08	4,74E+08	1,50E+08
3.0	4,70E+08	5,42E+08	5,53E+08	2,08E+08	4,43E+08	1,40E+08
6.0	4,35E+08	5,25E+08	4,82E+08	1,16E+08	3,90E+08	1,61E+08

Table 13: Arithmetic mean and S.D. of every resazurin fluorescence value of each parallel from SW948 colorectal cancer cells with 48 hours treatment with different concentrations of DCA. Pn displays the passage number for the replicate.

DCA (mM):	P12:	P13:	P13:	Arithmetic mean:	Standard deviation:
0	6,33E+08	5,95E+08	6,86E+08	6,38E+08	3,73E+07
0.25	6,19E+08	5,93E+08	6,96E+08	6,36E+08	4,37E+07
0.5	6,18E+08	6,07E+08	6,76E+08	6,34E+08	3,03E+07
1.0	6,20E+08	5,60E+08	7,19E+08	6,33E+08	6,56E+07
3.0	6,64E+08	6,40E+08	7,65E+08	6,90E+08	5,42E+07
6.0	6,97E+08	6,83E+08	8,40E+08	7,40E+08	7,09E+07

Table 14: % resazurin fluorescence values of passages from HCT116, 24 hours treatment with metformin normalized to the untreated control, the arithmetic means of all passages and their S.D. values. Pn displays the passage number for the replicate.

Metformin (mM):	P25:	P27:	P28:	Arithmetic mean:	Standard deviation:
0,25	99,64	103,97	97,23	100,28	2,79
0,5	103,46	110,13	119,55	111,05	6,60
1	89,17	116,01	112,96	106,05	12,00
3	93,63	82,62	111,55	95,94	11,92
6	79,86	87,50	85,54	84,30	3,24

Table 15: % resazurin fluorescence values of passages from HCT116, 48 hours treatment with metformin normalized to the untreated control, the arithmetic mean of all passages and their S.D. values. Pn displays the passage number for the replicate.

Metformin (mM):	P27:	P28:	P30:	Arithmetic mean:	Standard deviation:
0,25	112,28	87,65	76,79	92,24	14,84
0,5	103,16	83,31	78,20	88,22	10,77
1	79,48	71,71	69,71	73,63	4,21
3	70,60	60,54	48,28	59,81	9,13
6	73,80	53,95	44,35	57,36	12,26

Table 16: % resazurin fluorescence values of passages from SW948, 24 hours treatment with metformin normalized to the untreated control, the total arithmetic mean of all passages and their S.D. values. Pn displays the passage number for the replicate.

Metformin (mM):	P12:	P13:	P13:	P17:	Arithmetic mean:	Standard deviation:
0.25	102,50	98,66	94,66	103,87	99,92	3,59
0.5	103,84	99,81	95,76	99,03	99,61	2,88
1.0	103,51	95,84	105,19	85,12	97,41	7,93
3.0	94,32	75,58	99,74	57,45	81,77	16,66
6.0	89,32	65,34	104,93	68,93	82,13	16,03

Table 17: % resazurin fluorescence values of passages from SW948, 48 hours treatment with metformin normalized to the untreated control, the arithmetic mean of all passages and their S.D. values. Pn displays the passage number for the replicate

Metformin (mM):	P12:	P13:	P13:	P17:	Arithmetic mean:	Standard deviation:
0.25	97,48	88,56	94,56	85,43	91,51	4,76
0.5	96,69	85,94	95,67	64,31	85,65	13,02
1.0	84,56	87,29	105,30	57,81	83,74	16,96
3.0	76,79	75,67	99,73	49,45	75,41	17,80
6.0	46,41	65,39	105,03	26,43	60,81	29,01

Table 18: % resazurin fluorescence values of passages from HCT116, 24 hours treatment with DCA normalized to the untreated control, the arithmetic mean of all passages and their S.D. values. Pn displays the passage number for the replicate.

DCA (mM):	P25:	P27:	P28:	Arithmetic mean:	Standard deviation:
-----------	------	------	------	------------------	---------------------

0,25	92,58	99,16	113,71	101,82	8,83
0,5	89,85	98,14	117,03	101,67	11,37
1	93,91	101,06	120,13	105,04	11,07
3	101,37	109,83	124,48	111,89	9,54
6	110,61	84,28	146,00	113,63	25,29

Table 19: % resazurin fluorescence values of passages from HCT116, 48 hours treatment with DCA normalized to the untreated control, the arithmetic mean of all passages and their S.D. values. Pn displays the passage number for the replicate.

DCA (mM):	P25:	P27:	P28:	Arithmetic mean:	Standard deviation:
0,25	116,35	122,60	80,89	106,61	18,37
0,5	113,61	119,44	81,49	104,85	16,69
1	108,85	98,35	73,54	93,58	14,80
3	117,89	117,03	87,01	107,31	14,36
6	134,18	147,02	128,80	136,67	7,64

Table 20: % resazurin fluorescence values of passages from SW948, 24 hours treatment with DCA normalized to the untreated control, the arithmetic mean of all passages and their S.D. values. Pn displays the passage number for the replicate.

DCA (mM):	P12:	P13:	P13:	P17:	Arithmetic mean:	Standard deviation:
0.25	92,51	89,69	88,70	57,07	81,99	14,46
0.5	90,73	86,14	95,59	43,50	78,99	20,76
1.0	83,07	79,74	96,74	29,36	72,23	25,56
3.0	83,78	64,22	105,94	24,25	69,55	30,03
6.0	77,54	62,20	92,34	13,56	61,41	29,61

Table 21: % resazurin fluorescence values of passages from SW948, 48 hours treatment with DCA normalized to the untreated control, the arithmetic mean of all passages and their S.D. values. Pn displays the passage number for the replicate.

DCA (mM):	P12:	P13:	P13:	Arithmetic mean:	Standard deviation:
0.25	97,79	99,66	101,46	99,64	1,50
0.5	97,63	102,02	98,54	99,40	1,89
1.0	97,95	94,12	104,81	98,96	4,42
3.0	104,90	107,56	111,52	107,99	2,72
6.0	110,11	114,79	122,45	115,78	5,09

Appendix 3

Table 22: Arithmetic mean and S.D. of every CCK-8 absorbance value of each parallel from HCT116 colorectal cancer cells with 24 hours treatment with different concentrations of metformin. Pn displays the passage number for the replicate.

Metformin (mM):	P21	P27:	P28:	P30:	Arithmetic mean:	Standard deviation:
0	2,87E+00	2,45E+00	2,76E+00	2,75E+00	2,71E+00	1,59E-01
0,25	2,89E+00	2,28E+00	2,84E+00	2,85E+00	2,71E+00	2,50E-01
0,5	2,82E+00	2,48E+00	2,83E+00	2,62E+00	2,69E+00	1,45E-01
1	2,84E+00	2,49E+00	2,74E+00	2,54E+00	2,65E+00	1,44E-01
3	2,97E+00	2,38E+00	2,64E+00	2,69E+00	2,67E+00	2,09E-01
6	2,63E+00	1,99E+00	2,83E+00	2,67E+00	2,53E+00	3,21E-01

Table 23: Arithmetic mean and S.D. of every CCK-8 absorbance value of each parallel from HCT116 colorectal cancer cells with 48 hours treatment with different concentrations of metformin. Pn displays the passage number for the replicate.

Metformin (mM):	P27	P28:	P30:	Arithmetic mean:	Standard deviation:
0	2,78E+00	2,88E+00	1,87E+00	2,51E+00	4,55E-01
0,25	2,86E+00	2,92E+00	1,51E+00	2,43E+00	6,50E-01
0,5	2,80E+00	2,85E+00	1,14E+00	2,26E+00	7,94E-01
1	2,25E+00	2,31E+00	7,38E-01	1,77E+00	7,27E-01
3	1,88E+00	2,07E+00	5,03E-01	1,48E+00	6,97E-01
6	1,62E+00	1,92E+00	4,47E-01	1,33E+00	6,35E-01

Table 24: Arithmetic mean and S.D. of every CCK-8 absorbance value of each parallel from SW948 colorectal cancer cells with 24 hours treatment with different concentrations of metformin. Pn displays the passage number for the replicate.

Metformin (mM):	P12:	P13:	P13:	P17:	Arithmetic mean:	Standard deviation:
0	2,8818	2,6956	2,8516	2,7252	2,7886	0,0796
0.25	2,7863	2,6120	2,8481	2,5456	2,6980	0,1234
0.5	2,5262	2,2675	2,6769	2,1553	2,4065	0,2061
1.0	2,3397	1,7379	2,0695	1,7389	1,9715	0,2519
3.0	2,0047	1,4289	1,3160	1,1325	1,4705	0,3261
6.0	2,2147	1,3364	1,2251	1,2502	1,5066	0,4109

Table 25: Arithmetic mean and S.D. of every CCK-8 absorbance value of each parallel from SW948 colorectal cancer cells with 48 hours treatment with different concentrations of metformin. Pn displays the passage number for the replicate.

Metformin (mM):	P12:	P13:	P13:	P17:	Arithmetic mean:	Standard deviation:
0	2,6912	2,8818	2,7554	2,1238	2,6130	0,2907
0.25	2,5902	2,7863	2,6671	1,7249	2,4421	0,4199
0.5	2,2107	2,5262	2,3618	1,3422	2,1102	0,4572
1.0	1,6892	2,3397	1,6721	1,0693	1,6926	0,4494
3.0	1,3995	2,0047	1,3474	0,8350	1,3966	0,4146
6.0	0,3500	2,2147	0,8900	0,5403	0,9988	0,7282

Table 26: Arithmetic mean and S.D. of every CCK-8 absorbance value of each parallel from HCT116 colorectal cancer cells with 24 hours treatment with different concentrations of DCA. Pn displays the passage number for the replicate.

DCA (mM):	P27:	P28:	P30:	Arithmetic mean:	Standard deviation:
0	2,45E+00	2,76E+00	2,75E+00	1,99E+00	1,16E+00
0,25	2,16E+00	2,87E+00	2,92E+00	2,05E+00	1,08E+00
0,5	2,29E+00	2,87E+00	2,92E+00	2,14E+00	9,81E-01
1	2,29E+00	2,87E+00	2,91E+00	2,27E+00	7,72E-01
3	2,21E+00	2,90E+00	2,68E+00	2,70E+00	3,02E-01
6	2,21E+00	2,78E+00	2,77E+00	3,44E+00	1,50E+00

Table 27: Arithmetic mean and S.D. of every CCK-8 absorbance value of each parallel from HCT116 colorectal cancer cells with 48 hours treatment with different concentrations of DCA. Pn displays the passage number for the replicate.

DCA (mM):	P27:	P28:	P30:	Arithmetic mean:	Standard deviation:
0	2,78E+00	2,88E+00	1,87E+00	2,51E+00	4,55E-01
0,25	2,89E+00	2,97E+00	1,90E+00	2,59E+00	4,87E-01
0,5	2,83E+00	2,99E+00	1,82E+00	2,55E+00	5,19E-01
1	2,90E+00	3,00E+00	2,04E+00	2,65E+00	4,30E-01
3	2,87E+00	2,96E+00	1,93E+00	2,58E+00	4,65E-01
6	2,89E+00	2,93E+00	1,75E+00	2,53E+00	5,48E-01

Table 28: Arithmetic mean and S.D. of every CCK-8 absorbance value of each parallel from SW948 colorectal cancer cells with 24 hours treatment with different concentrations of DCA. Pn displays the passage number for the replicate.

DCA (mM):	P12:	P13:	P13:	P17:	Arithmetic mean:	Standard deviation:
0	2,8818	2,6956	2,8516	2,7252	2,7886	0,0796
0.25	2,7899	2,7915	2,8608	2,4910	2,7333	0,1428
0.5	2,9182	3,0078	2,9803	2,4411	2,8369	0,2308
1.0	2,5879	2,8287	2,9106	2,5208	2,7120	0,1621
3.0	2,6224	2,7865	2,8947	2,2518	2,6389	0,2436
6.0	2,3776	2,7673	2,7695	2,2527	2,5418	0,2309

Table 29: Arithmetic mean and S.D. of every CCK-8 absorbance value of each parallel from SW948 colorectal cancer cells with 48 hours treatment with different concentrations of DCA. Pn displays the passage number for the replicate.

DCA (mM):	P12:	P13:	P13:	P17:	Arithmetic mean:	Standard deviation:
0	2,6912	2,8818	2,7554	2,8491	2,7944	0,0755
0.25	2,8302	2,7899	2,8152	2,8928	2,8320	0,0379
0.5	2,7804	2,9182	2,8580	2,9850	2,8854	0,0755
1.0	2,8696	2,5879	2,6325	2,9481	2,7595	0,1527
3.0	2,8193	2,6224	2,8873	2,9892	2,8296	0,1340
6.0	2,8136	2,3776	2,8364	2,9141	2,7354	0,2099

Table 30: % CCK-8 absorbance values of passages from HCT116, 24 hours treatment with metformin normalized to the untreated control, the arithmetic means of all passages and their S.D. values. Pn displays the passage number for the replicate.

Metformin (mM):	P21	P27:	P28:	P30:	Arithmetic mean:	Standard deviation:
0,25	100,48	93,37	102,83	103,66	100,09	4,05
0,5	98,14	101,51	102,52	95,18	99,34	2,90
1	98,94	101,80	99,37	92,37	98,12	3,49
3	103,21	97,18	95,81	97,88	98,52	2,81
6	91,66	81,29	102,36	97,06	93,09	7,79

Table 31: % CCK-8 absorbance values of passages from HCT116, 48 hours treatment with metformin normalized to the untreated control, the arithmetic means of all passages and their S.D. values. Pn displays the passage number for the replicate.

Metformin (mM):	P27	P28:	P30:	Arithmetic mean:	Standard deviation:
0,25	102,87	101,13	80,66	94,89	10,08
0,5	100,79	98,74	60,89	86,80	18,35
1	81,14	80,04	39,48	66,89	19,39
3	67,69	71,69	26,94	55,44	20,22
6	58,54	66,46	23,89	49,63	18,48

Table 32: % CCK-8 absorbance values of passages from SW948, 24 hours treatment with metformin normalized to the untreated control, the arithmetic means of all passages and their S.D. values. Pn displays the passage number for the replicate.

Metformin (mM):	P12:	P13:	P13:	P17:	Arithmetic mean:	Standard deviation:
0	96,68	96,90	99,88	93,41	96,72	2,29

0.25	87,66	84,12	93,87	79,09	86,18	5,38
0.5	81,19	64,47	72,57	63,81	70,51	7,07
1.0	69,56	53,01	46,15	41,56	52,57	10,62
3.0	76,85	49,57	42,96	45,88	53,82	13,50
6.0	96,68	96,90	99,88	93,41	96,72	2,29

Table 33: % CCK-8 absorbance values of passages from SW948, 48 hours treatment with metformin normalized to the untreated control, the arithmetic means of all passages and their S.D. values. Pn displays the passage number for the replicate.

DCA (mM):	P12:	P13:	P13:	P17:	Arithmetic mean:	Standard deviation:
0	96,25	96,55	96,80	81,22	92,70	6,63
0.25	82,15	87,39	85,72	63,20	79,61	9,66
0.5	62,77	59,94	60,68	50,35	58,43	4,78
1.0	52,00	47,71	48,90	39,31	46,98	4,70
3.0	13,01	20,54	32,30	25,44	22,82	7,04
6.0	96,25	96,55	96,80	81,22	92,70	6,63

Table 34: % CCK-8 absorbance values of passages from HCT116, 24 hours treatment with DCA normalized to the untreated control, the arithmetic means of all passages and their S.D. values. Pn displays the passage number for the replicate.

DCA (mM):	P27:	P28:	P30:	Arithmetic mean:	Standard deviation:
0,25	88,37	103,99	106,30	99,55	7,97

0,5	93,77	103,82	106,09	101,22	5,35
1	93,75	103,94	105,92	101,20	5,33
3	90,55	104,93	97,38	97,62	5,87
6	90,22	100,73	100,86	97,27	4,98

Table 35: % CCK-8 absorbance values of passages from HCT116, 48 hours treatment with DCA normalized to the untreated control, the arithmetic means of all passages and their S.D. values. Pn displays the passage number for the replicate.

DCA (mM):	P27:	P28:	P30:	Arithmetic mean:	Standard deviation:
0,25	104,15	103,05	101,69	102,96	1,01
0,5	102,08	103,78	97,42	101,09	2,69
1	104,50	103,97	109,20	105,89	2,35
3	103,25	102,61	103,24	103,03	0,30
6	104,15	101,82	93,73	99,90	4,47

Table 36: % CCK-8 absorbance values of passages from SW948, 24 hours treatment with DCA normalized to the untreated control, the arithmetic means of all passages and their S.D. values. Pn displays the passage number for the replicate.

DCA (mM):	P12:	P13:	P13:	P17:	Arithmetic mean:	Standard deviation:
0	96,81	103,55	100,32	91,40	98,02	4,50
0.25	101,26	111,58	104,51	89,58	101,73	7,95

0.5	89,80	104,94	102,07	92,50	97,33	6,33
1.0	91,00	103,37	101,51	82,63	94,63	8,38
3.0	82,50	102,66	97,12	82,66	91,24	8,87
6.0	96,81	103,55	100,32	91,40	98,02	4,50

Table 37: % CCK-8 absorbance values of passages from SW948, 48 hours treatment with DCA normalized to the untreated control, the arithmetic means of all passages and their S.D. values. Pn displays the passage number for the replicate.

DCA (mM):	P12:	P13:	P13:	P17:	Arithmetic mean:	Standard deviation:
0	105,17	96,81	102,17	101,53	101,42	2,99
0.25	103,31	101,26	103,73	104,77	103,27	1,27
0.5	106,63	89,80	95,54	103,47	98,86	6,61
1.0	104,76	91,00	104,79	104,92	101,37	5,99
3.0	104,55	82,50	102,94	102,28	98,07	9,02
6.0	105,17	96,81	102,17	101,53	101,42	2,99

Appendix 4

Table 38: Resazurin fluorescence values of each passage from HCT116 with different concentration combinations of metformin and DCA 24 hours treatment, including arithmetic mean and S.D. The values have been normalized to its equivalent singular metformin value. Pn displays the passage number for the replicate.

Metformin and DCA (mM):	P29:	P30-1:	P30-2:	P31-1:	P31-2:	Arithmetic mean:	Standard deviation:	Normalized to metformin
Water		3,83E+08	4,85E+08	5,30E+08	6,71E+08	5,17E+08	1,04E+08	
0 mM control	5,99E+08	3,42E+08	4,37E+08	5,20E+08	6,62E+08	5,12E+08	1,14E+08	
1 mM met + 1 mM DCA	5,02E+08	3,36E+08	2,64E+08	4,23E+08	5,72E+08	4,19E+08	1,11E+08	87,29
1 mM met + 3 mM DCA	3,14E+08	4,34E+08	4,00E+08	4,88E+08	4,82E+08	4,24E+08	6,37E+07	88,33
1 mM met + 6 mM DCA	5,43E+08	4,27E+08	3,30E+08	3,90E+08	5,38E+08	4,46E+08	8,36E+07	92,92
3 mM met + 1 mM DCA	6,89E+08	5,22E+08	3,97E+08	5,05E+08	5,10E+08	5,25E+08	9,36E+07	107,36
3 mM met + 3 mM DCA	9,86E+08	4,95E+08	4,56E+08	6,19E+08	5,50E+08	6,21E+08	1,90E+08	126,99
3 mM met + 6 mM DCA	7,20E+08	5,48E+08	4,52E+08	5,30E+08	6,21E+08	5,74E+08	9,05E+07	117,38

6 mM met + 1 mM DCA	4,57E+08	4,04E+08	4,47E+08	5,78E+08	6,07E+08	4,99E+08	7,94E+07	87,85
6 mM met + 3 mM DCA	5,12E+08	3,81E+08	4,95E+08	5,90E+08	6,02E+08	5,16E+08	7,96E+07	90,85
6 mM met + 6 mM DCA	4,94E+08	3,64E+08	4,45E+08	6,79E+08	6,94E+08	5,35E+08	1,30E+08	94,19
1 mM met	4,47E+08	3,22E+08	4,96E+08	5,05E+08	6,28E+08	4,80E+08	9,88E+07	
3 mM met	3,94E+08	4,58E+08	5,28E+08	5,11E+08	5,54E+08	4,89E+08	5,70E+07	
6 mM met	4,59E+08	4,98E+08	4,90E+08	6,59E+08	7,33E+08	5,68E+08	1,08E+08	
1 mM DCA	4,06E+08	4,10E+08	3,69E+08	5,20E+08	5,86E+08	4,58E+08	8,14E+07	
3 mM DCA	4,27E+08	3,25E+08	2,63E+08	4,01E+08	6,19E+08	4,07E+08	1,21E+08	
6 mM DCA	4,95E+08	3,96E+08	3,47E+08	3,86E+08	6,52E+08	4,55E+08	1,10E+08	

Table 39: Resazurin fluorescence values of each passage from HCT116 with different concentration combinations of metformin and DCA 48 hours treatment, including arithmetic mean and S.D. The values have been normalized to its equivalent singular metformin value. Pn displays the passage number for the replicate.

Metformin and DCA (mM):	P30-1:	P30-2:	P31-1:	P31-2:	Arithmetic mean:	Standard deviation:	Normalized to metformin
Water	8,74E+08	1,16E+09	6,86E+08	7,61E+08	8,70E+08	1,79E+08	
0 mM control	8,35E+08	9,88E+08	8,87E+08	7,55E+08	8,66E+08	8,44E+07	
1 mM met + 1 mM DCA	7,21E+08	8,82E+08	5,12E+08	7,69E+08	7,21E+08	1,34E+08	107,29

1 mM met + 3 mM DCA	5,86E+08	8,52E+08	8,33E+08	6,01E+08	7,18E+08	1,25E+08	106,85
1 mM met + 6 mM DCA	7,23E+08	1,13E+09	8,78E+08	1,02E+09	9,37E+08	1,52E+08	139,43
3 mM met + 1 mM DCA	5,11E+08	4,95E+08	4,84E+08	5,60E+08	5,12E+08	2,92E+07	86,05
3 mM met + 3 mM DCA	6,32E+08	6,80E+08	6,22E+08	5,69E+08	6,26E+08	3,91E+07	105,21
3 mM met + 6 mM DCA	7,69E+08	7,34E+08	7,12E+08	6,85E+08	7,25E+08	3,09E+07	121,85
6 mM met + 1 mM DCA	4,24E+08	5,48E+08	4,01E+08	4,39E+08	4,53E+08	5,64E+07	82,07
6 mM met + 3 mM DCA	5,11E+08	5,47E+08	4,33E+08	3,82E+08	4,68E+08	6,48E+07	84,78
6 mM met + 6 mM DCA	5,93E+08	5,42E+08	5,14E+08	5,43E+08	5,48E+08	2,84E+07	99,28
1 mM met	7,74E+08	7,55E+08	6,20E+08	5,41E+08	6,72E+08	9,63E+07	
3 mM met	5,90E+08	6,00E+08	6,35E+08	5,56E+08	5,95E+08	2,83E+07	
6 mM met	5,71E+08	6,38E+08	5,09E+08	4,89E+08	5,52E+08	5,83E+07	
1 mM DCA	1,06E+09	1,02E+09	1,00E+09	9,51E+08	1,01E+09	3,83E+07	
3 mM DCA	1,11E+09	1,02E+09	1,00E+09	9,97E+08	1,03E+09	4,54E+07	
6 mM DCA	1,14E+09	1,13E+09	1,01E+09	9,65E+08	1,06E+09	7,45E+07	

Table 40: Resazurin fluorescence values of each passage from SW948 with different concentration combinations of metformin and DCA 24 hours treatment, including arithmetic mean and S.D. The values have been normalized to its equivalent singular metformin value. Pn displays the passage number for the replicate.

Metformin and DCA (mM):	P13:	P13:	P17:	Arithmetic mean:	Standard deviation	Normalization to metformin:
Water	5,55E+08	5,89E+08	5,99E+08	5,81E+08	1,86E+07	
0 mM control	4,40E+08	3,70E+08	6,42E+08	4,84E+08	1,15E+08	
1 mM met + 1 mM DCA	4,14E+08	3,91E+08	4,60E+08	4,21E+08	2,88E+07	80,96
1 mM met + 3 mM DCA	5,16E+08	4,36E+08	5,58E+08	5,03E+08	5,06E+07	96,73
1 mM met + 6 mM DCA	4,78E+08	4,53E+08	4,82E+08	4,71E+08	1,30E+07	90,58
3 mM met + 1 mM DCA	6,34E+08	5,65E+08	5,39E+08	5,79E+08	4,01E+07	103,39
3 mM met + 3 mM DCA	5,94E+08	6,14E+08	6,72E+08	6,26E+08	3,32E+07	111,79
3 mM met + 6 mM DCA	6,27E+08	5,64E+08	6,80E+08	6,24E+08	4,76E+07	111,43
6 mM met + 1 mM DCA	5,37E+08	4,97E+08	3,94E+08	4,76E+08	6,02E+07	93,52
6 mM met + 3 mM DCA	5,81E+08	5,27E+08	4,19E+08	5,09E+08	6,73E+07	100,00
6 mM met + 6 mM DCA	5,78E+08	4,94E+08	4,13E+08	4,95E+08	6,73E+07	97,25
1 mM met	4,71E+08	5,18E+08	5,73E+08	5,20E+08	4,19E+07	
3 mM met	5,57E+08	5,08E+08	6,15E+08	5,60E+08	4,38E+07	
6 mM met	5,13E+08	5,02E+08	5,12E+08	5,09E+08	4,81E+06	
1 mM DCA	3,34E+08	3,83E+08	6,81E+08	4,66E+08	1,53E+08	
3 mM DCA	3,47E+08	3,80E+08	6,55E+08	4,61E+08	1,38E+08	

6 mM DCA	3,75E+08	4,28E+08	6,70E+08	4,91E+08	1,29E+08
----------	----------	----------	----------	----------	----------

Table 41: Resazurin fluorescence values of each passage from SW948 with different concentration combinations of metformin and DCA 48 hours treatment, including arithmetic mean and S.D. The values have been normalized to its equivalent singular metformin value. Pn displays the passage number for the replicate.

Metformin and DCA (mM):	P13:	P13:	P17:	Arithmetic mean:	Standard deviation:	Normalization to metformin:
Water	6,18E+08	5,37E+08	6,31E+08	5,95E+08	4,16E+07	
0 mM control	5,63E+08	5,02E+08	7,54E+08	6,06E+08	1,07E+08	
1 mM met + 1 mM DCA	5,40E+08	4,92E+08	7,25E+08	5,86E+08	1,00E+08	115,35
1 mM met + 3 mM DCA	5,50E+08	5,16E+08	7,26E+08	5,97E+08	9,20E+07	117,52
1 mM met + 6 mM DCA	6,18E+08	4,69E+08	7,72E+08	6,20E+08	1,23E+08	122,05
3 mM met + 1 mM DCA	4,55E+08	4,06E+08	4,74E+08	4,45E+08	2,86E+07	103,01
3 mM met + 3 mM DCA	4,66E+08	4,83E+08	5,52E+08	5,00E+08	3,70E+07	115,74
3 mM met + 6 mM DCA	4,45E+08	5,11E+08	7,37E+08	5,64E+08	1,25E+08	130,56
6 mM met + 1 mM DCA	4,10E+08	3,37E+08	4,91E+08	4,13E+08	6,29E+07	107,55
6 mM met + 3 mM DCA	4,18E+08	3,11E+08	4,90E+08	4,06E+08	7,34E+07	105,73
6 mM met + 6 mM DCA	4,31E+08	3,32E+08	4,67E+08	4,10E+08	5,70E+07	106,77
1 mM met	5,10E+08	4,65E+08	5,48E+08	5,08E+08	3,41E+07	

3 mM met	3,83E+08	3,83E+08	5,30E+08	4,32E+08	6,93E+07
6 mM met	3,80E+08	3,34E+08	4,38E+08	3,84E+08	4,27E+07
1 mM DCA	5,73E+08	5,48E+08	6,12E+08	5,78E+08	2,63E+07
3 mM DCA	5,94E+08	6,26E+08	6,38E+08	6,19E+08	1,87E+07
6 mM DCA	6,36E+08	6,13E+08	6,31E+08	6,27E+08	9,86E+06

Table 47: CCK-8 absorbance values of each passage from HCT116 with different concentration combinations of metformin and DCA 24 hours treatment, including arithmetic mean and S.D. The values have been normalized to its equivalent singular metformin value. Pn displays the passage number for the replicate.

Metformin and DCA (mM):	P29:	P39-1:	P39-2:	Arithmetic mean	Standard deviation	Normalization to metformin:
Water		2,7230	2,7202	2,7216	0,0014	
0 mM control	1,6892	2,7771	2,8133	2,4265	0,5216	
1 mM met + 1 mM DCA	1,8088	2,0078	2,4115	2,0760	0,2507	89,1905826
1 mM met + 3 mM DCA	1,5219	2,3557	2,3586	2,0787	0,3937	89,3065819
1 mM met + 6 mM DCA	1,7912	2,3439	2,2675	2,1342	0,2445	91,6910122
3 mM met + 1 mM DCA	1,4236	2,5823	2,6856	2,2305	0,5721	105,891569
3 mM met + 3 mM DCA	1,5478	2,3988	2,5145	2,1537	0,4310	102,245537
3 mM met + 6 mM DCA	1,3099	2,3409	2,2387	1,9631	0,4638	93,1969237

6 mM met + 1 mM DCA	1,7393	2,6154	2,9397	2,4315	0,5070	112,102351
6 mM met + 3 mM DCA	1,5676	2,8436	2,5284	2,3132	0,5427	106,648225
6 mM met + 6 mM DCA	1,6070	2,6410	2,3955	2,2145	0,4411	102,097741
1 mM met	1,6438	2,6370	2,7020	2,3276	0,4843	
3 mM met	1,3860	2,6285	2,3048	2,1064	0,5263	
6 mM met	1,6192	2,2918	2,5962	2,1690	0,4082	
1 mM DCA	3,0074	2,2383	2,3445	2,5301	0,3403	
3 mM DCA	3,0445	2,3114	2,4880	2,6146	0,3124	
6 mM DCA	3,08	2,43	2,45	2,65	0,30	

Table 48: CCK-8 absorbance values of each passage from HCT116 with different concentration combinations of metformin and DCA 48 hours treatment, including arithmetic mean and S.D. The values have been normalized to its equivalent singular metformin value. Pn displays the passage number for the replicate.

Metformin and DCA (mM):	P31:	P39-1:	P39-2:	Arithmetic mean	Standard deviation	Normalized to metformin:
Water	2,7113	2,9637	2,9793	2,8847	0,1228	
0 mM control	2,7974	2,8590	2,9600	2,8721	0,0670	
1 mM met + 1 mM DCA	2,7453	1,7732	1,9839	2,1675	0,4176	82,0308065
1 mM met + 3 mM DCA	2,7440	2,0259	2,1008	2,2902	0,3223	86,6744881

1 mM met + 6 mM DCA	2,6225	2,0055	2,1914	2,2731	0,2584	86,0273247
3 mM met + 1 mM DCA	1,8109	2,9369	2,9215	2,5564	0,5272	99,9726252
3 mM met + 3 mM DCA	2,0596	2,4439	2,2176	2,2404	0,1577	87,6148762
3 mM met + 6 mM DCA	1,7836	1,8963	2,0731	1,9177	0,1192	74,9951116
6 mM met + 1 mM DCA	1,5899	2,9614	2,9854	2,5122	0,6522	99,7379705
6 mM met + 3 mM DCA	1,6009	2,9922	2,9930	2,5287	0,6561	100,393044
6 mM met + 6 mM DCA	1,7668	3,0157	3,0049	2,5958	0,5862	103,057011
1 mM met	2,0531	2,8948	2,9791	2,6423	0,4181	
3 mM met	1,7245	2,9460	3,0007	2,5571	0,5891	
6 mM met	1,7408	2,8697	2,9459	2,5188	0,5510	
1 mM DCA	2,8273	2,5067	2,2797	2,5379	0,2246	
3 mM DCA	2,7713	2,5097	2,2553	2,5121	0,2106	
6 mM DCA	2,7821	2,5991	2,6628	2,6813	0,0758	

Table 49: CCK-8 absorbance values of each passage from SW948 with different concentration combinations of metformin and DCA 24 hours treatment, including arithmetic mean and S.D. The values have been normalized to its equivalent singular metformin value. Pn displays the passage number for the replicate.

Metformin and DCA (mM):	P13:	P13:	P17:	Arithmetic mean:	Standard deviation:	Normalization to metformin:
-------------------------	------	------	------	------------------	---------------------	-----------------------------

Water	2,8362	2,6658	3,0017	2,8346	0,1372	
0 mM control	2,8814	2,7823	2,9360	2,8665	0,0636	
1 mM met + 1 mM DCA	2,8231	2,5539	2,9153	2,7641	0,1533	106,936707
1 mM met + 3 mM DCA	2,9320	2,7261	2,9531	2,8704	0,1024	111,049211
1 mM met + 6 mM DCA	2,9451	2,7239	2,9533	2,8741	0,1063	111,192355
3 mM met + 1 mM DCA	2,0110	1,7856	2,2798	2,0255	0,2020	107,836874
3 mM met + 3 mM DCA	2,1655	2,1415	2,2005	2,1692	0,0242	115,487409
3 mM met + 6 mM DCA	2,8255	2,6248	1,9920	2,4808	0,3552	132,076878
6 mM met + 1 mM DCA	1,7823	1,5450	1,5435	1,6236	0,1122	102,655539
6 mM met + 3 mM DCA	2,2451	1,9184	1,6118	1,9251	0,2586	121,718513
6 mM met + 6 mM DCA	1,7192	1,5843	1,7038	1,6691	0,0603	105,532372
1 mM met	2,6157	2,3055	2,8333	2,5848	0,2166	
3 mM met	1,6702	1,9110	2,0539	1,8783	0,1583	
6 mM met	1,2229	0,9814	2,5404	1,5816	0,6851	
1 mM DCA	2,9650	2,7282	2,9487	2,8806	0,1080	
3 mM DCA	2,9747	2,7505	3,0253	2,9169	0,1194	
6 mM DCA	2,9896	2,7618	2,9507	2,9007	0,0995	

Table 50: CCK-8 absorbance values of each passage from SW948 with different concentration combinations of metformin and DCA 48 hours treatment, including arithmetic mean and S.D. The values have been normalized to its equivalent singular metformin value. Pn displays the passage number for the replicate.

Metformin and DCA (mM):	P13:	P13:	P17:	Arithmetic mean:	Standard deviation:	Normalization to metformin:
Water	1,9086	1,9307	2,8023	2,2139	0,4162	
0 mM control	1,9673	1,9274	2,7905	2,2284	0,3978	
1 mM met + 1 mM DCA	1,8060	1,8717	2,0113	1,8964	0,0856	117,496902
1 mM met + 3 mM DCA	1,9560	1,9755	2,0517	1,9944	0,0413	123,568773
1 mM met + 6 mM DCA	1,9900	2,0261	2,0884	2,0348	0,0406	126,071871
3 mM met + 1 mM DCA	1,0708	1,0764	1,2271	1,1248	0,0724	123,672347
3 mM met + 3 mM DCA	1,2074	1,2122	1,9931	1,4709	0,3693	161,726223
3 mM met + 6 mM DCA	1,1782	1,0677	2,7720	1,6726	0,7787	183,903244
6 mM met + 1 mM DCA	0,7291	0,6880	1,2075	0,8749	0,2358	136,213607
6 mM met + 3 mM DCA	0,7404	0,7319	1,3269	0,9331	0,2785	145,274794
6 mM met + 6 mM DCA	0,7268	0,6260	0,9852	0,7793	0,1513	121,329597
1 mM met	1,6960	1,7360	1,4099	1,6140	0,1452	
3 mM met	0,8960	0,8027	1,0298	0,9095	0,0932	
6 mM met	0,6619	0,6531	0,6121	0,6423	0,0217	

1 mM DCA	2,0481	2,1401	2,0966	2,0949	0,0376
3 mM DCA	2,2822	2,5159	2,0907	2,2963	0,1739
6 mM DCA	2,3056	2,3603	1,3448	2,0036	0,4664

List of figures

Figure 1: showing a simplified overview showing the cell metabolism. The glycolysis, citric acid cycle and oxidative phosphorylation are depicted.....	13
Figure 2: Drawing of the glycolytic pathway, showing the intermediate steps, reactants, and products. (19)	15
Figure 3: The Citric Acid Cycle (22)	18
Figure 4: The Electron Transport Chain (24)	19
Figure 5: The Warburg Effect in Cancer Cells (25).....	26
Figure 6: The mechanism of action for Metformin	30
Figure 7: The mechanism of action for Dichloroacetate (DCA) (32).....	31
Figure 8: Example of results from Muse® Cell Analyzer count and viability assay.....	33
Figure 9: Basic structure of spectrophotometers (34).....	34
Figure 10: Activation of AMPK https://www.researchgate.net/publication/284563043_AMPK_An_Energy-Sensing_Pathway_with_Multiple_Inputs_and_Outputs	24
Figure 11: Total arithmetic mean (N=3) and S.D. of resazurin fluorescence values for HCT116 colorectal cancer cells with 24- and 48-hours exposure to different concentrations of metformin.	56
Figure 12: Total arithmetic mean (N=3) and S.D for resazurin fluorescence values normalized to the untreated control of HCT116 cell line with 24- and 48-hours exposure to various metformin concentrations.	57
Figure 13: Total arithmetic mean (N=4) and S.D. of resazurin fluorescence value from SW948 colorectal cancer cells with 24- and 48 hours treatment with various concentrations of metformin.....	58
Figure 14: Total arithmetic mean (N=4) and S.D. of resazurin fluorescence values normalized to the untreated control of SW948 with 24- and 48 hours treatment with metformin.....	59
Figure 15: Total arithmetic mean (N=3) and S.D. of resazurin fluorescence values for HCT116 colorectal cancer cells with 24 and 48 hours of exposure to different concentrations of DCA.....	60
Figure 16: Total arithmetic mean (N=3) and S.D for resazurin fluorescence values normalized to the untreated control of HCT116 cell line with 24- and 48-hours exposure to various DCA concentrations.	61
Figure 17: Total arithmetic mean (N=4) and S.D. of resazurin fluorescence value from SW948 colorectal cancer cells with 24- and 48 hours treatment with various concentrations of DCA.	62
Figure 18: Total arithmetic mean (N=4) and S.D. of resazurin fluorescence values normalized to the untreated control of SW948 with 24- and 48 hours treatment with DCA.	63
Figure 19: Total arithmetic mean (N=3) and S.D. of CCK-8 absorbance values for HCT116 colorectal cancer cells with 24- and 48-hours exposure to different concentrations of metformin.	66
Figure 20: Total arithmetic mean (N=3) and S.D. for CCK-8 absorbance values normalized to the untreated control of HCT116 cell line with 24- and 48-hours exposure to various metformin concentrations.	67
Figure 21: Total arithmetic mean (N=4) and S.D. of CCK-8 absorbance value from SW948 colorectal cancer cells with 24- and 48 hours treatment with various concentrations of metformin.	68

Figure 22: Total arithmetic mean (N=4) and S.D. of CCK-8 absorbance values normalized to the untreated control of SW948 with 24- and 48 hours treatment with metformin.....	69
Figure 23: Total arithmetic mean (N=3) and S.D. of CCK-8 absorbance values for HCT116 colorectal cancer cells with 24- and 48 hours exposure to different concentrations of DCA.	70
Figure 24: Total arithmetic mean (N=3) and S.D for CCK-8 absorbance values normalized to the untreated control of HCT116 cell line with 24- and 48 hours exposure to various DCA concentrations.	71
Figure 25: Total arithmetic mean (N=4) and S.D. of CCK-8 absorbance value from SW948 colorectal cancer cells with 24- and 48 hours treatment with various concentrations of DCA.....	72
Figure 26: Total arithmetic mean (N=4) and S.D. of CCK-8 absorbance values normalized to the untreated control of SW948 with 24- and 48 hours treatment with DCA.	73
Figure 27: Resazurin fluorescence values in percent normalized to its internal corresponding singular metformin treatment of HCT116 cell line with 24- and 48 hours exposure to various combinations of metformin and DCA.	75
Figure 28: Resazurin fluorescence values in percent normalized to its internal corresponding singular metformin treatment of SW948 cell line with 24- and 48 hours exposure to various combinations of metformin and DCA.	76
Figure 29: CCK-8 absorbance values in percent normalized to its internal corresponding singular metformin treatment of HCT116 cell line with 24- and 48 hours exposure to various combinations of metformin and DCA.	78
Figure 30: CCK-8 absorbance values in percent normalized to its internal corresponding singular metformin treatment of SW948 cell line with 24- and 48 hours exposure to various combinations of metformin and DCA.	79
Figure 31: Cell characteristics and gated areas of negative control for HCT116 (left) and SW948 (right) measured by a flow cytometry.....	80
Figure 32: Flow cytometry results of HCT116, treated with 48 hours exposure to metformin and DCA, on the expression of Akt and p-Akt.	81
Figure 33: Flow cytometry results of HCT116, treated with 48 hours exposure to metformin and DCA, on the expression of AMPK and p-AMPK.	82
Figure 34: Flow cytometry results of SW948, treated with 48 hours exposure to metformin and DCA, on the expression of Akt and p-Akt.	83
Figure 35: Flow cytometry results of SW948, treated with 48 hours exposure to metformin and DCA, on the expression of AMPK and p-AMPK.	84
Figure 36:	87

List of tables

Table 1: List of hazardous chemicals related to our project and their hazard/precaution classifications.	37
Table 2: List of non-hazardous chemicals related to our project.	38
Table 3: Listing of every instrument used in our project and their description.....	39

<i>Table 4: Listing of equipment used in our project and their description.</i>	<i>40</i>
<i>Table 5: Final medication concentrations used in our project for metformin and DCA, both separate and combined.</i>	<i>98</i>
<i>Table 6: Calculations of the amounts of medium and medications needed for each combination solution</i>	<i>99</i>
<i>Table 7: 96-well plate setup for alamarBlue assay on cell line HCT116 and SW948 containing viable cells ranging from 5000-30000, blank controls, and PBS.</i>	<i>100</i>
<i>Table 8: 96-well plate setup for alamarBlue treatment assay on cell line HCT116 and SW948 containing 10000- and 15000 viable cells, respectively, with different concentrations of metformin or DCA (mM), blank controls, and PBS.</i>	<i>101</i>
<i>Table 9: 96-well plate setup showing the placement of different medication combinations including wells treated with water rather than medication.</i>	<i>102</i>
<i>Table 10: 96-well plate setup showing the placement of different medication combinations in this setup no wells contain added water.</i>	<i>103</i>
<i>Table 11: Arithmetic mean and S.D. of every resazurin fluorescence value of each parallel from HCT116 colorectal cancer cells with 24 hours treatment with different concentrations of metformin. Pn displays the passage number for the replicate.</i>	<i>104</i>
<i>Table 12: Arithmetic mean and S.D. of every resazurin fluorescence value of each parallel from HCT116 colorectal cancer cells with 48 hours treatment with different concentrations of metformin. Pn displays the passage number for the replicate.</i>	<i>104</i>
<i>Table 13: Arithmetic mean and S.D. of every resazurin fluorescence value of each parallel from SW948 colorectal cancer cells with 24 hours treatment with different concentrations of metformin. Pn displays the passage number for the replicate.</i>	<i>105</i>
<i>Table 14: Arithmetic mean and S.D. of every resazurin fluorescence value of each parallel from SW948 colorectal cancer cells with 48 hours treatment with different concentrations of metformin. Pn displays the passage number for the replicate.</i>	<i>105</i>
<i>Table 15: Arithmetic mean and S.D. of every resazurin fluorescence value of each parallel from HCT116 colorectal cancer cells with 24 hours treatment with different concentrations of DCA. Pn displays the passage number for the replicate.</i>	<i>106</i>
<i>Table 16: Arithmetic mean and S.D. of every resazurin fluorescence value of each parallel from HCT116 colorectal cancer cells with 48 hours treatment with different concentrations of DCA. Pn displays the passage number for the replicate.</i>	<i>106</i>
<i>Table 17: Arithmetic mean and S.D. of every resazurin fluorescence value of each parallel from SW948 colorectal cancer cells with 24 hours treatment with different concentrations of DCA. Pn displays the passage number for the replicate.</i>	<i>107</i>
<i>Table 18: Arithmetic mean and S.D. of every resazurin fluorescence value of each parallel from SW948 colorectal cancer cells with 48 hours treatment with different concentrations of DCA. Pn displays the passage number for the replicate.</i>	<i>107</i>

<i>Table 19: % resazurin fluorescence values of passages from HCT116, 24 hours treatment with metformin normalized to the untreated control, the arithmetic mean of all passages and their S.D. values. Pn displays the passage number for the replicate.</i>	<i>108</i>
<i>Table 20: % resazurin fluorescence values of passages from HCT116, 48 hours treatment with metformin normalized to the untreated control, the arithmetic mean of all passages and their S.D. values. Pn displays the passage number for the replicate.</i>	<i>108</i>
<i>Table 21: % resazurin fluorescence values of passages from SW948, 24 hours treatment with metformin normalized to the untreated control, the total arithmetic mean of all passages and their S.D. values. Pn displays the passage number for the replicate.</i>	<i>109</i>
<i>Table 22: % resazurin fluorescence values of passages from SW948, 48 hours treatment with metformin normalized to the untreated control, the arithmetic mean of all passages and their S.D. values. Pn displays the passage number for the replicate</i>	<i>109</i>
<i>Table 23: % resazurin fluorescence values of passages from HCT116, 24 hours treatment with DCA normalized to the untreated control, the arithmetic mean of all passages and their S.D. values. Pn displays the passage number for the replicate.</i>	<i>109</i>
<i>Table 24: % resazurin fluorescence values of passages from HCT116, 48 hours treatment with DCA normalized to the untreated control, the arithmetic mean of all passages and their S.D. values. Pn displays the passage number for the replicate.</i>	<i>110</i>
<i>Table 25: % resazurin fluorescence values of passages from SW948, 24 hours treatment with DCA normalized to the untreated control, the arithmetic mean of all passages and their S.D. values. Pn displays the passage number for the replicate.</i>	<i>110</i>
<i>Table 26: % resazurin fluorescence values of passages from SW948, 48 hours treatment with DCA normalized to the untreated control, the arithmetic mean of all passages and their S.D. values. Pn displays the passage number for the replicate.</i>	<i>110</i>
<i>Table 27: Arithmetic mean and S.D. of every CCK-8 absorbance value of each parallel from HCT116 colorectal cancer cells with 24 hours treatment with different concentrations of metformin. Pn displays the passage number for the replicate.....</i>	<i>112</i>
<i>Table 28: Arithmetic mean and S.D. of every CCK-8 absorbance value of each parallel from HCT116 colorectal cancer cells with 48 hours treatment with different concentrations of metformin. Pn displays the passage number for the replicate.....</i>	<i>112</i>
<i>Table 29: Arithmetic mean and S.D. of every CCK-8 absorbance value of each parallel from SW948 colorectal cancer cells with 24 hours treatment with different concentrations of metformin. Pn displays the passage number for the replicate.....</i>	<i>113</i>
<i>Table 30: Arithmetic mean and S.D. of every CCK-8 absorbance value of each parallel from SW948 colorectal cancer cells with 48 hours treatment with different concentrations of metformin. Pn displays the passage number for the replicate.....</i>	<i>113</i>
<i>Table 31: Arithmetic mean and S.D. of every CCK-8 absorbance value of each parallel from HCT116 colorectal cancer cells with 24 hours treatment with different concentrations of DCA. Pn displays the passage number for the replicate.....</i>	<i>113</i>

<i>Table 32: Arithmetic mean and S.D. of every CCK-8 absorbance value of each parallel from HCT116 colorectal cancer cells with 48 hours treatment with different concentrations of DCA. Pn displays the passage number for the replicate.....</i>	<i>114</i>
<i>Table 33: Arithmetic mean and S.D. of every CCK-8 absorbance value of each parallel from SW948 colorectal cancer cells with 24 hours treatment with different concentrations of DCA. Pn displays the passage number for the replicate.....</i>	<i>114</i>
<i>Table 34: Arithmetic mean and S.D. of every CCK-8 absorbance value of each parallel from SW948 colorectal cancer cells with 48 hours treatment with different concentrations of DCA. Pn displays the passage number for the replicate.....</i>	<i>115</i>
<i>Table 35: % CCK-8 absorbance values of passages from HCT116, 24 hours treatment with metformin normalized to the untreated control, the arithmetic means of all passages and their S.D. values. Pn displays the passage number for the replicate.</i>	<i>115</i>
<i>Table 36: % CCK-8 absorbance values of passages from HCT116, 48 hours treatment with metformin normalized to the untreated control, the arithmetic means of all passages and their S.D. values. Pn displays the passage number for the replicate.</i>	<i>116</i>
<i>Table 37: % CCK-8 absorbance values of passages from SW948, 24 hours treatment with metformin normalized to the untreated control, the arithmetic means of all passages and their S.D. values. Pn displays the passage number for the replicate.</i>	<i>116</i>
<i>Table 38: % CCK-8 absorbance values of passages from SW948, 48 hours treatment with metformin normalized to the untreated control, the arithmetic means of all passages and their S.D. values. Pn displays the passage number for the replicate.</i>	<i>117</i>
<i>Table 39: % CCK-8 absorbance values of passages from HCT116, 24 hours treatment with DCA normalized to the untreated control, the arithmetic means of all passages and their S.D. values. Pn displays the passage number for the replicate.</i>	<i>117</i>
<i>Table 40: % CCK-8 absorbance values of passages from HCT116, 48 hours treatment with DCA normalized to the untreated control, the arithmetic means of all passages and their S.D. values. Pn displays the passage number for the replicate.</i>	<i>118</i>
<i>Table 41: % CCK-8 absorbance values of passages from SW948, 24 hours treatment with DCA normalized to the untreated control, the arithmetic means of all passages and their S.D. values. Pn displays the passage number for the replicate.</i>	<i>118</i>
<i>Table 42: % CCK-8 absorbance values of passages from SW948, 48 hours treatment with DCA normalized to the untreated control, the arithmetic means of all passages and their S.D. values. Pn displays the passage number for the replicate.</i>	<i>119</i>
<i>Table 43: Resazurin fluorescence values of each passage from HCT116 with different concentration combinations of metformin and DCA 24 hours treatment, including arithmetic mean and S.D. Pn displays the passage number for the replicate.</i>	<i>120</i>
<i>Table 44: Resazurin fluorescence values of each passage from HCT116 with different concentration combinations of metformin and DCA 48 hours treatment, including arithmetic mean and S.D. Pn displays the passage number for the replicate.</i>	<i>121</i>

<i>Table 45: Resazurin fluorescence values of each passage from SW948 with different concentration combinations of metformin and DCA 24 hours treatment, including arithmetic mean and S.D. Pn displays the passage number for the replicate.</i>	<i>122</i>
<i>Table 46: Resazurin fluorescence values of each passage from SW948 with different concentration combinations of metformin and DCA 48 hours treatment, including arithmetic mean and S.D. Pn displays the passage number for the replicate.</i>	<i>124</i>
<i>Table 47: % Resazurin fluorescence values of each passage of SW948 with different concentration combinations of metformin and DCA 48 hours treatment normalized to the untreated control, including arithmetic mean and S.D. Pn displays the passage number for the re</i>	<i>129</i>
<i>Table 48: CCK-8 absorbance values of each passage from HCT116 with different concentration combinations of metformin and DCA 24 hours treatment, including arithmetic mean and S.D. Pn displays the passage number for the replicate.</i>	<i>125</i>
<i>Table 49: CCK-8 absorbance values of each passage from HCT116 with different concentration combinations of metformin and DCA 48 hours treatment, including arithmetic mean and S.D. Pn displays the passage number for the replicate.</i>	<i>126</i>
<i>Table 50: % CCK-8 absorbance values of each passage of HCT116 with different concentration combinations of metformin and DCA 48 hours treatment normalized to the untreated control, including arithmetic mean and S.D. Pn displays the passage number for the replicate</i>	<i>133</i>
<i>Table 51: CCK-8 absorbance values of each passage from SW948 with different concentration combinations of metformin and DCA 24 hours treatment, including arithmetic mean and S.D. Pn displays the passage number for the replicate.</i>	<i>127</i>
<i>Table 52: CCK-8 absorbance values of each passage from SW948 with different concentration combinations of metformin and DCA 48 hours treatment, including arithmetic mean and S.D. Pn displays the passage number for the replicate.</i>	<i>129</i>

List of equations

<i>Equation 1</i>	<i>44</i>
<i>Equation 2</i>	<i>45</i>
<i>Equation 3</i>	<i>45</i>
<i>Equation 4</i>	<i>47</i>
<i>Equation 5</i>	<i>47</i>
<i>Equation 6</i>	<i>50</i>
<i>Equation 7</i>	<i>50</i>
<i>Equation 8</i>	<i>55</i>